THE ROLE OF MYOGENIC CONSTRICTION IN HYPERTENSION AND CHRONIC

KIDNEY DISEASE

MYOGENIC CONSTRICTION: ITS REGULATION, ROLE IN HYPERTENSIVE

KIDNEY DISEASE, AND ASSOCIATION WITH URINARY UROMODULIN

By SAMERA NADEMI, Hon. B.Sc.

A Thesis Submitted to the School of Graduate Studies in Partial Fulfilment of the

Requirements of the Doctorate of Philosophy Degree

McMaster University

McMaster University DOCTOR OF PHILOSOPHY (2022)

Hamilton, Ontario (Medical Sciences)

TITLE: Proteinuria, including uromodulin overexcretion is correlated with renal disease

AUTHOR: Samera Nademi, B.Sc. (University of Victoria)

SUPERVISOR: Jeffrey G. Dickhout, Ph.D.

NUMBER OF PAGES: 282

THESIS ABSTRACT

Chronic kidney disease (CKD) is defined as glomerular filtration rate (GFR) less than 60 mL/min/1.73 m^2 for 3 months and is characterized by progressive loss of renal function. The second leading cause of CKD is hypertension. More than half of CKD patients also suffer from hypertension. Arteries and arterioles adjust to the fluctuations in the systematic blood pressure through a mechanism called autoregulation. In the kidneys, autoregulation protects the delicate glomeruli capillaries from high blood pressure and occurs through myogenic constriction (MC). MC refers to contraction of arterioles in response to an increase in the blood pressure. Chronically hypertensive individuals and animal models have an enhanced MC, leading to minimal renal injury despite their elevated blood pressure. Experimental and clinical evidence point to a role for the MC in the pathogenesis of the CKD, however, the mechanism through which preglomerular arterial MC contributes to CKD has not been fully elucidated. This thesis showed that augmented MC in chronically hypertensive animal models was due to increased thromboxane A2 prostaglandin that was not released from the endothelium (**Chapter 2**). Nevertheless, inhibiting MC while also reducing the blood pressure prevented salt-induced renal injury even though the blood pressure was still not normalized compared to the normotensive controls (**Chapter 3**). The resulting improvement in renal structure and function could be attributed to the reduction in the blood pressure, albumin, and uromodulin (UMOD) excretion (**Chapter 3**). UMOD is a kidney-specific glycoprotein that, based on a genome-wide association study have the strongest association to CKD (**Chapter 3**). Comparing two CKD hypertensive animal models further revealed that

CKD progression was independent of the blood pressure and strongly associated with UMOD excretion levels (**Chapter 4**). Collectively, the data discussed in this thesis demonstrates potential therapeutic targets in CKD hypertensive animal models.

ACKNOWLEDGEMENTS

First, I would like to express sincere gratitude to my supervisor, Dr. Jeffrey G. Dickhout who over the years, kindly and patiently guided and supported me. I am very grateful for all the things that you have done for me. You helped me when I needed the most and I will never forget this.

I also would like to thank my committee members, Dr. Luke Janssen and Dr. Joan Krepinsky for their exceptional support, input, and encouragement. Thanks very much for your on-going insights and for making our Nephrology meetings enjoyable to attend. I feel very lucky to have such knowledgeable and supportive supervisor and committee members.

Additionally, I would like to express much gratitude to Dr. Kamal Bali, Dr. Kim Madden, and Dr. Vickas Khanna for giving me the opportunity to participate in their research teams. I was very fortunate to collaborate with such wonderful people and appreciate this opportunity a great deal.

And last but not least, I am also very grateful to my parents, Reza and Roya, and my precious brother, Sepehr. You are the brightness and the colors of my life. I could have never made it this far if it was not for the pure love and support you always gave me. Thank you so much for always being there for me.

TABLE OF CONTENTS

Page number

NIFEDIPINE PREVENTED SALT-INDUCED RENAL INJURY IN OLDER

SPONTANEOUSLY HYPERTENSIVE RATS

LIST OF FIGURES

CHAPTER 3

**NIFEDIPINE PREVENTED SALT-INDUCED RENAL INJURY IN
OLDER SPONTANEOUSLY HYPERTENSIVE RATS**

CHAPTER 4

RENAL DISEASE IN THE DAHL SALT SENSITIVE (DSS) IS ASSOCIATED WITH EXCESSIVE UROMODULIN EXCRETION, (PREPARED FOR SUBMISSION)

LIST OF TABLES

LIST OF ABBREVIATIONS

20-HETE	20-hydroxyeicosatetraenoic acid
4-PBA	4-phenylbutyric acid
ACE	Angiotensin converting enzyme
ACh	Acetylcholine
BK	Large conductance potassium channel (or big potassium channels)
BL	baseline
Ca2+	calcium
CKD	Chronic kidney disease
COX	Cyclooxygenase enzymes
DAG	Diacylglycerol
DBP	Diastolic blood pressure
DCT	distal convoluted tubules
DOCA	Deoxycorticosterone acetate
DSS	Dahl salt-sensitive
EGF	Epidermal growth factor
ENaC	Epithelial sodium channels
eNOS	endothelial NO synthase
EP	endpoint
ER	Endoplasmic reticulum
ERS	Endoplasmic reticulum stress
ESRD	End state renal disease

ET1	Endothelin-1
FHH	Fawn hooded hypertensive
FHL	Fawn-hooded low blood pressure
GFR	Glomerular filtration rate
GPCRs	G-Protein-Coupled Receptors
HBSS	Hank's Balanced Salt Solution
HS	High salt
HSD	High salt diet
HSN	High salt co-administered with Nifedipine
HSP	High Salt co-administered with 4-PBA
IP3	Inositol trisphosphate
L-NNA	N-Nitro-L-arginine
LSD	low salt diet
L-VGCC	L-type voltage gated calcium channel
MAP	Mean arterial pressure
MC	Myogenic constriction
MP	midpoint
MR	Myogenic response
NaCl	sodium chloride
NKCC2	Na+, K+, 2Cl- cotransporter
NO	Nitric Oxide
NOS	Nitric Oxide synthase

NS	Normal salt
PGH2	prostaglandin H2
PGI2	Prostacyclin
PGs	Prostaglandins
PIP2	Phosphotidylinositol 4,5-Bisphosphate
PKC	Protein kinase C
PLC	Phospholipase C
Plekha7	Pleckstrin homology domain containing family A member 7
RBF	renal blood flow
SBP	Systolic blood pressure
SEM	Scanning Electron Microscopy
SHR	Spontaneously hypertensive rats
SMCs	smooth muscle cells
SNPs	Single Nucleotide Polymorphisms
SR	Sarcoplasmic reticulum
TAL	thick ascending limb
TEM	Transmission Electron Microscopy
TGF	Tubuloglomerular feedback
TGF-β	Transforming growth factor betaa
TM	Tunicamycin
TRPC6	Transient receptor potential canonical 6
TRPM4	Transient receptor potential melastatin 4

T-Tubule   Transverse-tubule

TXA2   Thromboxane A2

UMOD   Uromodulin

UPR   unfolded Protein response

VSMCs   Vascular smooth muscle cells

WKY   Wistar-Kyoto

WR   Wistar rats

PREFACE

This thesis is formatted as a sandwich thesis composed of six chapters based on the instructions outlined in the "Guide for the Preparation of Master's and Doctoral Theses" and provided by the School of Graduate Studies at McMaster University. Chapter 1 of this thesis is an introductory chapter that provides a background information on the following chapters. Chapter 2 through 4 are empirical articles that were either published, submitted for publication, or prepared for submission at the time that this thesis was prepared. Even though I am the primary author, the original articles presented in this thesis were the results of collaborative efforts and thereby are multi-authored. Chapter 5 is a concluding chapter that discusses the findings of this thesis in the context of the available literature, provides future directions, summarizes conclusions, and expresses the significance of our studies in the context of nephrology and hypertension. The manuscripts that comprise this thesis are listed below:

CHAPTER 1: Zahraa Mohammad-Ali, Racheal E. Carlisle, **Samera Nademi,** Jeffrey G. Dickhout. (2017). Animal Models of Kidney Disease. In Animal Models for the Study of Human Disease (pp. 379-417), *Elsevier* (Published). A small section of this manuscript was paraphrased in Chapter 1.

CHAPTER 2: Samera Nademi, Chao Lu, Jeffrey G. Dickhout (2019). Enhanced Myogenic Constriction in the SHR Preglomeruar Vessels is Mediated by Thromboxane A2 Synthesis. *Frontiers in Physiology (Renal Section),* (Published)

CHAPTER 3: Samera Nademi, Chao Lu, Rushank Patel, Jeffrey G. Dickhout (2022). Nifedipine Prevented Salt-Induced Renal Injury in Older Spontaneously Hypertensive Rats. *The Public Library of Science*, (Submitted)

CHAPTER 4: Samera Nademi, Chao Lu, Victoria Yum, Jeffrey G. Dickhout (2022). Renal Disease in the Dahl Salt Sensitive (DSS) is Associated with Excessive Uromodulin Excretion, (Prepared for submission)

In addition to the precedent articles that were used to compile this thesis, I also contributed to the following manuscripts during my doctoral studies:

Faris Bdair, Sophia Mangala, Imad Kashir, Darren Young Shing, John Price, Murtaza Sohaib, Breanne Flood, **Samera Nademi**, Lehana Thabane, Kim Madden (2022). The Reporting Quality and Transparency of Orthopaedic Studies Using Bayesian Analysis Requires Improvement: A Systematic Survey of the Completeness of Reporting in Orthopedic Surgery, *Elsevier Contemporary Clinical Trials Communications* (Submitted)

Rachel E. Carlisle, Zahraa Mohammed-Ali, Chao Lu, Tamana Yousof, Victor Tat, **Samera Nademi**, Melissa E. MacDonald, Richard C. Austin, Jeffrey G. Dickhout (2021). TDAG51 Induces Renal Interstitial Fibrosis through Modulation of TGFβ Receptor 1 in Chronic Kidney Disease, *Cell death & disease*, *12*(10), 1-12, (Published)

Samera Nademi, Kamal Bali, Danielle Petruccelli, Mitch Winemaker (2021). The Effects of a Targeted Preoperative Education Session on Primary Total Knee Arthroplasty Outcomes: A Pilot Randomized Controlled Trial, (In preparation)

Rubinger L, **Nademi S**, Flood B, Kashir I, Khosravi A, Young Shing D, Zhao D, Tushinski D, Shanthanna H, Madden K. (2021). Interventions to Reduce Opioid Use in Arthroplasty: A Meta-Analysis, (Submitted)

Samera Nademi, Jeffrey G. Dickhout (2019). Protein Misfolding in Endoplasmic Reticulum Stress with Applications to Renal Diseases. *Advances in Protein Chemistry and Structural Biology*, *118*, 217-247, (Published)

CHAPTER 1

INTRODUCTION

1.1 CHRONIC KIDNEY DISEASE AND ITS COMPLICATIONS

1.1.1 Chronic Kidney Disease

Chronic Kidney Disease (CKD), a gradual and persistent loss of kidney function [1], is a serious public health burden in Canada and world-wide. Over 2.9 million Canadians have CKD, with millions more being at risk of developing CKD [2, 3]. CKD often progresses to End-Stage Renal Disease (ESRD) which requires dialysis or renal replacement therapy and costs the Canadian health care system over $40 billion per year [4]. The diagnosis of CKD requires a glomerular filtration rate (GFR) decline (<60 mL/min/1.73 m^2) for at least 3 months or evidence of renal damage (i.e., albuminuria, abnormal kidney biopsy) [1]. To assist doctors in providing optimum care, the National Kidney Foundation categorized CKD into 5 stages: **Stage 1**) kidney damage with normal or increased GFR (>90 mL/min/1.73 m^2); **Stage 2**) mild reduction in GFR (60-89 mL/min/1.73 m^2); **Stage 3**) moderate reduction in GFR (30-59 mL/min/1.73 m^2); **Stage 4**) severe reduction in GFR (15-29 mL/min/1.73 m^2); and **Stage 5**) kidney failure (<15 mL/min/1.73 m^2 or dialysis) [1, 5]. One of the powerful risk factors for the development and progression of CKD to ESRD is damage to the glomerular filtration barrier structure [6]. Glomerular filtration barrier consists of 3 layers, listed here from the blood to the urinary side: 1) fenestrated endothelium, 2) glomerular basement membrane, and 3) highly specialized podocytes [5]. The podocytes have foot processes that wrap around the glomerular basement membrane and endothelial cells of glomerular capillaries [5]. In between the glomerular capillaries, there are mesangial cells that produce

glomerular extracellular matrix (ECM, also called mesangial matrix) and provide structural support for the glomerular capillaries [5]. Glomerular capillaries and mesangial cells are all located inside a hollow capsule called Bowman's capsule, which is lined with a cell layer called parietal epithelial cells [5]. Unfortunately, sometimes glomerular capillaries, mesangial cells, and parietal cells develop abnormalities characterized by mesangial cell proliferation, immune cell accumulation (i.e. leukocytes), immune deposits, overproduction of glomerular ECM, and necrosis with segmental or global scarring [5, 7]. These characteristics are commonly referred to as glomerular sclerosis or scarring of the glomeruli [5]. Glomerular sclerosis may compromise the glomerular capillary's ability to keep red blood cells and proteins (such as albumin) circulating inside the blood, causing them to leak into the urine. This results in proteinuria, albuminuria, hematuria, and altered GFR [5, 8, 9]. Glomerular injury can be semi-quantitively evaluated using a technique called glomerular damage scoring, commonly used based on a scoring system that was demonstrated by El Nahas in 1987 [10]. El Nahas scored glomeruli based on 5 grades: Grade 0 for healthy glomerulus, Grade 1 for basement membrane thickening, Grade 2 for approximately 50% glomerular deterioration, Grade 3 for about 75% glomerular degeneration, and Grade 4 for a complete glomerular obliteration [10]. This scoring system helps evaluate the glomeruli healthiness – a parameter that is related to proteinuria and albuminuria levels. Another major contributor to the development and progression of chronic renal failure is obstruction of renal tubules through formation of protein casts which are mainly composed of a kidney-specific protein called uromodulin (UMOD) [11].

1.1.2 Uromodulin and Chronic Kidney Disease

UMOD, also called Tamm-Horsfall protein, is the most abundant glycoprotein in normal urine, being excreted at a rate of 50-150 mg per day in human [12]. UMOD is synthesized exclusively in the kidney by epithelial cells of the thick ascending limb (TAL) of the loop of Henle and distal convoluted tubules (10% of TAL expression) [13]. After synthesis, UMOD enters the endoplasmic reticulum (ER) where it is cleaved during maturation, sorted, and sent to the Golgi and ultimately cell membrane. UMOD is anchored to the membrane by a glycosylphosphatidylinositol (GPI) anchoring site. The GPI signal is then cleaved by a membrane-bound serine protease called hepsin and UMOD is secreted into the renal tubule. The cleavage occurs directly downstream from the Zona Pellucida (ZP) domain (essential for polymerization) at the C-terminus end of the protein which mediates the luminal release of the UMOD [14]. In the tubules, UMOD polymerizes and becomes excreted into the urine [15]. Suboptimal environmental conditions such as acidic pH, high salt content, and low GFR can trigger UMOD to denature, aggregate, and precipitate [16]. The aggregated UMOD can then attract the adhesion of other elements such as albumin, immunoglobulins (i.e., Bence Jones proteins [17]), tubular cells, leukocytes, and hemoglobin [11]. This leads to the formation of various types of casts. The most commonly found type is hyalin cast, which is primarily composed of UMOD and also sometimes albumin [18-20]. Albumin interacts with UMOD and is particularly effective at precipitating UMOD [20]. Protein casts are mainly formed in the distal convoluted tubules and collecting ducts of the nephrons [16]. These casts obstruct the nephron tubules and prevent them from functioning properly [21]. As

more nephrons become dysfunctional, CKD develops and can eventually lead to ESRD [22].

In 2009, genome-wide association studies (GWAS) examined association of 900,000 single nucleotide polymorphisms (SNPs) across human genome with CKD and identified common non-coding variants for UMOD gene to have the strongest association with incident CKD [23]. This association was even stronger in older CKD patients [24]. Previously, it was believed that there was only an association between high UMOD expression and excretion with the incident and development of CKD [25]. However, new research by Sjaard et al.used a Mendelian randomization to demonstrate that UMOD is a causal mediator of CKD [5]. Specifically, a meta-analysis by Olden et al. showed that UMOD promoter and non-coding variants induce overexpression and overexcretion of UMOD and are associated with CKD [26]. These variations cannot be explained by mutations in the coding region of UMOD, which induce UMOD-associated kidney disease (UAKD) [6, 7].

UMOD knockout mice show normal kidney structure [9, 10]. However, several UMOD knockout and patient studies have revealed critical functions for this kidney-specific protein such as protection against urinary tract infections, innate immunity, preventing kidney stone formation, and salt-electrolyte balance [13, 24, 25]. Liu, et al. demonstrated that UMOD deficiency impairs an active cotransporter of sodium, potassium, and chloride (Na^+, K^+, $2Cl^-$ cotransporter, NKCC2) causing an electrolyte

imbalance in the kidney and induces hypertension and hyperuricemia [14, 27]. UMOD also regulates another renal outer medullary potassium channel (ROMK) that is an ATP-dependent channel transporting potassium out of cells [25, 27, 28]. High dietary salt intake leads to increased UMOD expression and excretion [25, 29], which may be due to its role in the regulation of NKCC2 channel [27, 29, 30]. Modulation of NKCC2 and ROMK expression and activities have been shown to affect its affinity for sodium chloride (NaCl) and ability to concentrate urine, leading to hypertension [27, 28, 31].

1.1.3 High Salt and Chronic Kidney Disease

Sodium is essential in maintaining physiological homeostasis. Nevertheless, recent studies showed that average sodium consumption by adults in Canada (3400 mg [32, 33]), America (>3200 mg [34]), and Europe (2800-7200 mg [35]) well exceeded the recommended amounts (2000 mg) by World Health Organization (WHO) ([36]). The majority of this sodium is acquired through processed, packaged, and restaurant foods [36]; the content of which are not directly controlled by the consumers. Excess sodium intake induces numerous abnormalities such as hypertension, proteinuria, albuminuria, calciuria (leading to kidney stone formation and osteoporosis), renal interstitial fibrosis, decreased GFR, oxidative stress, damaged podocytes, renal and cardiac hypertrophy, and endothelium dysfunction [37-40]. Some of these abnormalities follow the development of hypertension, yet others are independent of the elevated blood pressure (i.e., the effects on endothelium, GFR, and proteinuria) [39, 41-43]. This suggests the involvement of multiple mechanisms through which excess salt insults the body's homeostasis [39]. Most

of these mechanisms are largely unknown [39]. Studies have shown that a reduction in salt consumption leads to a significant decrease in all-cause mortality in normotensive and hypertensive patients [44, 45]. In this study, we used HS diet to induce CKD in hypertensive animal models such as Dahl Salt Sensitive (DSS) and Spontaneously Hypertensive Rats (SHR) and their normotensive controls, Brown Norway 13 (BN13) and Wistar Kyoto (WKY) rats. We also utilized older SHR rats to further induce renal injury upon salt congestion as being older is a risk factor for CKD [46].

1.1.4 Aging and Chronic Kidney Disease

The proportion of people over 60 years of age are increasing worldwide due to improved medical care, longer life expectancies, and reduced fertility rates [46, 47]. As the body ages, so do the kidneys [46]. The nephrology community is still divided over what is a normal GFR decline for elderly patients as about one-third of older individuals experience a decline in the GFR that is associated with normal urinalysis [46, 48]. Nevertheless, around two-thirds of elderly patients experience reduced GFR as well as kidney function [48]. In fact amongst individuals over 60 years old, the risk of ESRD is higher than non-renal related mortalities [47, 49]. According to a study by Nicola et al., proteinuria presence increased the incidence of ESRD in older patients versus the younger, suggesting that CKD may advance more belligerently in elderly patients [49].

1.1.5 Hypertension and Chronic Kidney Disease

Hypertension is defined as systolic and/or diastolic blood pressure ≥ 140 and/or 90 mmHg respectively [50, 51]. There are two main types of hypertensions - essential or primary and secondary hypertension. Essential hypertension occurs in 90 to 95% of hypertensive patients and is when the cause is unknown. Physicians diagnose patients in this category after observing high blood pressure three consecutive times with no known causality. Secondary hypertension is caused by a known medical condition [50, 52]. One in three adults in the United States suffers from hypertension but the prevalence of hypertension is substantially higher amongst CKD patients [53, 54]. According to epidemiology studies, depending on the stage and cause of the CKD, approximately 50-90% of CKD patients also suffer from hypertension in the United States. More advanced CKD patients are more likely to have hypertension [54, 55]. In fact, hypertension is the second leading cause of CKD after diabetes mellitus [56]. CKD and hypertension exacerbate each other in two ways [57]. Firstly, chronic high blood pressure can damage, narrow, weaken, or harden the vasculature around the kidneys including the glomerular capillaries [57, 58]. Consequently, blood delivery to the glomeruli is reduced and the filtration capability of the injured kidneys is decreased. Secondly, hypertension can be a complication of CKD as damaged kidneys may not adequately regulate the renin-angiotensin-aldosterone (RAAS) pathway. As a result, CKD in hypertensive individuals may progress faster to ESRD. It is critically important to control blood pressure in CKD patients to less than 130/80 mmHg through non-pharmacological (i.e., salt intake restriction, healthy diet, and exercising) and pharmacological treatments.

Pharmacological treatments include RAAS blockade, diuretics, calcium channel blockers, and adrenoceptor (α and β) antagonists [57]. One of the critical homeostasis mechanisms in the kidneys that help prevent renal damage as a result of chronic hypertension is a renal autoregulation mechanism called myogenic constriction (MC) [59].

1.2 MYOGENIC CONSTRICTION

1.2.1 Myogenic Constriction and Chronic Kidney Disease

MC is stretch-induced reduction in blood vessels' diameters in order to protect the organ(s) they feed from wide variations in the systematic blood pressure. Multiple literature reports established a link between MC and renal disease. One such piece of evidence came from the work of Mori et al. which suggested that renal autoregulation protects from kidney injury [60]. The researchers induced hypertension in 8-9-weeks-old DSS rats by feeding them HS diet for 2 weeks. HS diet has been shown to obliterate MC in preglomerular arteries of the DSS rats [61]. An inflatable servocontrol pump was placed in the left renal artery. When inflating, this pump imitated MC corresponding to pulses. Consequently, they removed MC in the right kidney (by administrating HS over 2 weeks, uncontrolled kidney), while artificially placed MC in the left kidney (controlled kidney). As a result, compared to the controlled (left) kidney, the uncontrolled (right) kidney suffered from significantly more interstitial fibrosis, glomeruli injury, interlobular arterial injury (higher wall-thickness ratio), inflammation (more activated microglia cells), and tubular injury due to experiencing high renal perfusion pressure over 2 weeks

(kidneys were compared in the same rats) [60]. There is also another response in the kidneys that contributes to renal protection and autoregulation, called tubuloglomerular feedback. When renal blood flow and GFR change, the amount of sodium chloride delivery to the nephrons changes accordingly. The fluctuations in the lumen sodium chloride are sensed by macula densa cells in the distal tubule, which adjust the diameter of the afferent arteriole, returning the renal blood flow and GFR back to homeostasis [62-65]. Together, MC and Tubuloglomerular feedback maintain renal intraglomerular pressure within a narrow range, with Tubuloglomerular feedback happening at 0.01 Hz (slow response) and MC occurring at 1 Hz (fast response) [66].

1.2.2 Importance of Myogenic Constriction

The significance of MC can be realized from consequences of its dysfunction or augmentation. Impaired MC has been observed in variety of human disorders such as diabetes, salt-sensitive hypertension (as sometimes found in the African Americans population), CKD; and rat models of renal pathology such as fawn hooded hypertensive and the DSS [67-69]. Defective MC in these patients and animal models has been associated with progressive albuminuria, proteinuria, glomerulosclerosis, and fibrosis in the kidneys [62, 70-74]. On the contrary, an augmented MC seems to be reno-protective as some hypertensive rats (i.e., SHR) and some patients with essential hypertension, do not develop significant renal injury possibly due to an enhanced MC [73, 75-77]. Effective treatment of MC dysfunction requires an understanding of its mechanism.

1.2.3 Mechanism of Myogenic Constriction

The following figure (**Figure 1**) presents a schematic of the MC mechanism. Even though MC was first described more than a century ago, its mechanism of sensing mechanical distension and the downstream pathways are not fully understood [74, 78, 79]. Vascular smooth muscle cells (VSMCs) are the main players in generating MC. They contain mechanosensitive G-Protein-Coupled Receptors (GPCRs) that become activated by membrane stretch as a result of increased blood flow, leading to the activation of a downstream second-messenger signaling pathway [80-82]. In this pathway, two sources provide the calcium (Ca^{2+}) concentration needed for the contraction of VSMCs: (1) Intracellular Ca^{2+} from sarcoplasmic reticulum, and (2) extracellular Ca^{2+} entering through T-type and L-type voltage-gated Ca^{2+} channels (T- and L-VGCC) [83]. After becoming activated by membrane stretch, GPCR activates Phospholipase C (PLC), which converts Phosphotidylinositol 4,5-Bisphosphate (PIP2) to inositol trisphosphate (IP3) and Diacylglycerol (DAG). DAG activates transient receptor potential canonical 6 (TRPC6) channels and protein kinase C (PKC) to phosphorylate and sensitize transient receptor potential melastatin 4 (TRPM4) channels. TRPM4 are non-selective cation channels in VSMCs which, when activated, allow influx of cations (i.e. sodium), leading to membrane depolarization. IP3, on the other hand, promotes efflux of Ca^{2+} from the sarcoplasmic reticulum into the cytosol. Ca^{2+} binds to calmodulin causing phosphorylation of myosin light chain kinase (MLCK) and activation of actinomyosin-based contractile mechanisms [84, 85]. Knockdown of TRPM4 and TRPC6 expressions in VSMCs impairs MC in cerebral arteries [82, 86]. Evidence shows that these TRP

channels are co-expressed with GPCRs, such as the angiotensin type 1, endothelin, vasopressin, or histamine receptors; and this co-expression is required for the activation of TRP channels [80]. The membrane depolarization induced by TRPM4 and TRPC6 channel openings, activate L-VGCC to allow Ca^{2+} influx. Ca^{2+} binds to calmodulin and this leads to actinomyosin-based contraction [84, 85]. This is followed by activation of additional mechanisms that further sensitize the contractile mechanism to Ca^{2+}. Intracellular Ca^{2+} increase also activates phospholipase A2 (PLA2) to stimulate release of arachidonic acid, which becomes converted to 20-HETE by cytochrome P450 enzymes. 20-HETE activates downstream kinases [74], inhibits large conductance potassium (BK) channels [87-90], and augments cellular depolarization (through TRPC6 channels). This leads to sustained T- and L-VGCC activation, and further Ca^{2+} influx. Furthermore, Endres et al. identified a gene, pleckstrin homology domain containing family A member 7 (Plekha7), that contributes to a defective MC and renal pathology. The authors placed Plekha7-KO DSS and wild-type (WT) rats on 8% NaCl diet for 4 weeks. The Plekha7-mutant rats showed significantly lower mean arterial pressure, systolic pressure, albuminuria, proteinuria, total peripheral resistance, and perivascular fibrosis in their heart and kidneys. Also, upon treatment with acetylcholine (ACh), both flow-mediated and endothelial-dependent vasodilations were improved in isolated mesenteric arteries of Plekha7-mutant compared to the WT [91].
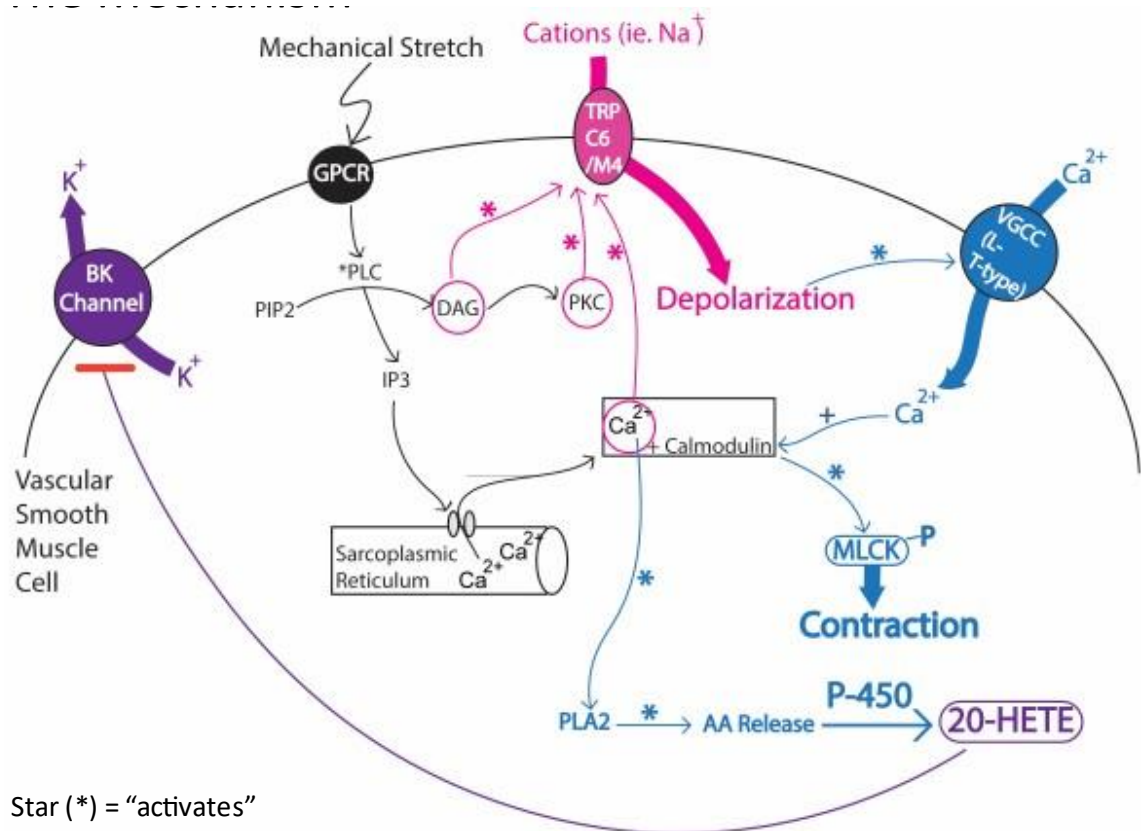
Figure 1. The mechanism of myogenic constriction (MC). The event orders are black, red, blue, & purple. Asterisk (*) depicts active/ed.

1.2.4 Regulation of Myogenic Constriction

Factors regulating MC include systolic pressure, shear stress, nitric oxide (NO), and prostaglandins. Loutzenhiser et al. discovered that when mean arterial pressure was held constant, increase in systolic pressure induced vasoconstriction; but when systolic pressure was held constant, reductions in mean arterial pressure or diastolic pressure did not change MC. The

authors concluded that MC in the kidneys only depends on systolic pressure [92]. Moreover, shear stress stimulates endothelial cells to secrete vasodilators such as NO, prostaglandins, and epoxyeicosatrienoic acids. These compounds relax the vessels by opening BK channels, hyperpolarizing the cell, and hence, inhibiting Ca^{2+} influx [93-96]. Prostaglandins are synthesized through cyclooxygenase (COX) enzymes, which convert arachidonic acid to prostaglandin H2 (PGH2), an intermediate that coverts to other prostanoids [97-100] (**Figure 2**). COX 1 and COX 2 have been found in both endothelium and smooth muscle cells of renal vasculature [101-104]. The smooth muscle cells and endothelium regulate MC by producing vasodilators and vasoconstrictors [100, 105] through various mechanisms. Some of these mechanisms are briefly explained below.

Prostaglandin I2 (PGI$_2$). There are two types of COX: (a) COX 1 is constitutively expressed in the endothelial cells, and (b) COX 2 is expressed in the endothelium in response to inflammatory stimulation with cytokines or endotoxins [98-100]. In endothelium, both COX types convert arachidonic acid to PGH2, which is subsequently converted by downstream enzymes to various prostanoids such as thromboxane A2 (TXA2), prostaglandin I$_2$, and prostaglandin E2 [97]. After being synthesized from PGH2, prostaglandin I$_2$ exits the endothelium and binds to its receptor on the VSMC. The binding activates a second messenger-signaling cascade involving cyclic adenosine monophosphate and protein kinase A that leads to the relaxation of VSMC. In contrast to prostaglandin I2, TXA2 induces vasoconstriction in arteries.

Thromboxane A2 (TXA2). After being synthesized from PGH2 by thromboxane synthase, TXA2 exits the endothelium and binds to thromboxane-prostanoid receptors located on the VSMCs, leading to an increase in intracellular $[Ca^{2+}]$ and vasoconstriction [106, 107]. TXA2 is also synthesized and released in the VSMCs [108].
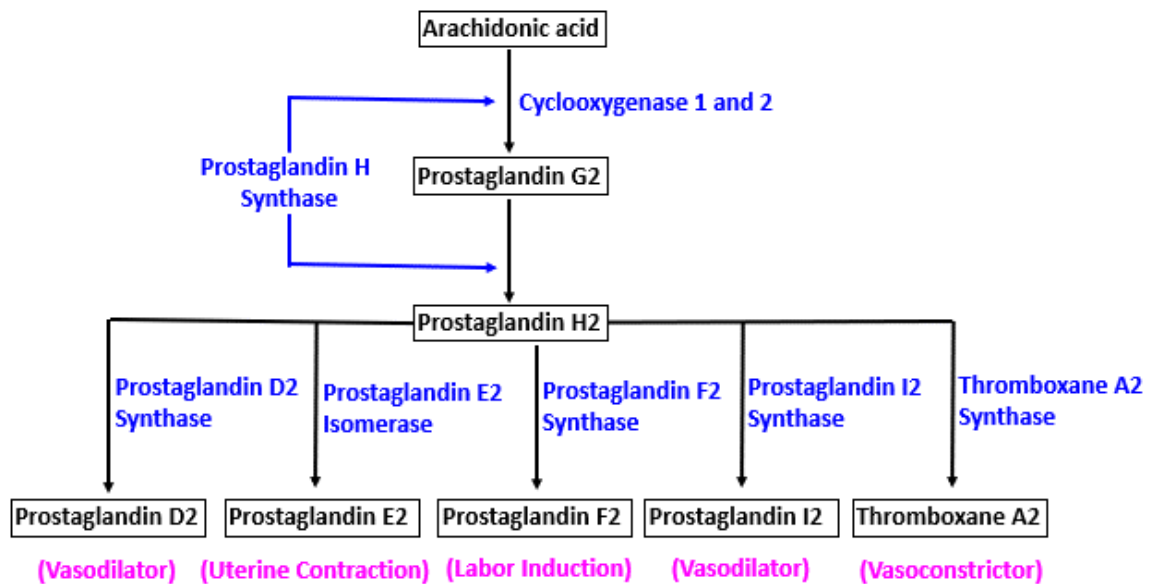
Figure 2. A schematic of main prostaglandin synthesis pathways. The enzymes are shown in blue. An example of function is indicated for each prostaglandin in pink. This diagram was constructed based on the information presented in [105, 109].

Nitric Oxide. Even though not a prostaglandin, NO has a critical role in vascular contractility. The flow of blood in vessels induces a mechanical stretch on the membrane of endothelial cells. This stretch on the membrane is also called shear stress and causes

opening of mechanically sensitive channels on the endothelium membrane: (1) specialized Ca^{2+}-activated K^+ channels, inducing K^+ efflux and Ca^{2+} influx [100, 110]; and (2) GPCRs which activate IP3 second messenger signaling pathway, leading to the opening of endoplasmic reticulum (ER) and Ca^{2+} influx into the cytoplasm [110, 111]. Ca^{2+} in the cytosol binds to calmodulin and the complex binds to caveolae. Caveolae are invaginations of plasma membrane that contain inactive endothelial NO synthase (eNOS) bound to caveolin protein [112]. Calcium-calmodulin complex detaches eNOS from caveolin and activates this enzyme to convert L-arginine into NO [113]. NO then diffuses into VSMCs and binds to the enzyme soluble guanylyl cyclase (sGC), activating it to convert guanosine triphosphate (GTP) to cGMP. cGMP then reduces Ca^{2+} release from sarcoplasmic reticulum and decreases sensitivity of actin-myosin chain to Ca^{2+}, thereby decreasing VSMC contractions and relaxing the vessel [114-116].

1.2.5 Dependence of Myogenic Constriction on Endothelium

Even though MC is essential in renal autoregulation, there are conflicting literature reports on the dependency of MC on the endothelium (**Table 1**). As illustrated in Table 1, studies in different species and tissues have reported that endothelium removal abolished [117-121], enhanced [122-127], reduced [124], or did not change [126, 128-130] MC. Endothelial cells can release different vasoactive substances in variable quantities in different vascular beds or even different sections of the same vascular bed [131-133]. Thus, it is important to investigate the function of endothelium in different vascular beds. Although a few studies removed endothelium from mesenteric

and renal arterioles [134-140], the effects of endothelium removal on MC in hypertensive (SHR) and normotensive (WKY) arcuate and mesenteric arteries have never been investigated before. There are several methods for removing endothelium established in the literature, which are described in the next section.

Table 1. Literature reports on the dependence of myogenic constriction on endothelium

Species / Tissue	Vessel	intramural pressure	Denudation method	Denudation confirmation	Endothelium dependent	Cite
Rabbit / Kidney	afferent a.	Flow (40-120 mmHg)	antibody-complement treatment	ACh elicited no dilation	**No** (**enhanced** in free flow but **no change** in no-flow)	[122]
Mice / Gastrointest-inal tract	3rd-order mesenteric a.	10-80 mmHg	Air-bolus injection	----	**No,** (**enhanced** in WT; **No change** in eNOS-KO)	[126]
Rat / Gastrointest-inal tract	mesenteric a. (~200 μm)	(20-160 mmHg)	Mechanical rubbing (Hair abrasion)	ACh elicited no dilation	**No** (**enhanced**)	[125]
Mice/ Gastrointest inal tract	isolated mesenteric a.	----	Knocked out Connexin 40 in endothelial cells, disrupted EC junctions	----	**No** (**enhanced**)	[127]

Cat / Brain	Middle cerebral a.	40-160 mmHg ␣	Collagenase and elastase treatment	Transmission Electron Microscopy	**Yes,** (**abolished**)	[117]
Rat / Muscle	cremaster muscle arterioles (50 µm)	Flow (20-160 mm Hg)	Air injection	ACh elicited no dilation, sodium nitroprusside induced dilation	**No** (**enhance** in WKY, **reduced** in SHR)	[124]
Rat / Muscle	Cremaster a.	No flow	Mechanical rubbing (abrasive pipette)	Transmission Electron Microscopy	**No,** (**No change**)	[130]
Dog / Neck	Common carotid a.	Flow (0-38 mmHg)	Mechanical rubbing (stainless wire)	----	**Yes,** (**abolished**)	[120]

Table abbreviations:

a. = arteriole

ACh = Acetylcholine

EC = endothelial cells

1.2.6 Methods of Endothelium Denudation

Endothelium can be removed from blood vessels by chemical or physical means. Chemical methods include using collagenase, elastase, or antibodies. Collagenase and elastase are enzymes that dissolve intercellular matrix between endothelium, but might also damage the underneath VSMC layer [141]. Antibodies against specific endothelial antigens, such as factor VIII-related antigens, can also be used. Factor VIII-related antigens are plasma glycoprotein that mediate platelet attachments to the endothelium and serve as stabilizers for coagulation factor VIII. Juncos et al. showed that antibody-mediated removal abolished endothelium functionality (based on drug treatments), but did not completely remove the endothelium (revealed in their transmission electron micrograph) [142].

Physical methods of denuding endothelium involve abrading the inner surface of the vessel using an applicator such as cotton, filter paper [143], wood, wire, air bolus, or human hair [141]. Mechanical abrasion with wire, wood, cotton, and filter paper pose a challenge due to the inherent fragility of some of these applicators or difficulties in applying them towards small vessels such as preglomerular arteries [141]. Also, air bolus injections are appropriate methods for large arteries, but may not remove the endothelium in smaller arterioles [144]. In 1989, Osol et al. suggested an effective method for removing the endothelium from small arteries involving human hair, which provided sufficient degree of abrasion to damage the endothelium but not the VSMCs. The authors demonstrated successful endothelium removal through electron microscopy and

acetylcholine treatment (did not induce endothelium-dependent dilation). They also showed intact VSMCs by treating the vessels with endothelium-independent vasodilator (diltiazem) and vasoconstrictor (potassium), which elicited no alterations in MC compared to the endothelium-intact controls [141]. After reviewing the aforementioned methods, we decided to use human hair to mechanically abrade endothelium from renal and mesenteric arterioles.

1.2.7 Inhibiting Myogenic Constriction with Nifedipine

Nifedipine is a synthetic dihydropyridine antihypertensive drug that is prescribed to patients with hypertension, angina (chest pain), Raynaud syndrome (sudden spasm of arteries that cause reduced blood flow to the feeding organ), and premature labor [145, 146]. It functions through inhibiting L-type Ca^{2+} channels and relaxing the cardiac and smooth muscle cells [147, 148]. Blocking L-type Ca^{2+} channels has been shown to diminish MC [149] as Ca^{2+} is a vital signaling molecule in muscle contractions [150].

Nifedipine is mainly administered orally, but also sublingually and rectally; and about 90% of it is absorbed by the gastrointestinal tract, evident by its plasma levels [151]. Approximately 92-98 % of the absorbed circulating nifedipine is bound to plasma proteins such as albumin [152-154]. Nevertheless, only about 65-70 % enters the systematic circulation due to a significant first-pass effect in the liver [153, 155, 156]. Cytochrome P450 3A4, located in the liver and to a lesser degree in the intestinal mucosa [157], metabolizes nifedipine to 2,6-dimethyl-4-(2-nitrophenyl)-5-methoxycarbonyl-

pyridine-3-carboxylic acid, and then further to 2-hydroxymethyl-pyridine carboxylic acid. The bioavailability of nifedipine is about 56% to 77% while its half life is approximately 2-5 hours [151, 154]. Nifedipine is excreted in the urine or feces as inactive metabolites while about 1% of the absorbed nifedipine is excreted unchanged [154]. To determine how MC functions, we examined the roles of L-type Ca^{2+} channels, endothelium, NO, and prostaglandins in preglomerular arcuate and mesenteric arterioles.

1.2.8 Measuring Myogenic Constriction

In-vitro vascular studies can be divided into three main areas: structural, mechanics, and vasoreactivity [158]. Vascular structures are usually examined through different microscopy techniques such as light, electron, and fluorescent microscopies. Vascular mechanics are frequently studied with wire myography in vessels larger than 500 μm in diameter [159]. In wire myography, two wires are passed through an artery to keep the diameter constant (isometric condition) and tension changes are measured and recorded [159]. A major disadvantage of the wire myography is damaging the endothelial cell layer due to the insertion of wires [160, 161]. Another method commonly used to study endothelial functioning and vascular vasoreactivity is pressure myography which measures vessel's diameter under isobaric conditions [158]. A pressure myograph system contains a pressure myograph chamber that is connected to a peristaltic pump (to pressurize the arteries), a stereo microscope (to visualize the artery), and a servocontrolled video camera (to video-record the artery). In the pressure myograph chamber, small arterioles are mounted onto a glass pipet, cannulated at one end to create

a blind sac, pressurized with a physiological buffer (pressure is kept constant for a selected time-period), and their diameter is measured and recorded. Pressure myography simulates vessels' conditions *in-vivo* and is specifically designed to measure MC, endothelial functioning, and vascular responses to various pharmacological agents [162]. In this thesis study, we utilized pressure myography technique to measure MC and endothelial functioning in second-branch mesenteric as well as renal arcuate arteries.

1.2.9 Measuring Myogenic Constriction in Arcuate Arteries

A schematic of the kidney's vasculature is demonstrated in **Figure 3**. The abdominal aorta branches off to the right and left renal arteries just below the superior mesenteric artery [163]. As the renal arteries enter renal hilum and sinuses, they divide into anterior and posterior segmental arteries which in turn branch off to interlobar arteries supplying renal pyramids [164]. Interlobar arteries then transverse along the corticomedullary border to become arcuate arteries. Arcuate arteries sprout into the renal cortex constructing interlobular arteries. Small afferent arterioles branch off from the interlobular arteries and lead to glomerular capillaries [164] consisting of a network of approximately 50 capillary loops called a tuft [165].

MC is present in all segments of preglomerular arterioles including afferent arteriole, interlobular, and arcuate arteries [166-168]. Although the afferent arteriole was reported in the literature to play a significant role in renal autoregulation [167, 168], MC in arcuate arteries is also critical in renal autoregulation. MC has been largely

investigated in afferent arterioles [169-175], yet there is a paucity of data in the study of MC in arcuate arteries. It is important to investigate MC in various vascular beds because different vascular beds or even different sections of the same vascular beds may show different MC responses due to the release of variable types and quantities of vasoactive substances [131-133]. In this thesis study, we investigated MC in two anatomically parallel vascular beds: arcuate and mesenteric (second branch) arteries.
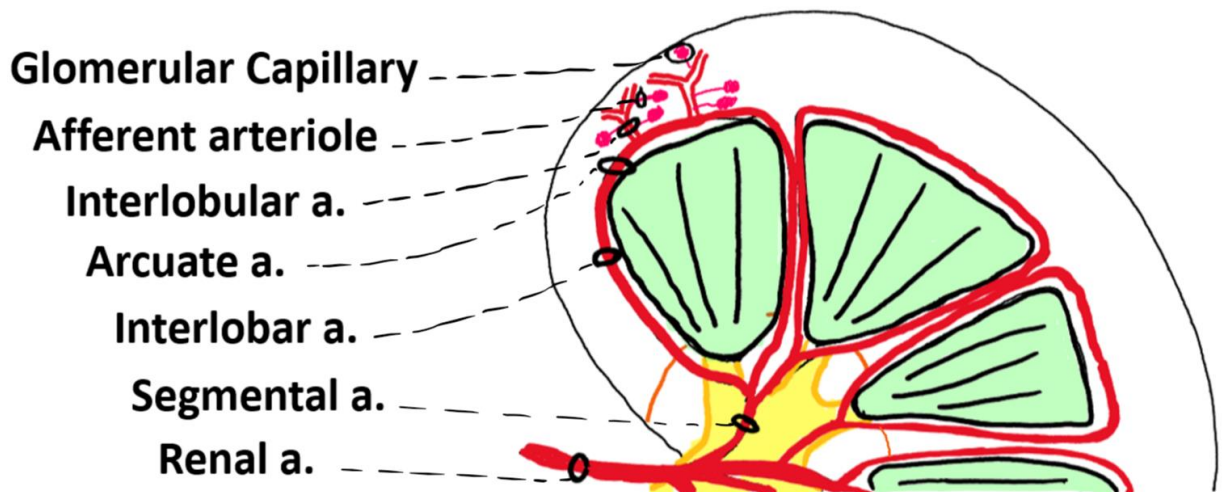
Figure 3. A schematic of renal vasculature. The term "artery" was abbreviated to "a.".

1.3 ANIMAL MODELS OF KIDNEY DISEASE

* This section was paraphrased from the following manuscript:

Zahraa Mohammad-Ali, Racheal E. Carlisle, **Samera Nademi,** Jeffrey G. Dickhout. (2017). Animal Models of Kidney Disease. In Animal Models for the Study of Human Disease (pp. 379-417), *Elsevier*

1.3.1 The Spontaneously Hypertensive Rat (SHR): A Genetic Model of Essential Hypertension

In 1960s, Okamoto et al. selectively bred WKY rats that demonstrated high blood pressure [176]. The result was a hypertensive rat that spontaneously developed high blood pressure from 5-6 weeks of age until about 17-19 weeks old, when the blood pressure stabilized at approximately 180-200 mmHg [177, 178]. This rat model was named the SHR and has been commonly used in hypertension and other cardiovascular disease research to this date. SHR rats have an enhanced preglomerular MC that prevents glomerular hyperfiltration and severe renal disease, despite having a very high systematic blood pressure [75, 179]. Nevertheless, SHR may develop renal disease particularly at older ages [180]. Even though SHR rats are mostly salt-resistant, their renal disease can exacerbate upon salt feeding [180]. GFR starts to decline in the SHR at around 30 weeks of age [181], but other cardiovascular and renal disease characteristics typically present at around 40-50 weeks old [182-184]. These characteristics include proteinuria,

glomerulosclerosis, renal interstitial fibrosis, intratubular protein casts, and hypertrophy (cardiac and vascular) [182-184].

1.3.2 The Dahl Salt-Sensitive (DSS) Rat: A Genetic Model of Hypertensive Proteinuric Chronic Kidney Disease

Another rat model commonly used in hypertensive CKD research is the DSS, representing salt-sensitive human populations. Similar to hypertensive black Americans and diabetic nephropathy patients, the DSS rats develop hypertension and renal injury [185-188]. When the DSS is fed a high salt diet (HS, 4-8% NaCl), they develop severe hypertensive CKD characteristics such as proteinuria, albuminuria, mesangial expansion, glomerulosclerosis, intratubular protein casts, interstitial fibrosis, and inflammation [189]. Nonetheless, DSS can develop hypertensive CKD even on a normal salt diet (NS, 0.1-0.4% NaCl) compared to the control rats [180, 190-192]. The control rodents used for the DSS are normotensive Brown Norway rats that had their chromosome 13 introgressed (BN13) to make a type of consomic DSS rat [193]. Introgression is defined as the transfer of genetic material between two animal strains following hybridization and through repeated backcrossing to one of its parent strains [194, 195]. An example of introgression process is generation of a consomic rat that contains an entire chromosome from another rat strain [195].

1.4 PROJECT RATIONALE, HYPOTHESIS, OBJECTIVE, AND THESIS OUTLINE

1.4.1 Overall and Specific Objectives

The **overall objective** of this thesis is to determine if inhibiting MC worsens salt-induced hypertensive CKD and the involved mechanism(s). To investigate this objective, we first need to determine how MC in renal pre-glomerular vessels functions.

Specifically, the goal of this research project was to:

1) Examine the underlying reason for the enhanced MC in pre-glomerular arterioles of chronically hypertensive SHR rats and whether this response is endothelium-dependent.

2) Determine if impaired MC exacerbates CKD in older hypertensive animal models.

3) Compare DSS and SHR rats that were fed a high salt diet to investigate the role of impaired MC, hypertension, and urinary UMOD in CKD progression.

1.4.2 Hypotheses and Rationales

Objective 1. After examining the WKY and SHR cremaster muscle arteriole responses to PGH2 synthesis inhibitor (indomethacin), PGH2 receptor blocker (SQ 29,548), and endothelium removal, Huang et al. concluded that overproduction of endothelium-derived PGH2 was responsible for the observed enhanced myogenic tone in the SHR compared to the WKY rats [196]. Additionally, Lesniewske et al. suggested that alterations in NO signaling may be responsible for the observed up-regulation of MC in skeletal muscle arterioles of hypertensive rats (i.e., Zucker Diabetic Fatty rats) [197]. Thus, we hypothesized that the enhanced MC in the SHR preglomerular arteries is due to increased production of PGH2 and decreased release of NO compared to the WKY vessels. Since PGH2 was reported to be primarily found in the endothelial cells [3], we further hypothesized that removing endothelium abolishes MC in mesenteric and preglomerular arteries.

Objective 2. Mori et al. impaired MC in the right kidney while preserving it for the left kidney in the same rat. The investigators observed that the right kidney suffered significantly more renal injuries compared to the left kidney [60]. Other studies examining the effects of dihydropyridine calcium channel blockers in 5/6 ablation or streptozotocin-induced diabetic CKD models also showed that inhibiting MC further exacerbated the CKD progression in these animal models [198-200]. Conversely, augmented MC observed in animal models and humans with essential hypertension has been associated with minimal renal injury, despite the chronically elevated blood pressure

[75, 76, 201]. HS diet has also been shown to induce hypertension and renal damage in various animal models including SHR and WKY rats [180]. We hypothesized that feeding HS diet to older SHR and WKY rats increases their blood pressure, while co-administrating HS and nifedipine reduces their blood pressure, but abolishes MC in the kidneys and thus worsens the salt-induced CKD progression.

Objective 3. Two animal models commonly used in CKD and hypertension research are DSS and SHR [202]. Both of these animal models are hypertensive however DSS is susceptible while SHR is resistant to salt-induced renal injury [61, 203]. A previously published study in our research group demonstrated that MC is impaired in the DSS rats that were fed high dietary sodium [61]. We hypothesized that HS diet impairs MC in the DSS but not the SHR, leading to an extensive renal damage in the DSS-HS but not the SHR-HS rats.

Recap. In summary, my Ph.D. thesis hypothesis consists of three subsections: 1) enhanced MC in the SHR preglomerular arteries is due to increased PGH2 and decreased NO synthesis and is dependent on the endothelium; 2) impairing MC exacerbates salt-induced CKD progression in older SHR versus WKY rats; 3) HS diet impairs MC in the DSS but not age-matched SHR, leading to significantly more renal damage in the DSS compared to the SHR.

1.4.3 Experimental Approach

To investigate the aforementioned hypotheses, *in-vivo* and *ex-vivo* experiments were conducted as briefly outlined below.

Two parallel vascular networks, renal preglomerular and mesenteric [204], were used to investigate the contractility of resistant arterioles as well as the role of endothelium in vascular functionality in hypertension. Arcuate arterioles were extracted from hypertensive animals, SHR and DSS, as well as their controls, WKY and BN13 respectively. Second branch mesenteric arterioles were extracted from SHR and WKY rats. To investigate the role of endothelium in MC, endothelium was removed from both mesenteric and arcuate arterioles using a human hair as an organic ablator and MC was measured in both endothelium-intact and -removed arteries. To explore the role of prostanoids in MC, a cyclooxygenase (COX-1 and -2) inhibitor, indomethacin, was added to both endothelium-intact and -removed arcuate arteries; and MC was measured in these vessels. Similarly, furegrelate, which is a TXA2 synthase inhibitor, was used to examine the role of TXA2 prostaglandin in the augmented MC of the SHR arcuate arteries. Nifedipine was also used to study the effects of inhibiting L-type calcium channels in MC of arcuate and mesenteric arterioles.

In addition to the *ex-vivo* vascular experiments, *in-vivo* studies were performed. Younger male SHR rats (12 weeks old) were used as a model of essential hypertension with almost no renal injury, along with their age-matched controls WKY. Older male

SHR rats (43-46 weeks old) were also used as a model of essential hypertension with renal injury. Older SHR exhibit reduced afferent arteriolar responsiveness and lack the protective augmented MC in their preglomerular arteries [205, 206]. These are accompanied by proteinuria and progressive glomerular sclerosis in older SHR rats. The DSS was used as a model of hypertension and salt-induced renal injury with reduced renal function, proteinuria, and albuminuria [207, 208]. DSS age-matched controls, BN13, have a subsection of their chromosome 13 replaced, but are 98% identical to the DSS rats [193]. All animals were either purchased from Charles River or bred at McMaster University. All animal works were conducted according to the McMaster University Animal Research Ethics Board guidelines. To induce renal disease, high dietary salt was fed to the SHR and DSS rats, although it was expected that the DSS would suffer more extensive renal damage. Being older is a risk factor for renal disease, thus older SHR rats were also utilized. While inducing renal damage through feeding HS diet to older rats, a MC inhibitor that also reduces blood pressure, nifedipine, was used as an intervention and then CKD characteristics (i.e., proteinuria, albuminuria, protein casts depositions, fibrosis) were measured. To elucidate the pathogenesis of CKD, SHR and DSS rats were compared in terms of blood pressure, MC, and urinary UMOD excretion levels.

REFERENCES

1.   Levin, A., R. Bilous, and J. Coresh, *Chapter 1: Definition and classification of CKD.* Kidney Int Suppl, 2013. **3**(1): p. 19-62.

2.   Kalatharan, V., M. Lemaire, and M.B. Lanktree, *Opportunities and challenges for genetic studies of end-stage renal disease in Canada.* Canadian journal of kidney health and disease, 2018. **5**: p. 2054358118789368.

3.   Kottgen, A., et al., *Uromodulin levels associate with a common UMOD variant and risk for incident CKD.* J Am Soc Nephrol, 2010. **21**(2): p. 337-44.

4.   Manns, B., et al., *The Financial Impact of Advanced Kidney Disease on Canada Pension Plan and Private Disability Insurance Costs.* Can J Kidney Health Dis, 2017. **4**: p. 2054358117703986.

5.   Kitching, A.R. and H.L. Hutton, *The players: cells involved in glomerular disease.* Clinical Journal of the American Society of Nephrology, 2016. **11**(9): p. 1664-1674.

6.   Iseki, K., *Ikemiya Y, Iseki C, Takishita S.* Proteinuria and the risk of developing end-stage renal disease. Kidney Int, 2003. **63**: p. 1468-1474.

7.   Zhong, J., et al., *Mechanisms of scarring in focal segmental glomerulosclerosis.* Journal of Histochemistry & Cytochemistry, 2019. **67**(9): p. 623-632.

8.   Daehn, I.S. and J.S. Duffield, *The glomerular filtration barrier: a structural target for novel kidney therapies.* Nature Reviews Drug Discovery, 2021. **20**(10): p. 770-788.

9.   Iseki, K., et al., *Proteinuria and the risk of developing end-stage renal disease.* Kidney international, 2003. **63**(4): p. 1468-1474.

10.   El Nahas, A.M., et al., *Chronic renal failure after nephrotoxic nephritis in rats: contributions to progression.* Kidney international, 1987. **32**(2): p. 173-180.

11.   Wu, T.-H., et al., *Tamm–Horsfall protein is a potent immunomodulatory molecule and a disease biomarker in the urinary system.* Molecules, 2018. **23**(1): p. 200.

12.   Reindl, J., et al., *Uromodulin-related autosomal-dominant tubulointerstitial kidney disease—pathogenetic insights based on a case.* Clinical Kidney Journal, 2018.

13.   Tokonami, N., et al., *Uromodulin is expressed in the distal convoluted tubule, where it is critical for regulation of the sodium chloride cotransporter NCC.* Kidney international, 2018. **94**(4): p. 701-715.

14.   Olinger, E., et al., *Hepsin-mediated processing of uromodulin is crucial for salt-sensitivity and thick ascending limb homeostasis.* Scientific reports, 2019. **9**(1): p. 1-15.

15.   Brunati, M., et al., *The serine protease hepsin mediates urinary secretion and polymerisation of Zona Pellucida domain protein uromodulin.* Elife, 2015. **4**: p. e08887.

16.   Lerma, E.V., M.A. Sparks, and J. Topf, *Nephrology Secrets E-Book.* 2018: Elsevier Health Sciences.

17. Sanders, P.W. and B.B. Booker, *Pathobiology of cast nephropathy from human Bence Jones proteins.* The Journal of clinical investigation, 1992. **89**(2): p. 630-639.

18. Sanders, P.W., et al., *Mechanisms of intranephronal proteinaceous cast formation by low molecular weight proteins.* The Journal of clinical investigation, 1990. **85**(2): p. 570-576.

19. Fan, S.-L. and S. Bai, *Urinalysis*, in *Contemporary Practice in Clinical Chemistry*. 2020, Elsevier. p. 665-680.

20. McQueen, E., *The nature of urinary casts.* Journal of Clinical Pathology, 1962. **15**(4): p. 367-373.

21. Fogo, A.B. and M. Kashgarian, *Diagnostic Atlas of Renal Pathology E-Book*. 2021: Elsevier Health Sciences.

22. Sanders, P.W., *Dysproteinemias and amyloidosis.* Primer on Kidney Diseases E-Book, 2009: p. 232.

23. Kottgen, A., et al., *Multiple loci associated with indices of renal function and chronic kidney disease.* Nat Genet, 2009. **41**(6): p. 712-7.

24. Gudbjartsson, D.F., et al., *Association of variants at UMOD with chronic kidney disease and kidney stones—role of age and comorbid diseases.* PLoS genetics, 2010. **6**(7): p. e1001039.

25. Devuyst, O., E. Olinger, and L. Rampoldi, *Uromodulin: from physiology to rare and complex kidney disorders.* Nat Rev Nephrol, 2017. **13**(9): p. 525-544.

26.   Olden, M., et al., *Common variants in UMOD associate with urinary uromodulin levels: a meta-analysis*. 2014, Am Soc Nephrol. p. 1869-1882.

27.   Liu, Y., et al., *Tamm-Horsfall protein/uromodulin deficiency elicits tubular compensatory responses leading to hypertension and hyperuricemia.* American Journal of Physiology-Renal Physiology, 2018. **314**(6): p. F1062-F1076.

28.   Mutig, K., et al., *Activation of the bumetanide-sensitive Na+, K+, 2Cl− cotransporter (NKCC2) is facilitated by Tamm-Horsfall protein in a chloride-sensitive manner.* Journal of Biological Chemistry, 2011. **286**(34): p. 30200-30210.

29.   Mount, D.B., *Thick ascending limb of the loop of Henle.* Clin J Am Soc Nephrol, 2014. **9**(11): p. 1974-86.

30.   Mutig, K., et al., *Activation of the bumetanide-sensitive Na+,K+,2Cl-cotransporter (NKCC2) is facilitated by Tamm-Horsfall protein in a chloride-sensitive manner.* J Biol Chem, 2011. **286**(34): p. 30200-10.

31.   Trudu, M., et al., *Common noncoding UMOD gene variants induce salt-sensitive hypertension and kidney damage by increasing uromodulin expression.* Nature medicine, 2013. **19**(12): p. 1655-1660.

32.   *Sodium in Canada*. 2017; Available from: http://www.hc-sc.gc.ca/fn-an/nutrition/sodium/index-eng.php.

33.   Zhang, C., et al., *Genetic susceptibility of hypertension-induced kidney disease.* Physiological Reports, 2021. **9**(1): p. e14688.

34.   Bernstein, A.M. and W.C. Willett, *Trends in 24-h urinary sodium excretion in the United States, 1957–2003: a systematic review.* The American journal of clinical nutrition, 2010: p. ajcn. 29367.

35.   *Implementation of the EU Salt Reduction Frame.* 2012; Available from: http://ec.europa.eu/health/home_en.

36.   Härtl, G. *WHO issues new guidance on dietary salt and potassium.* 2013; Available from: http://www.who.int/mediacentre/news/notes/2013/salt_potassium_20130131/en/.

37.   Berger, R.C., et al., *Renal Effects and Underlying Molecular Mechanisms of Long-Term Salt Content Diets in Spontaneously Hypertensive Rats.* PLoS One, 2015. **10**(10): p. e0141288.

38.   Henry, C., et al., *Salt induces myocardial and renal fibrosis in normotensive and hypertensive rats.* Circulation, 1998. **98**(23): p. 2621-2628.

39.   Farquhar, W.B., et al., *Dietary sodium and health: more than just blood pressure.* J Am Coll Cardiol, 2015. **65**(10): p. 1042-50.

40.   Yatabe, M.S., et al., *Effects of a high-sodium diet on renal tubule Ca2+ transporter and claudin expression in Wistar-Kyoto rats.* BMC nephrology, 2012. **13**(1): p. 1-9.

41.   Oberleithner, H., et al., *Salt overload damages the glycocalyx sodium barrier of vascular endothelium.* Pflugers Arch, 2011. **462**(4): p. 519-28.

42.   Gates, P.E., et al., *Dietary sodium restriction rapidly improves large elastic artery compliance in older adults with systolic hypertension.* Hypertension, 2004. **44**(1): p. 35-41.

43.   Todd, A.S., et al., *Dietary salt loading impairs arterial vascular reactivity.* Am J Clin Nutr, 2010. **91**(3): p. 557-64.

44.   Whelton, P.K., et al., *Sodium, blood pressure, and cardiovascular disease.* Circulation, 2012. **126**(24): p. 2880-2889.

45.   He, F.J. and G.A. MacGregor, *Salt reduction lowers cardiovascular risk: meta-analysis of outcome trials.* Lancet, 2011. **378**(9789): p. 380-2.

46.   Mallappallil, M., et al., *Chronic kidney disease in the elderly: evaluation and management.* Clinical practice (London, England), 2014. **11**(5): p. 525.

47.   Nitta, K., et al., *Aging and chronic kidney disease.* Kidney and Blood Pressure Research, 2013. **38**(1): p. 109-120.

48.   Kithas, P.A. and M.A. Supiano, *Hypertension and chronic kidney disease in the elderly.* Advances in chronic kidney disease, 2010. **17**(4): p. 341-347.

49.   De Nicola, L., et al., *The effect of increasing age on the prognosis of non-dialysis patients with chronic kidney disease receiving stable nephrology care.* Kidney international, 2012. **82**(4): p. 482-488.

50.   Iqbal, A.M. and S.F. Jamal, *Essential hypertension.* StatPearls [Internet], 2020.

51.   Singh, S., R. Shankar, and G.P. Singh, *Prevalence and associated risk factors of hypertension: a cross-sectional study in urban Varanasi.* International journal of hypertension, 2017. **2017**.

52.   Carretero, O.A. and S. Oparil, *Essential hypertension: part I: definition and etiology.* Circulation, 2000. **101**(3): p. 329-335.

53.   Egan, B.M., Y. Zhao, and R.N. Axon, *US trends in prevalence, awareness, treatment, and control of hypertension, 1988-2008.* Jama, 2010. **303**(20): p. 2043-2050.

54.   System, U.R.D., *USRDS 2013 annual data report: atlas of chronic kidney disease and end-stage renal disease in the United States.* National Institutes of Health, National Institute of Diabetes and Digestive and Digestive and Kidney Diseases, Vol. 2014, 2013.

55.   Tedla, F., et al., *Hypertension in chronic kidney disease: navigating the evidence.* International journal of hypertension, 2011. **2011**.

56.   Van Buren, P.N. and R. Toto, *Hypertension in diabetic nephropathy: epidemiology, mechanisms, and management.* Advances in chronic kidney disease, 2011. **18**(1): p. 28-41.

57.   Pugh, D., P.J. Gallacher, and N. Dhaun, *Management of hypertension in chronic kidney disease.* Drugs, 2019. **79**(4): p. 365-379.

58.   Textor, S.C., *Renal arterial disease and hypertension.* Medical Clinics, 2017. **101**(1): p. 65-79.

59.   Hayashi, K., M. Epstein, and T. Saruta, *Altered myogenic responsiveness of the renal microvasculature in experimental hypertension.* Journal of hypertension, 1996. **14**(12): p. 1387-1401.

60.   Mori, T., et al., *High perfusion pressure accelerates renal injury in salt-sensitive hypertension.* Journal of the American Society of Nephrology, 2008. **19**(8): p. 1472-1482.

61.   Yum, V., et al., *Endoplasmic reticulum stress inhibition limits the progression of chronic kidney disease in the Dahl salt-sensitive rat.* American Journal of Physiology-Renal Physiology, 2017. **312**(1): p. F230-F244.

62.   Bidani, A.K., et al., *Protective importance of the myogenic response in the renal circulation.* Hypertension, 2009. **54**(2): p. 393-8.

63.   Loutzenhiser, R., et al., *Renal autoregulation: new perspectives regarding the protective and regulatory roles of the underlying mechanisms.* Am J Physiol Regul Integr Comp Physiol, 2006. **290**(5): p. R1153-67.

64.   Loutzenhiser, R., A. Bidani, and L. Chilton, *Renal myogenic response: kinetic attributes and physiological role.* Circulation research, 2002. **90**(12): p. 1316-1324.

65.   Loutzenhiser, R., A.K. Bidani, and X. Wang, *Systolic pressure and the myogenic response of the renal afferent arteriole.* Acta Physiologica, 2004. **181**(4): p. 407-413.

66.   Moss, N.G., T.K. Gentle, and W.J. Arendshorst, *Modulation of the myogenic mechanism: concordant effects of NO synthesis inhibition and O2− dismutation on renal autoregulation in the time and frequency domains.* American Journal of Physiology-Renal Physiology, 2016. **310**(9): p. F832-F845.

67.   *<Burke, 2014 (molecular mech of renal autoregulation.pdf>.*

68.   *<Carlsson, 1987 (The role of myogenic relaxation, adenosine and prostaglandins in human forearm reactive hyperaemia).pdf>*.

69.   Carlström, M., C.S. Wilcox, and W.J. Arendshorst, *Renal autoregulation in health and disease.* Physiological reviews, 2015. **95**(2): p. 405-511.

70.   Endlich, N., et al., *Analysis of differential gene expression in stretched podocytes: osteopontin enhances adaptation of podocytes to mechanical stress.* The FASEB Journal, 2002. **16**(13): p. 1850-1852.

71.   Ingram, A.J., et al., *Activation of mesangial cell signaling cascades in response to mechanical strain.* Kidney international, 1999. **55**(2): p. 476-485.

72.   Noble, N.A. and W.A. Border. *Angiotensin II in renal fibrosis: should TGF-beta rather than blood pressure be the therapeutic target?* in *Seminars in nephrology*. 1997.

73.   Bidani, A.K. and K.A. Griffin, *Pathophysiology of hypertensive renal damage: implications for therapy.* Hypertension, 2004. **44**(5): p. 595-601.

74.   Burke, M., et al., *Molecular mechanisms of renal blood flow autoregulation.* Curr Vasc Pharmacol, 2014. **12**(6): p. 845-58.

75.   Arendshorst, W.J. and W.H. Beierwaltes, *Renal and nephron hemodynamics in spontaneously hypertensive rats.* American Journal of Physiology-Renal Physiology, 1979. **236**(3): p. F246-F251.

76.   Griffin, K.A., et al., *Differential salt-sensitivity in the pathogenesis of renal damage in SHR and stroke prone SHR.* American journal of hypertension, 2001. **14**(4): p. 311-320.

77.   Imig, J.D., et al., *Formation and actions of 20-hydroxyeicosatetraenoic acid in rat renal arterioles.* American Journal of Physiology-Regulatory, Integrative and Comparative Physiology, 1996. **270**(1): p. R217-R227.

78.   Carlstrom, M., C.S. Wilcox, and W.J. Arendshorst, *Renal autoregulation in health and disease.* Physiol Rev, 2015. **95**(2): p. 405-511.

79.   Jernigan, N.L. and H.A. Drummond, *Myogenic vasoconstriction in mouse renal interlobar arteries: role of endogenous β and γENaC.* American Journal of Physiology-Renal Physiology, 2006. **291**(6): p. F1184-F1191.

80.   y Schnitzler, M.M., et al., *Gq-coupled receptors as mechanosensors mediating myogenic vasoconstriction.* The EMBO Journal, 2008. **27**(23): p. 3092-3103.

81.   Earley, S., B.J. Waldron, and J.E. Brayden, *Critical role for transient receptor potential channel TRPM4 in myogenic constriction of cerebral arteries.* Circulation research, 2004. **95**(9): p. 922-929.

82.   Brayden, J.E., et al., *Transient receptor potential (TRP) channels, vascular tone and autoregulation of cerebral blood flow.* Clinical and Experimental Pharmacology and Physiology, 2008. **35**(9): p. 1116-1120.

83.   Cribbs, L.L., *Vascular smooth muscle calcium channels: could "T" be a target?* Circ Res, 2001. **89**(7): p. 560-2.

84.   Hill, M.A., et al., *Arteriolar myogenic signalling mechanisms: Implications for local vascular function.* Clinical hemorheology and microcirculation, 2006. **34**(1-2): p. 67-79.

85.   Mogford, J.E., et al., *Vascular smooth muscle αvβ3 integrin mediates arteriolar vasodilation in response to RGD peptides.* Circulation Research, 1996. **79**(4): p. 821-826.

86.   Earley, S., B.J. Waldron, and J.E. Brayden, *Critical role for transient receptor potential channel TRPM4 in myogenic constriction of cerebral arteries.* Circ Res, 2004. **95**(9): p. 922-9.

87.   Sun, C.-W., et al., *Role of tyrosine kinase and PKC in the vasoconstrictor response to 20-HETE in renal arterioles.* Hypertension, 1999. **33**(1): p. 414-418.

88.   Zou, A.-P., et al., *20-HETE is an endogenous inhibitor of the large-conductance Ca (2+)-activated K+ channel in renal arterioles.* American Journal of Physiology-Regulatory, Integrative and Comparative Physiology, 1996. **270**(1): p. R228-R237.

89.   Sun, C.W., et al., *Nitric oxide-20-hydroxyeicosatetraenoic acid interaction in the regulation of K+ channel activity and vascular tone in renal arterioles.* Circ Res, 1998. **83**(11): p. 1069-79.

90.   Lange, A., et al., *20-Hydroxyeicosatetraenoic acid-induced vasoconstriction and inhibition of potassium current in cerebral vascular smooth muscle is dependent on activation of protein kinase C.* Journal of Biological Chemistry, 1997. **272**(43): p. 27345-27352.

91.   Endres, B.T., et al., *Mutation of Plekha7 attenuates salt-sensitive hypertension in the rat.* Proc Natl Acad Sci U S A, 2014. **111**(35): p. 12817-22.

92.   Loutzenhiser, R., A.K. Bidani, and X. Wang, *Systolic pressure and the myogenic response of the renal afferent arteriole.* Acta Physiol Scand, 2004. **181**(4): p. 407-13.

93.   Schnermann, J. and D.Z. Levine, *Paracrine factors in tubuloglomerular feedback: adenosine, ATP, and nitric oxide.* Annu Rev Physiol, 2003. **65**: p. 501-29.

94.   Blantz, R.C., et al., *The complex role of nitric oxide in the regulation of glomerular ultrafiltration.* Kidney Int, 2002. **61**(3): p. 782-5.

95.   Morsing, P. and A.E. Persson, *Effect of prostaglandin synthesis inhibition on the tubuloglomerular feedback control in the rat kidney.* Ren Physiol Biochem, 1992. **15**(2): p. 66-72.

96.   Roman, R.J., *P-450 metabolites of arachidonic acid in the control of cardiovascular function.* Physiol Rev, 2002. **82**(1): p. 131-85.

97.   Brock, T.G., R.W. McNish, and M. Peters-Golden, *Arachidonic acid is preferentially metabolized by cyclooxygenase-2 to prostacyclin and prostaglandin E2.* Journal of Biological Chemistry, 1999. **274**(17): p. 11660-11666.

98.   Caughey, G.E., et al., *Roles of Cyclooxygenase (COX)-1 and COX-2 in Prostanoid Production by Human Endothelial Cells: Selective Up-Regulation of Prostacyclin Synthesis by COX-2.* The Journal of Immunology, 2001. **167**(5): p. 2831-2838.

99.   Morita, I., *Distinct functions of COX-1 and COX-2.* Prostaglandins & other lipid mediators, 2002. **68**: p. 165-175.

100.   Sandoo, A., et al., *The endothelium and its role in regulating vascular tone.* The

        open cardiovascular medicine journal, 2010. **4**: p. 302.

101.   Harris, R.C., *COX-2 and the kidney.* Journal of cardiovascular pharmacology,

        2006. **47**: p. S37-S42.

102.   Komhoff, M., et al., *Localization of cyclooxygenase-1 and-2 in adult and fetal*

        human kidney: implication for renal function. American Journal of Physiology-

        Renal Physiology, 1997. **272**(4): p. F460-F468.

103.   Nantel, F., et al., *Immunolocalization of cyclooxygenase-2 in the macula densa of*

        human elderly. FEBS letters, 1999. **457**(3): p. 475-477.

104.   Adegboyega, P.A. and O. Ololade, *Immunohistochemical expression of*

        cyclooxygenase-2 in normal kidneys. Applied Immunohistochemistry &

        Molecular Morphology, 2004. **12**(1): p. 71-74.

105.   Allaj, V., C. Guo, and D. Nie, *Non-steroid anti-inflammatory drugs,*

        prostaglandins, and cancer. Cell & bioscience, 2013. **3**(1): p. 1-13.

106.   Bunting, S., S. Moncada, and J.R. Vane, *The prostacyclin-thromboxane A2*

        balance: pathophysiological and therapeutic implications. British Medical

        Bulletin, 1983. **39**(3): p. 271-276.

107.   Alexander, R.W. and K.K. Griendling, *Signal transduction in vascular smooth*

        muscle. Journal of hypertension. Supplement: official journal of the International

        Society of Hypertension, 1996. **14**(5): p. S51-4.

108.   Rucker, D. and A.S. Dhamoon, *Physiology, thromboxane A2.* StatPearls

        [Internet], 2020.

109. Davidge, S.T., *Prostaglandin H synthase and vascular function.* Circulation research, 2001. **89**(8): p. 650-660.

110. *<Burke, 2014- Molecular Mechanisms of Renal Blood Flow Autoregulation .pdf>.*

111. Chachisvilis, M., Y.-L. Zhang, and J.A. Frangos, *G protein-coupled receptors sense fluid shear stress in endothelial cells.* Proceedings of the National Academy of Sciences, 2006. **103**(42): p. 15463-15468.

112. Bucci, M., et al., *In vivo delivery of the caveolin-1 scaffolding domain inhibits nitric oxide synthesis and reduces inflammation.* Nature medicine, 2000. **6**(12): p. 1362.

113. Palmer, R.M.J., D.S. Ashton, and S. Moncada, *Vascular endothelial cells synthesize nitric oxide from L-arginine.* Nature, 1988. **333**(6174): p. 664.

114. Fleming, I. and R. Busse, *Signal transduction of eNOS activation.* Cardiovascular research, 1999. **43**(3): p. 532-541.

115. Ignarro, L.J., et al., *Activation of purified soluble guanylate cyclase by endothelium-derived relaxing factor from intrapulmonary artery and vein: stimulation by acetylcholine, bradykinin and arachidonic acid.* Journal of Pharmacology and Experimental Therapeutics, 1986. **237**(3): p. 893-900.

116. Bae, S.W., et al., *Rapid increase in endothelial nitric oxide production by bradykinin is mediated by protein kinase A signaling pathway.* Biochemical and biophysical research communications, 2003. **306**(4): p. 981-987.

117.   Harder, D.R., *Pressure-induced myogenic activation of cat cerebral arteries is dependent on intact endothelium.* Circ Res, 1987. **60**(1): p. 102-7.

118.   Hughes, J.M. and S.J. Bund, *Arterial myogenic properties of the spontaneously hypertensive rat.* Experimental physiology, 2002. **87**(5): p. 527-534.

119.   Katusic, Z.S., J.T. Shepherd, and P.M. Vanhoutte, *Endothelium-dependent contraction to stretch in canine basilar arteries.* Am J Physiol, 1987. **252**(3 Pt 2): p. H671-3.

120.   Rubanyi, G.M., *Endothelium-dependent pressure-induced contraction of isolated canine carotid arteries.* American Journal of Physiology-Heart and Circulatory Physiology, 1988. **255**(4): p. H783-H788.

121.   Kuo, L., M.J. Davis, and W.M. Chilian, *Endothelium-dependent, flow-induced dilation of isolated coronary arterioles.* American Journal of Physiology-Heart and Circulatory Physiology, 1990. **259**(4): p. H1063-H1070.

122.   Juncos, L.A., et al., *Flow modulates myogenic responses in isolated microperfused rabbit afferent arterioles via endothelium-derived nitric oxide.* J Clin Invest, 1995. **95**(6): p. 2741-8.

123.   Garcia-Roldan, J.-L. and J.A. Bevan, *Flow-induced constriction and dilation of cerebral resistance arteries.* Circulation research, 1990. **66**(5): p. 1445-1448.

124.   Huang, A., et al., *Contribution of 20-HETE to augmented myogenic constriction in coronary arteries of endothelial NO synthase knockout mice.* Hypertension, 2005. **46**(3): p. 607-13.

125.   Gschwend, S., et al., *Myogenic constriction is increased in mesenteric resistance arteries from rats with chronic heart failure: instantaneous counteraction by acute AT1 receptor blockade.* British journal of pharmacology, 2003. **139**(7): p. 1317-1325.

126.   Scotland, R.S., et al., *An Endothelium-Derived Hyperpolarizing Factor–Like Factor Moderates Myogenic Constriction of Mesenteric Resistance Arteries in the Absence of Endothelial Nitric Oxide Synthase–Derived Nitric Oxide.* Hypertension, 2001. **38**(4): p. 833-839.

127.   Chaston, D.J., et al., *Polymorphism in endothelial connexin40 enhances sensitivity to intraluminal pressure and increases arterial stiffness.* Arterioscler Thromb Vasc Biol, 2013. **33**(5): p. 962-70.

128.   Daneshtalab, N. and J.S. Smeda, *Alterations in the modulation of cerebrovascular tone and blood flow by nitric oxide synthases in SHRsp with stroke.* Cardiovascular research, 2010. **86**(1): p. 160-168.

129.   Hwa, J.J. and J.A. Bevan, *Stretch-dependent (myogenic) tone in rabbit ear resistance arteries.* American Journal of Physiology-Heart and Circulatory Physiology, 1986. **250**(1): p. H87-H95.

130.   Falcone, J.C., M.J. Davis, and G.A. Meininger, *Endothelial independence of myogenic response in isolated skeletal muscle arterioles.* American Journal of Physiology-Heart and Circulatory Physiology, 1991. **260**(1): p. H130-H135.

131.   Ferrer, M., et al., *Heterogeneity of endothelium-dependent mechanisms in different rabbit arteries.* Journal of vascular research, 1995. **32**(5): p. 339-346.

132.   Thorin, E., et al., *Human vascular endothelium heterogeneity: A comparative study of cerebral and peripheral cultured vascular endothelial cells.* Stroke, 1997. **28**(2): p. 375-381.

133.   Hill, C.E., J.K. Phillips, and S.L. Sandow, *Heterogeneous control of blood flow amongst different vascular beds.* Medicinal research reviews, 2001. **21**(1): p. 1-60.

134.   Morita, T., et al., *Mechanisms underlying impairment of endothelium-dependent relaxation by fetal bovine serum in organ-cultured rat mesenteric artery.* European journal of pharmacology, 2011. **668**(3): p. 401-406.

135.   Gao, Y.J. and R.M. Lee, *Hydrogen peroxide is an endothelium-dependent contracting factor in rat renal artery.* Br J Pharmacol, 2005. **146**(8): p. 1061-8.

136.   Rabelo, F.A.W., et al., *Nonendothelial NO blunts sympathetic response of normotensive rats but not of SHR.* Hypertension, 2001. **38**(3): p. 565-568.

137.   Wang, Z.-T., et al., *Vasorelaxant effects of cardamonin and alpinetin from Alpinia henryi K. Schum.* Journal of cardiovascular pharmacology, 2001. **37**(5): p. 596-606.

138.   Hisanobu, S., et al., *Endothelial cells modulate the vasoinhibitory effect of NKY-722, a Ca2+ channel antagonist., in canine mesenteric arteries.* European journal of pharmacology, 1991. **196**(2): p. 197-199.

139.   Gerkens, J.F., *Unclipping of two-kidney, one clip hypertensive rats produces endothelium-dependent inhibition of sympathetic vasoconstriction.* Journal of hypertension, 1989. **7**(12): p. 961-966.

140. Venugopalan, C.S., et al., *Biphasic responses of equine colonic vessel rings to vasoactive inflammatory mediators.* Autonomic and Autacoid Pharmacology, 1998. **18**(4): p. 231-238.

141. Osol, G., M. Cipolla, and S. Knutson, *A new method for mechanically denuding the endothelium of small (50–150 μm) arteries with a human hair.* Journal of Vascular Research, 1989. **26**(5): p. 320-324.

142. Juncos, L.A., et al., *Removal of endothelium-dependent relaxation by antibody and complement in afferent arterioles.* Hypertension, 1994. **23**(1 Suppl): p. I54.

143. Molina, R., A. Hidalgo, and M.J. de Boto García, *Influence of mechanical endothelium removal techniques and conservation conditions on rat aorta responses.* Methods and findings in experimental and clinical pharmacology, 1992. **14**(2): p. 91-96.

144. Ralevic, V., et al., *A new protocol for removal of the endothelium from the perfused rat hind-limb preparation.* Circulation research, 1989. **64**(6): p. 1190-1196.

145. Aronson, J.K., *Meyler's side effects of drugs: the international encyclopedia of adverse drug reactions and interactions*. 2015: Elsevier.

146. Gordon, A.C. and J.A. Myburgh, *Vasodilators and antihypertensives*, in *Oh's Intensive Care Manual*. 2014, Elsevier. p. 923-934. e2.

147. *Nifedipine.* Drugs.com.

148.   McCormack, T., T. Krause, and N. O'Flynn, *Management of hypertension in adults in primary care: NICE guideline.* Br J Gen Pract, 2012. **62**(596): p. 163-164.

149.   Coats, P., et al., *Signalling mechanisms underlying the myogenic response in human subcutaneous resistance arteries.* Cardiovascular research, 2001. **49**(4): p. 828-837.

150.   Berchtold, M.W., H. Brinkmeier, and M. Muntener, *Calcium ion in skeletal muscle: its crucial role for muscle function, plasticity, and disease.* Physiological reviews, 2000. **80**(3): p. 1215-1265.

151.   Raemsch, K.D. and J. Sommer, *Pharmacokinetics and metabolism of nifedipine.* Hypertension, 1983. **5**(4_pt_2): p. II18.

152.   Otto, J. and L. Lesko, *Protein binding of nifedipine.* Journal of pharmacy and pharmacology, 1986. **38**(5): p. 399-400.

153.   *ADALAT ® CC (nifedipine) Extended Release Tablets For Oral Use.* FDA/CDER, 2011.

154.   Snider, M.E., D.S. Nuzum, and A. Veverka, *Long-acting nifedipine in the management of the hypertensive patient.* Vascular health and risk management, 2008. **4**(6): p. 1249.

155.   Herman, T.F. and C. Santos, *First pass effect.* 2019.

156.   GRUNDY, J.S., L.A. ELIOT, and R.T. FOSTER, *Extrahepatic first-pass metabolism of nifedipine in the rat.* Biopharmaceutics & drug disposition, 1997. **18**(6): p. 509-522.

157.   Thelen, K. and J.B. Dressman, *Cytochrome P450-mediated metabolism in the human gut wall.* Journal of pharmacy and pharmacology, 2009. **61**(5): p. 541-558.

158.   Wenceslau, C.F., et al., *Guidelines for the measurement of vascular function and structure in isolated arteries and veins.* American Journal of Physiology-Heart and Circulatory Physiology, 2021. **321**(2): p. H77-H111.

159.   Lu, X. and G.S. Kassab, *Assessment of endothelial function of large, medium, and small vessels: a unified myograph.* American Journal of Physiology-Heart and Circulatory Physiology, 2011. **300**(1): p. H94-H100.

160.   Dunn, W.R., G.C. Wellman, and J.A. Bevan, *Enhanced resistance artery sensitivity to agonists under isobaric compared with isometric conditions.* American Journal of Physiology-Heart and Circulatory Physiology, 1994. **266**(1): p. H147-H155.

161.   Falloon, B.J., et al., *Comparison of small artery sensitivity and morphology in pressurized and wire-mounted preparations.* American Journal of Physiology-Heart and Circulatory Physiology, 1995. **268**(2): p. H670-H678.

162.   Jadeja, R.N., et al., *Assessing myogenic response and vasoactivity in resistance mesenteric arteries using pressure myography.* JoVE (Journal of Visualized Experiments), 2015(101): p. e50997.

163.   Solez, K. and R.H. Heptinstall, *The anatomy of the renal circulation*, in *Structure and Function of the Circulation*. 1980, Springer. p. 631-660.

164.   Leslie, S.W. and H. Sajjad, *Anatomy, abdomen and pelvis, renal artery.* 2017.

165.   Johns, E. and A. Ahmeda, *Renal circulation.* Reference Module in Biomedical Sciences. Elsevier, p. Elsevier, 2014.

166.   Kaplan, N.M. and B.F. Palmer, *Impaired renal autoregulation: implications for the genesis of hypertension and hypertension-induced renal injury.* The American journal of the medical sciences, 2001. **321**(6): p. 388-400.

167.   Carmines, P.K., E.W. Inscho, and R.C. Gensure, *Arterial pressure effects on preglomerular microvasculature of juxtamedullary nephrons.* American Journal of Physiology-Renal Physiology, 1990. **258**(1): p. F94-F102.

168.   Takenaka, T., et al., *Biophysical signals underlying myogenic responses in rat interlobular artery.* Hypertension, 1998. **32**(6): p. 1060-1065.

169.   Harder, D.R., R. Gilbert, and J.H. Lombard, *Vascular muscle cell depolarization and activation in renal arteries on elevation of transmural pressure.* American Journal of Physiology-Renal Physiology, 1987. **253**(4): p. F778-F781.

170.   Kauser, K., et al., *Inhibitors of cytochrome P-450 attenuate the myogenic response of dog renal arcuate arteries.* Circulation research, 1991. **68**(4): p. 1154-1163.

171.   Narayanan, J., et al., *Pressurization of isolated renal arteries increases inositol trisphosphate and diacylglycerol.* American Journal of Physiology-Heart and Circulatory Physiology, 1994. **266**(5): p. H1840-H1845.

172.   Juncos, L.A., et al., *Flow modulates myogenic responses in isolated microperfused rabbit afferent arterioles via endothelium-derived nitric oxide.* The Journal of clinical investigation, 1995. **95**(6): p. 2741-2748.

173.   Ito, S., L.A. Juncos, and O.A. Carretero, *Pressure-induced constriction of the afferent arteriole of spontaneously hypertensive rats.* Hypertension, 1992. **19**(2_supplement): p. II164.

174.   Ren, Y., et al., *Enhanced myogenic response in the afferent arteriole of spontaneously hypertensive rats.* American Journal of Physiology-Heart and Circulatory Physiology, 2010. **298**(6): p. H1769-H1775.

175.   Yip, K. and D. Marsh, *[Ca2+] i in rat afferent arteriole during constriction measured with confocal fluorescence microscopy.* American Journal of Physiology-Renal Physiology, 1996. **271**(5): p. F1004-F1011.

176.   Okamoto, K. and K. Aoki, *Development of a strain of spontaneously hypertensive rats.* Japanese circulation journal, 1963. **27**(3): p. 282-293.

177.   Bianchi, G., et al., *Blood pressure changes produced by kidney cross-transplantation between spontaneously hypertensive rats and normotensive rats.* Clinical science and molecular medicine, 1974. **47**(5): p. 435-448.

178.   Dickhout, J.G. and R.M. Lee, *Structural and functional analysis of small arteries from young spontaneously hypertensive rats.* Hypertension, 1997. **29**(3): p. 781-789.

179.   Kimura, G. and B.M. Brenner, *Implications of the linear pressure–natriuresis relationship and importance of sodium sensitivity in hypertension.* Journal of hypertension, 1997. **15**(10): p. 1055-1061.

180.   Yu, H.C., et al., *Salt induces myocardial and renal fibrosis in normotensive and hypertensive rats.* Circulation, 1998. **98**(23): p. 2621-2628.

181.   Reckelhoff, J.F., H. Zhang, and J.P. Granger, *Decline in renal hemodynamic function in aging SHR: role of androgens.* Hypertension, 1997. **30**(3): p. 677-681.

182.   Conrad, C.H., et al., *Myocardial fibrosis and stiffness with hypertrophy and heart failure in the spontaneously hypertensive rat.* Circulation, 1995. **91**(1): p. 161-170.

183.   Feld, L.G., et al., *Renal lesions and proteinuria in the spontaneously hypertensive rat made normotensive by treatment.* Kidney international, 1981. **20**(5): p. 606-614.

184.   Ofstad, J. and B.M. Iversen, *Glomerular and tubular damage in normotensive and hypertensive rats.* American Journal of Physiology-Renal Physiology, 2005. **288**(4): p. F665-F672.

185.   Campese, V.M., *Salt sensitivity in hypertension. Renal and cardiovascular implications.* Hypertension, 1994. **23**(4): p. 531-550.

186.   Cowley, A.W. and R.J. Roman, *The role of the kidney in hypertension.* Jama, 1996. **275**(20): p. 1581-1589.

187.   O'Bryan, G.T. and T.H. Hostetter. *The renal hemodynamic basis of diabetic nephropathy*. in *Seminars in nephrology*. 1997.

188.   Ritz, E. and S.R. Orth, *Nephropathy in patients with type 2 diabetes mellitus.* New England Journal of Medicine, 1999. **341**(15): p. 1127-1133.

189.   Hye Khan, M.A., et al., *Orally active epoxyeicosatrienoic acid analog attenuates kidney injury in hypertensive dahl salt–sensitive rat.* Hypertension, 2013. **62**(5): p. 905-913.

190. De Miguel, C., et al., *T lymphocytes mediate hypertension and kidney damage in Dahl salt-sensitive rats.* American Journal of Physiology-Regulatory, Integrative and Comparative Physiology, 2010. **298**(4): p. R1136-R1142.

191. Hayakawa, K., et al., *ER stress depresses NF-κB activation in mesangial cells through preferential induction of C/EBPβ.* Journal of the American Society of Nephrology, 2010. **21**(1): p. 73-81.

192. Rapp, J.P. and H. Dene, *Development and characteristics of inbred strains of Dahl salt-sensitive and salt-resistant rats.* Hypertension, 1985. **7**(3_pt_1): p. 340-349.

193. Cowley Jr, A.W., et al., *Brown Norway chromosome 13 confers protection from high salt to consomic Dahl S rat.* Hypertension, 2001. **37**(2): p. 456-461.

194. Harrison, R.G. and E.L. Larson, *Hybridization, introgression, and the nature of species boundaries.* Journal of Heredity, 2014. **105**(S1): p. 795-809.

195. Cowley Jr, A., et al., *Consomic rat model systems for physiological genomics.* Acta physiologica scandinavica, 2004. **181**(4): p. 585-592.

196. Huang, A., D. Sun, and A. Koller, *Endothelial dysfunction augments myogenic arteriolar constriction in hypertension.* Hypertension, 1993. **22**(6): p. 913-921.

197. Lesniewski, L.A., et al., *Decreased NO signaling leads to enhanced vasoconstrictor responsiveness in skeletal muscle arterioles of the ZDF rat prior to overt diabetes and hypertension.* American Journal of Physiology-Heart and Circulatory Physiology, 2008. **294**(4): p. H1840-H1850.

198.   Bidani, A.K., et al., *Protective importance of the myogenic response in the renal circulation.* Hypertension, 2009. **54**(2): p. 393-398.

199.   Griffin, K.A., et al., *Effects of calcium channel blockers on "dynamic" and "steady-state step" renal autoregulation.* American Journal of Physiology-Renal Physiology, 2004. **286**(6): p. F1136-F1143.

200.   Griffin, K.A., M.M. Picken, and A.K. Bidani, *Deleterious effects of calcium channel blockade on pressure transmission and glomerular injury in rat remnant kidneys.* The Journal of clinical investigation, 1995. **96**(2): p. 793-800.

201.   Burke, M., et al., *Molecular mechanisms of renal blood flow autoregulation.* Current vascular pharmacology, 2014. **12**(6): p. 845-858.

202.   Lerman, L.O., et al., *Animal models of hypertension: a scientific statement from the American Heart Association.* Hypertension, 2019. **73**(6): p. e87-e120.

203.   Mattson, D.L., et al., *Influence of diet and genetics on hypertension and renal disease in Dahl salt-sensitive rats.* Physiological genomics, 2004. **16**(2): p. 194-203.

204.   Grisk, O. and H.M. Stauss, *Frequency modulation of mesenteric and renal vascular resistance.* American Journal of Physiology-Regulatory, Integrative and Comparative Physiology, 2002.

205.   Tolbert, E.M., et al., *Onset of glomerular hypertension with aging precedes injury in the spontaneously hypertensive rat.* American Journal of Physiology-Renal Physiology, 2000. **278**(5): p. F839-F846.

206.   Weinstein, J.R. and S. Anderson, *The aging kidney: physiological changes.* Advances in chronic kidney disease, 2010. **17**(4): p. 302-307.

207.   Rafiq, K., et al., *Regression of glomerular and tubulointerstitial injuries by dietary salt reduction with combination therapy of angiotensin II receptor blocker and calcium channel blocker in Dahl salt-sensitive rats.* PloS one, 2014. **9**(9): p. e107853.

208.   Mohammed-Ali, Z., et al., *Animal models of kidney disease*, in *Animal Models for the Study of Human Disease*. 2017, Elsevier. p. 379-417.

CHAPTER 2

Enhanced Myogenic Constriction in the SHR Preglomerular Vessels is Mediated by Thromboxane A2 Synthesis

Samera Nademi, Chao Lu, and Jeffrey G. Dickhout

Copyright Permission:

The paper, "Enhanced Myogenic Constriction in the SHR Preglomerular Vessels is Mediated by Thromboxane A2 Synthesis" authors, Samera Nademi, Chao Lu, and Jeffrey G. Dickhout, is published in Frontiers in Physiology (2020). 11: p. 853. Doi: 10.3389/fphys.2020.00853 under a Creative Commons Attribution ("CC BY") license.

The current version is CC-BY, version 4.0 linked here http://creativecommons.org/licenses/by/4.0/.

This license allows:

Share — copy and redistribute the material in any medium or format,

Adapt — remix, transform, and build upon the material,

for any purpose, even commercially.

The licensor cannot revoke these freedoms as long as you follow the license terms.

Attribution — You must give appropriate credit, provide a link to the license, and indicate if changes were made. You may do so in any reasonable manner, but not in any way that suggests the licensor endorses you or your use.

No additional restrictions — You may not apply legal terms or technological measures that legally restrict others from doing anything the license permits.

Chapter Summary:

Autoregulation is a process through which blood vessels' diameters are changed to adjust to fluctuations in the systematic blood pressure. In the kidneys, autoregulation protects the delicate glomeruli capillaries from high blood pressure and occurs through a slow (tubuloglomerular feedback) and a fast (MC) process. Defective MC is associated with diabetes, chronic kidney disease, and secondary hypertension (hypertension with a known cause). Conversely, enhanced MC protects the kidneys from hypertension-induced renal injury in chronically hypertensive human and animal models. Our work was the first to show that the enhanced MC in rat models of human chronic hypertension is mediated by thromboxane A2 synthesis, independently from the endothelium. We also showed that MC is not dependent on endothelium in the preglomerular and mesenteric arteries of normotensive and hypertensive animal models. These results shed light onto the mechanism through which chronically hypertensive individuals preserve their renal function despite their high blood pressure.

Author's Contribution:

S. Nademi and J.G. Dickhout designed the study. S. Nademi and C. Lu performed the experiments, analyzed the data, and interpreted the results. SN prepared the figures and drafted the manuscript. S. Nademi and J.G. Dickhout edited and revised the manuscript. All authors approved the final version of the manuscript, contributed to the article and approved the submitted version.

Title: Enhanced Myogenic Constriction in the SHR Preglomerular Vessels is Mediated

by Thromboxane A2 Synthesis

Authors: Samera Nademi [1], Chao Lu [2], Jeffrey G. Dickhout [1, 2]

Authors' Affiliations: 1. Department of Medicine, Division of Nephrology, McMaster

University; 2. St. Joseph's Healthcare Hamilton, Hamilton, Ontario, Canada

Address Correspondence to:

Jeffrey G. Dickhout, PhD

Department of Medicine, Division of Nephrology

McMaster University and St. Joseph's Healthcare Hamilton

50 Charlton Avenue East, T-3312

Hamilton, ON, Canada, L8N 4A6

Tel: 905-522-1155 ext. 35334

Fax: 905-540-6589

Email: jdickhou@stjosham.on.ca

ABSTRACT

Background

Spontaneously Hypertensive Rats (SHR) have chronically elevated blood pressures at 30 weeks of age (systolic: 191.0 ± 1.0, diastolic: 128.8 ± 0.9). However, despite this chronic malignant hypertension, SHR kidneys remain relatively free of pathology due to having an augmented myogenic constriction (MC). We hypothesized that the enhanced MC in the SHR preglomerular vessels was due to increased prostaglandin and decreased nitric oxide (NO) synthesis, providing renal protection.

Methods

SHR and Wistar Kyoto (WKY) arcuate and mesenteric arteries were treated with indomethacin (prostaglandin synthesis inhibitor), N omega-nitro-L-arginine (L-NNA, nitric oxide synthase inhibitor), and nifedipine (L-type calcium channel blocker); and MC was measured in these vessels. The role of endothelium in MC was examined by removing endothelium from WKY and SHR preglomerular and mesenteric arteries using human hair, and measuring MC. We also studied the source of prostaglandin in the SHR by treating endothelium-removed arcuate arteries with indomethacin and furegrelate (thromboxane synthase inhibitor).

Results

MC was enhanced in the SHR preglomerular vessels but not the mesenteric arteries. Indomethacin and LNNA removed the enhanced MC in the SHR. Nifedipine also inhibited MC in both WKY and SHR arcuate and mesenteric arteries. Removing endothelium did not change MC in either arcuate or mesenteric arteries of WKY and

SHR rats; and did not remove the augmented MC in the SHR arcuate arteries. Indomethacin and furegrelate decreased MC in endothelium-removed SHR arcuate arteries and obliterated the enhanced MC in the SHR.

Conclusions

The enhanced MC in the SHR arcuate arteries was due to thromboxane A2 synthesis from the tunica media and/or adventitia layers. MC was not dependent on endothelium, but was dependent on L-type calcium channels. Nevertheless, SHR arcuate arteries displayed differential intracellular calcium signalling compared to the WKYs.

INTRODUCTION

In 1901, Bayliss observed that small resistant arteries from different vascular beds of rabbits, cats, and dogs decreased in diameter when he increased intraluminal pressure, and increased diameter with decreasing pressure. Bayliss believed that this response was "myogenic in nature," and thus later this phenomenon was termed myogenic constriction (MC) [179, 180]. MC is stretch-induced reduction in small arteriole diameters in order to regulate the amount of intraluminal blood flow [55]. In the kidneys, renal blood flow autoregulation is an important homeostatic mechanism that protects the delicate glomerular capillaries from fluctuations in the systematic blood pressure, allowing the kidneys to maintain a constant blood flow and glomerular filtration rate (GFR). MC is one of the two mechanisms through which kidneys autoregulate their blood flow (the other mechanism is tubuloglomerular feedback). The significance of MC can be realized from consequences of its' dysfunction or augmentation. Impaired MC has been observed in a variety of diseases such as diabetes, low-renin and salt-sensitive hypertensions (i.e. in African Americans), and chronic kidney disease (CKD) [58, 181, 182]. On the contrary, enhanced myogenic constriction protects the kidneys from renal injury. It has been observed that some chronically hypertensive human (i.e. essential hypertensives) and rats (i.e. spontaneously hypertensive rats, SHR) do not develop significant renal injuries despite highly elevated blood pressures. It appears that this renal protection is due to an augmented MC response in the pre-glomerular vessels [52, 62, 64-66, 183, 184]. We hypothesized that the enhanced MC found in the SHR rats is due to increased prostaglandin H2 (PGH2) and decreased nitric oxide (NO) synthesis in the endothelium

compared to their normotensive controls, Wistar Kyoto (WKY) rats. To test this hypothesis, we treated SHR and WKY arcuate and mesenteric arteries with indomethacin and N omega-nitro-L-arginine (LNNA, NO synthase inhibitor) and measured MC. We also examined the role of endothelium in the SHR enhanced MC by removing the endothelium, based on a method that was described by Osol involving the use of human hair [128], and measured MC in SHR and WKY arcuate and mesenteric arteries. We utilized both younger and older animals since the augmentation of MC in the SHR may be the result of endothelial dysfunction and we hypothesized this dysfunction would be more severe in the old animals, since they would have been exposed to elevated blood pressure for a longer period of time.

METHODS

Animal Studies. Older WKY and SHR male rats (30 to 40 weeks old) as well as younger male SHR and WKY rats (12 to 16 weeks old) were utilized for the vessel studies. Rats' blood pressure was measured using tail cuff plethysmography (Kent Scientific, CODA system) and their body weights were recorded (Table 1). All rats were bred at McMaster University Central Animal Facility and maintained at St Joseph's Healthcare Hamilton Animal Facility. All animal work was performed with McMaster University Animal Research Ethics Board's approval and in accordance with their guidelines. Animals were housed with a 12-hour light-dark cycle and had free access to food and drinking water. After *anesthetizing the rodents with isoflurane and perfusing the vasculature with* Hank's basic salt solution (HBSS) to remove blood, arcuate and

second branch mesenteric arteries were dissected out of their kidneys and mesenteries respectively to conduct vascular studies, as previously [150].

Myogenic response measurements in endothelium-intact arteries. Renal arcuate and second-branch mesenteric arteries were dissected out of their tissues and transferred into a pressure myograph chamber (PMC) containing 37^0C oxygenated HBSS. The PMC was connected to a PS-200 system and a peristaltic pump with a servo-controller to pressurize the arteries (Living Systems, Burlington VT, USA), and a Leica WILD M3C microscope and Hitachi KP-113 CCD camera to video-record the vessels. In the PMC, the arteries were mounted on a glass micropipette, a blind-sac was created, and the vessels were allowed 30 mins to equilibrate to 80 mmHg pressure (P80 mmHg) as previously described [150]. To test the functional presence of the endothelium, 3 µM phenylephrine (endothelium-independent vasoconstrictor) was added to pre-constrict the arteries followed by 10 µM carbachol (endothelium-dependent vasodilator), and the diameter-changes were recorded. The chamber was subsequently washed with HBSS and vessels were re-allowed 30 mins to equilibrate at P80 mmHg. MC was measured by increasing intraluminal pressure in 20 mmHg increments until 180 mmHg with 5-minute-intervals between each pressure change and the lumen diameters were recorded (E-intact MC). To investigate the effects of prostanoid and NO synthesis, 10 µM indomethacin and 100 µM LNNA respectively and independently were added to the PMC, the vessels were allowed 30 mins to equilibrate, and MC was measured as described. Passive diameter at each pressure point was measured by replacing HBSS with Ca^{2+}-Free HBSS containing

5mM Ca^{2+} chelator, ethylene glycol tetraacetic acid (EGTA), and re-measuring MC as aforementioned. MC measurements in this study were conducted serially in the following order: normal HBSS (control), drug-treated HBSS, and Ca^{2+}-Free HBSS (passive diameter). To investigate the dependency of MC on endothelium, the tunica intima was denuded from the arteries using a human hair.

Removing endothelium using human hair. A human hair was glued to a small petri dish and the arteries were moved through the length of the hair about 10 times, according to a method that was described by [128]. The arteries were then re-mounted in the PMC, remnant endothelium was flushed out for 5 mins with HBSS, the blind-sac was re-created, and the vessels were allowed 30 mins to equilibrate at P80 mmHg. To test the functional absence of the endothelium, 3 µM phenylephrine was added to pre-constrict the arteries followed by 10 µM carbachol and the diameter-changes were recorded. MC was then re-measured (E-removed MC) as described above.

Myogenic response measurements in endothelium-removed arteries. To investigate the effects of prostaglandin and thromboxane A synthesis on endothelium-removed vessels, 10 µM indomethacin and 100 µM furegrelate respectively and independently were added to the PMC, the vessels were allowed 30 mins to adjust, and MC was measured as previously explained. Passive diameter at each pressure point was measured at the end of each experiment by replacing HBSS with Ca^{2+}-free HBSS (5mM EGTA). Physical absence of the endothelium was further investigated.

Scanning Electron Microscopy (SEM) to ensure physical absence of endothelium. Endothelium-removed and -intact arcuate arteries were cut in half, fixed with 2% glutaraldehyde (in 0.1 M sodium cacodylate buffer), post-fixed with 2% osmium tetroxide, dehydrated with increasing ethanol concentration, critical point dried, mounted onto microscope stubs, and examined under SEM.

Data and statistical analysis. Percent diameter change was calculated by subtracting lumen diameter at each pressure point in Ca^{2+}-free HBSS ($D_{n\,(Ca2+\,free)}$) from the lumen diameter at the same pressure point in normal HBSS (D_n), divided by the diameter in Ca^{2+}-free HBSS ($D_{n\,(Ca2+\,free)}$), and multiplied by 100 (% Diameter Change $= \left(\frac{D_n - D_{n\,(Ca-Free)}}{D_{n\,(Ca-Free)}}\right) * 100$); this is illustrated in Figure 1 (A & B). Percent relaxation due to carbachol was calculated by subtracting lumen diameter at P80 mmHg after adding carbachol (D_{after}) from lumen diameter before adding carbachol (D_{before}), divided by diameter before carbachol (D_{before}), and multiplied by 100 (% Carbachol Relaxation $= \left(\frac{D_{before} - D_{after}}{D_{before}}\right) * 100$). Paired t-test was used to compare carbachol-induced responses before and after endothelium removal. Independent t-test was used to compare WKY and SHR population means. 2-way ANOVA was used to compare MC from different rat strains or treatments. If differences were found by ANOVA, post-hoc comparisons at different pressure points (Holm-Sidak post-hoc test) were conducted to determine differences in the means. Significant differences were evaluated using GraphPad prism

and 95% confidence intervals. P-values less than or equal to 0.05 were deemed statistically significant.

Reagents. The following reagents were purchased from Sigma- Aldrich: phenylephrine (P6126), carbachol (C4382), furegrelate (F3764), indomethacin (I7378), LNNA (N5501), and EGTA (E3889).

RESULTS

Effects of inhibiting PGH2 and NO synthesis on Endothelium-intact vessels derived from older rats. We used indomethacin, a non-selective cyclooxygenase (COX-1 and COX-2) inhibitor, to block PGH2 synthesis [185]. Indomethacin reduced MC in the SHR but not the WKY arcuate arteries (Figure 2 (A & B)). SHR arcuate arteries demonstrated an enhanced MC compared to the WKY arteries (Figure 2 (C)), and the augmented MC in the SHR was abolished by indomethacin treatment (Figure 2 (D)). Comparably, indomethacin decreased MC in both SHR and WKY mesenteric arteries (Figure 3 (A & B)). Nevertheless, an enhanced MC was not observed in the SHR mesenteric arteries compared to the WKY (Figure 3 (C)). Also, indomethacin-treated SHR and WKY mesenteric vessels showed similar MC (Figure 3 (D)). We also investigated the effects of blocking nitric oxide synthase (NOS) by *LNNA* on MC in the SHR and WKY rats. Similar to the indomethacin, LNNA reduced MC in the SHR arcuate arteries at P80, P160, and P180 mmHg; but did not change MC in the WKY pre-glomerular vessels (Figure 4 (A & B)). LNNA also removed the augmented MC in the

SHR arcuate arteries compared to the WKY (Figure 4 (C)). In mesenteric arteries, LNNA treatment did not change MC in either WKY or SHR, and there were no differences between WKY and SHR LNNA-treated vessels (Figure 5 (A, B, C, & D)).

Effects of inhibiting L-type calcium channels on MC in Endothelium-intact vessels. L-type Ca^{2+} channel blocker, nifedipine, significantly reduced MC in both WKY and SHR arcuate (Figure 6 (A & B)) and mesenteric arteries (Figure 7 (A & B)) of older rats. Nonetheless in older rats, nifedipine-treated SHR arcuate arteries showed significantly more MC compared to the WKY arcuate arteries (Figure 6 (C)) at P140 to P180 mmHg; this difference was not observed in the SHR and WKY mesenteric arteries (Figure 7 (C)). Further, we also investigated the effects of nifedipine in arcuate arteries from younger WKY and SHR rats (12-16 weeks old). Similar to the older rats (30-40 weeks old), nifedipine blocked MC in both WKY and SHR arcuate arteries of the younger rats (Figure 8 (A & B)). However, there were no differences between nifedipine-treated WKY and SHR arcuate arteries (Figure 8 (C)).

Endothelium was successfully removed using human hair. SEM micrographs showed complete physical absence of the endothelium in WKY arcuate arteries. The endothelium was oriented longitudinally, whereas the smooth muscle cell (SMC) layer was oriented cross-sectionally (Figure 9 (A)). In response to carbachol, WKY and SHR pre-constricted arcuate arteries (by 3 µM phenylephrine) showed almost no relaxation to 10 µM carbachol after removing the endothelium. WKY endothelium-intact arcuate

vessels relaxed significantly more than SHR endothelium-intact vessels (Figure 9 (B)). Pre-constricted mesenteric arteries (by 3 µM phenylephrine) in WKY and SHR also showed lack of relaxation to 10 µM carbachol after removing the endothelium. There were no statistically significant differences between WKY and SHR endothelium-intact carbachol-induced relaxation (Figure 9 (C)).

Effects of removing endothelium on myogenic constriction in the WKY and SHR. Removing endothelium did not change MC in the WKY and SHR arcuate (Figure 10 (A & B)) and mesenteric arteries (Figure 11 (A & B)). Moreover, SHR endothelium-intact arcuate arteries demonstrated enhanced MC compared to the WKY endothelium-intact arcuate arteries at P140 to P180 mmHg (Figure 10 (C)), but this enhancement was absent in the SHR mesenteric arteries (Figure 11 (C)). Denuding endothelium did not remove the augmented MC in the SHR arcuate arteries (Figure 10 (D)). Furthermore, MC was similar in endothelium -removed WKY and SHR mesenteric arcades (Figure 11 (D)).

Effects of inhibiting prostaglandin H2 and Thromboxane A2 synthesis in endothelium-removed arcuate arteries of younger SHRs. Similar to the older rats (30-40 weeks old), arcuate arteries of younger SHR rats (12-16 weeks old) showed enhanced MC at P140, P160, and P180 mmHg (Figure 12 (A)). Inhibiting prostaglandin H2 synthesis by indomethacin in endothelium-removed arcuate arteries significantly decreased MC at P160 and P180 mmHg in the SHR (compared to both E-intact and E-removed vessels), but did not change MC in the WKY (Figure 12 (B & C)). **Similarly,**

inhibiting thromboxane A2 synthesis by furegrelate in endothelium-removed arcuate arteries also significantly decreased MC at P120 to P180 mmHg (compared to both E-intact and E-removed vessels), but did not change MC in the WKY (Figure 12 (D & E)). There were no differences in endothelium-removed arcuate arteries that had been treated with indomethacin or furegrelate in either WKY or SHR (Figure 12 (F & G)).

MC was still enhanced in endothelium-removed SHR arcuate arteries compare to endothelium-removed WKY arcuate arteries (Figure 13 (A)). Treating SHR endothelium-removed preglomerular arteries with indomethacin and furegrelate obliterated the enhanced MC in these vessels compared to the WKY arcuate arteries (Figure 13 (B & C)).

DISCUSSION

We observed an augmented MC in the SHR pre-glomerular arteries compared to the WKY pre-glomerular arteries (Figure (2C, 4C, 10C, & 12 A)). This augmented MC was absent in the SHR mesenteric vessels (Figure (3C, 5C, & 11C)). This occurred regardless of age (present in both younger and older SHR). We also found that inhibiting prostaglandin synthesis (by indomethacin) obliterated the enhanced MC that was observed in the SHR preglomerular arteries (Figure (2D)) by reducing MC in these vessels (Figure (2B)). L-type Ca^{2+} channel blocker, nifedipine, reduced MC in all vessels (Figure (6A, 6B, 7A, 7B, 8A, & 8B)), although SHR arcuate arteries of older rats showed more myogenic tone than WKY arcuate arteries after treating with nifedipine (Figure

(6C)). Our work showed that MC in WKY and SHR arcuate and mesenteric arteries is independent of endothelium as removing endothelium did not change MC (Figure (10A, 10B, 11A, & 11B)). As well, removing endothelium did not eradicate the enhanced MC in the SHR preglomerular vessels (Figure (10D)), suggesting that this augmentation is endothelium-independent. Our results also showed that indomethacin (prostaglandin H2 synthesis inhibitor) and furegrelate (thromboxane A2 synthase inhibitor) abolished the enhanced MC in the SHR independently from endothelium (Figure (12C & 12E)) suggesting that the source of thromboxane A2 synthesis in the SHR pre-glomerular arteries is the tunica media and/or adventitia layers, and not the endothelium (Figure (14)). In omental arteries, thromboxane synthase has been found in both the tunica media and adventitia layers in both normal and preeclamptic women [186]. This is the first study, to our knowledge, to show that MC is independent of endothelium in arcuate and mesenteric arteries of WKY and SHR rats. We were also the first to show that the enhanced MC in the SHR arcuate arteries was due to increased thromboxane A2 synthesis.

The enhanced myogenic constriction in the SHR. Several studies investigated the reason for the observed enhanced MC during chronic hypertension in different vascular beds. Huang and Koller (1993) examined WKY and SHR cremaster muscle arteriole responses to indomethacin (PGH2 synthesis inhibitor) and SQ 29,548 (PGH2 receptor blocker), as well as the effects of endothelium removal. Contrary to our results, they suggested that increased PGH2 production from endothelium was responsible for the

observed enhanced MC in the SHR cremaster muscle arterioles [166]. This could be because different vascular beds display different vasoactive mechanisms in the endothelium and vascular SMCs [118-120]. Other studies conducted in skeletal muscle arterioles and aorta showed that in hypertension, endothelium synthesizes endothelin [187-189] and TxA2 (formed from PGH2) [190, 191] which increase sensitivity of smooth muscle contractile apparatus, inducing greater contractions in response to similar raise in intracellular calcium in the SHR SMC layer compared to the Wistar Rats (WR) [191]. This is consistent with our findings that also suggest a heightened intracellular calcium response in the SHR preglomerular arteries versus the WKY, as nifedipine-treated SHR vessels showed higher myogenic tone compared to the WKY nifedipine-treated vessels (Figure (6C)). This enhanced sensitivity of SHR pre-glomerular arteries to intracellular calcium-rise may be due to activation of Rho-kinase pathway in SMCs [192, 193]. Moreover, diminished NO signaling in skeletal muscle arterioles of hypertensive rats (i.e. Zucker Diabetic Fatty rats) has been shown to contribute to the exaggerated MC [194], which is contrary to our finding that NO synthesis may have a small constrictor effect on the SHR arcuate arteries at high intraluminal pressures (P160 and P180 mmHg) (Figure (4B)). NO is predominantly produced by the endothelium and is very unstable with a half-life of seconds [195-197]. After being produced, NO can rapidly react with oxygen species $(O_2, O_2^- \text{ and } H_2O_2)$ and thiol groups to produce nitrite, nitrate, peroxynitrite (ONOO), and nitrosothiols. The effects of NO on vessels can be mediated by the potential presence of thiol and oxygen species [196, 198]. The small vasoconstrictor effects of NO (at high intraluminal pressures) that was observed in this

study may be due to the reaction of NO with superoxide to create peroxynitrite in the

SHR vessels [199] and thereby augmenting constrictor responses [200]. The resulting

peroxynitrite may promote the release of TXA2 leading to arteriolar constriction, as was

shown in gracilis muscle arterioles of hyperhomocysteinemia (induced by methionine

diet) mouse model [200]. As well, in rat models of high-fat high-sucrose (HFHS) and

levothyroxine (L-T$_4$) diets, endothelium-denuded thoracic aortic rings from HFHS+LT$_4$

rats showed stronger vasoconstriction than HFHS rats due to increase NO and superoxide

production that led to peroxynitrite formation, independent from the endothelium [201].

Other contributing mechanisms to the enhanced MC have also been reported such as

increased superoxide generation through activation of Nicotinamide Adenine

Dinucleotide Phosphate (NADPH) oxidase in afferent arterioles [202]; increased

activation of angiotensin II type 1 receptor in cremaster muscle arteries [203]; and

increased production of 20-hydroxyeicosatrienoic acid (20-HETE) through activation of

cytochrome P450 in afferent and cerebral arterioles [66, 204-206]. Consistent with our

observation of an augmented MC in the SHR arcuate arteries, Imig and his colleagues, in

1993, found an enhanced MC in the SHR (4 week-old prehypertensive SHRs)

interlobular as well as proximal and distal portions of the afferent arterioles of

juxtamedullary glomeruli. The researchers also discovered that inhibiting cytochrome P-

450 enzyme (with ketoconazole or 7-ethoxyresorufin) had variable effects in different

segments of the preglomerular arteries. In interlobular, proximal afferent, and distal

afferent arterioles, inhibiting cytochrome P-450 did not remove, removed, and partially

removed the enhanced MC in the SHR arterioles, respectively, compared to the WKY

arteries [204]. These findings suggest that cytochrome P-450 metabolites of arachidonic acid have a critical role in the enhanced MC in the SHR preglomerular vessels [66]. To investigate if the enhanced MC in the SHR vessels is endothelium-dependent, we removed the endothelium using human hair.

Removing the endothelium. Endothelium can be removed from blood vessels by chemical or physical means. Chemical methods include using collagenase, elastase, or antibodies. Collagenase and elastase are enzymes that dissolve intercellular matrix between endothelium, but might also damage the vascular SMC layer [128]. Antibodies against specific endothelial antigens may also not completely remove the endothelium [207]. Physical methods of denuding endothelium involve abrading the inner surface of the vessel by an applicator such as cotton, filter paper [130], wood, wire, air bolus, or human hair; most of which are fragile or difficult to apply to small arteries [128] such as pregomerular vessels. Air bolus injections also are appropriate methods for large arteries, but may not completely remove the endothelium in small arterioles [131]. In 1989, Osol et al. suggested an effective method for removing endothelium from small arteries involving human hair, which provided sufficient degree of abrasion to damage the endothelium but not the vascular SMC layer. After reviewing the aforementioned methods, we decided to use human hair to mechanically abrade endothelium from preglomerular and mesenteric arteries in order to investigate the role of endothelium on MC.

Role of endothelium in MC. Even though MC is essential in renal autoregulation, its dependency on endothelium is controversial. Studies in different species and tissues have reported that endothelium removal abolished [104-108], enhanced [109-114], reduced [111], or did not change [113, 115-117] MC. This controversy may be because endothelial cells can release different vasoactive substances in variable quantities in different vascular beds or even different sections of the same vascular bed [118-120]. Thus, it is important to investigate the function of endothelium in different vascular beds. In rabbit afferent arterioles, Juncos and his colleagues reported that removing endothelium enhanced MC in free-flow vessels but did not change MC in no-flow arteries. Nevertheless, the authors used factor VIII-related antigen antibodies which did not completely remove the endothelium, revealed in their transmission electron micrographs [207]. Another study conducted by Harder demonstrated a dependency of MC on endothelium in cat cerebral arteries. Harder subjected these arteries to 40 to 60 mmHg pressure and recorded a depolarization of 0.35 mV/mmHg, which was abolished when he removed the endothelium [104]. In mesenteric arteries, endothelial cells may have roles in MC under hypoxic conditions. Earley and Walker exposed Sprague-Dawley rats to chronic hypoxia and found that myogenic responsiveness in their mesenteric arteries was abolished. This obliteration was restored by removing the endothelium [208].

NSAIDs in hypertension and CKD. Non-steroidal anti-inflammatory drugs (NSAIDs) are a class of drugs that block prostaglandins synthesis by inhibiting COX-1 and COX-2 enzymes. While healthy people rarely have adverse renal side effects upon

using NSAIDs, individuals (particularly elderly patients) who have hypertension and CKD may develop acute kidney failure [209]. In fact, administering indomethacin to renal failure rat models (Sprague–Dawley rats that have been administered adenine to have chronic renal failure) significantly decreased their survival rate [210]. Every year, about 2.5 million Americans who use NSAIDs experience renal-related side effects [211].

CONCLUSIONS

MC is augmented in the SHR preglomerular arteries but not the mesenteric arteries, compared to the WKY respective vessels. The augmented MC in the SHR pre-glomerular vessels appears to be due to increased prostanoid production, particularly TXA2 synthesis, from the tunica media and/or adventitia layers. Moreover, MC is not dependent on the endothelium in the WKY and SHR pre-glomerular and mesenteric arteries, as removing endothelium did not change the MC. L-type Ca^{2+} channels are critical to MC as inhibiting them tremendously decreases MC in both WKY and SHR arcuate and mesenteric arteries. Nevertheless, SHR pre-glomerular arteries seem to have a differential intracellular Ca^{2+} signaling at higher intraluminal pressures (P140-P180 mmHg) compared to the WKY vessels.

ACKNOWLEDGEMENTS

DISCLOSURES

Authors declare no conflict of interest.

AUTHOR CONTRIBUTIONS

SN and CL performed experiments, analyzed data, and interpreted results. SN prepared figures and drafted manuscript. SN and JD edited and revised manuscript. SN, CL, and JD approved final version of manuscript. JD conceived and designed research.

REFERENCES

1.   Sabolić, I., et al., *The AQP2 water channel: effect of vasopressin treatment, microtubule disruption, and distribution in neonatal rats.* The Journal of membrane biology, 1995. **143**(3): p. 165-175.

2.   Bayliss, W.M., *On the local reactions of the arterial wall to changes of internal pressure.* The Journal of physiology, 1902. **28**(3): p. 220-231.

3.   Kaplan, N.M. and B.F. Palmer, *Impaired renal autoregulation: implications for the genesis of hypertension and hypertension-induced renal injury.* The American journal of the medical sciences, 2001. **321**(6): p. 388-400.

4.   Le Goff, X., et al., *Aggregation dynamics and identification of aggregation-prone mutants of the von Hippel-Lindau tumor suppressor protein.* J Cell Sci, 2016. **129**(13): p. 2638-50.

5.   Atala, A., *Re: A Structured Interdomain Linker Directs Self-Polymerization of Human Uromodulin.* J Urol, 2016. **196**(3): p. 958.

6.   Carlström, M., C.S. Wilcox, and W.J. Arendshorst, *Renal autoregulation in health and disease.* Physiological reviews, 2015. **95**(2): p. 405-511.

7.   Loutzenhiser, R., A. Bidani, and L. Chilton, *Renal myogenic response: kinetic attributes and physiological role.* Circulation research, 2002. **90**(12): p. 1316-1324.

8.   Loutzenhiser, R., A. Bidani, and X. Wang, *Systolic pressure and the myogenic response of the renal afferent arteriole.* Acta physiologica Scandinavica, 2004. **181**(4): p. 407-413.

9.   Loutzenhiser, R., K.A. Griffin, and A.K. Bidani, *Systolic blood pressure as the trigger for the renal myogenic response: protective or autoregulatory?* Current opinion in nephrology and hypertension, 2006. **15**(1): p. 41-49.

10.   Arendshorst, W.J. and W.H. Beierwaltes, *Renal and nephron hemodynamics in spontaneously hypertensive rats.* American Journal of Physiology-Renal Physiology, 1979. **236**(3): p. F246-F251.

11.   Griffin, K.A., et al., *Differential salt-sensitivity in the pathogenesis of renal damage in SHR and stroke prone SHR.* American journal of hypertension, 2001. **14**(4): p. 311-320.

12.   Bidani, A.K. and K.A. Griffin, *Pathophysiology of hypertensive renal damage: implications for therapy.* Hypertension, 2004. **44**(5): p. 595-601.

13.   Imig, J.D., et al., *Formation and actions of 20-hydroxyeicosatetraenoic acid in rat renal arterioles.* American Journal of Physiology-Regulatory, Integrative and Comparative Physiology, 1996. **270**(1): p. R217-R227.

14.   Osol, G., M. Cipolla, and S. Knutson, *A new method for mechanically denuding the endothelium of small (50–150 μm) arteries with a human hair.* Journal of Vascular Research, 1989. **26**(5): p. 320-324.

15.   Dickhout, J.G. and R.M. Lee, *Structural and functional analysis of small arteries from young spontaneously hypertensive rats.* Hypertension, 1997. **29**(3): p. 781-789.

16.   Lucas, S., *The pharmacology of indomethacin.* Headache: The Journal of Head and Face Pain, 2016. **56**(2): p. 436-446.

17.   Mousa, A.A., J.F. Strauss III, and S.W. Walsh, *Reduced methylation of the thromboxane synthase gene is correlated with its increased vascular expression in preeclampsia.* Hypertension, 2012. **59**(6): p. 1249-1255.

18.   Huang, A., D. Sun, and A. Koller, *Endothelial dysfunction augments myogenic arteriolar constriction in hypertension.* Hypertension, 1993. **22**(6): p. 913-921.

19.   Ferrer, M., et al., *Heterogeneity of endothelium-dependent mechanisms in different rabbit arteries.* Journal of vascular research, 1995. **32**(5): p. 339-346.

20.   Thorin, E., et al., *Human vascular endothelium heterogeneity: A comparative study of cerebral and peripheral cultured vascular endothelial cells.* Stroke, 1997. **28**(2): p. 375-381.

21.   Hill, C.E., J.K. Phillips, and S.L. Sandow, *Heterogeneous control of blood flow amongst different vascular beds.* Medicinal research reviews, 2001. **21**(1): p. 1-60.

22.   Lemne, C.E., et al., *Increased basal concentrations of plasma endothelin in borderline hypertension.* Journal of hypertension, 1994. **12**(9): p. 1069-1074.

23.   Schiffrin, E.L., et al., *Enhanced expression of endothelin-1 gene in resistance arteries in severe human essential hypertension.* Journal of hypertension, 1997. **15**(1): p. 57-63.

24.   Schiffrin, E.L. and G.E.L. Thibault, *Plasma endothelin in human essential hypertension.* American journal of hypertension, 1991. **4**(4_Pt_1): p. 303-308.

25.   Mayhan, W.G., *Role of prostaglandin H2-thromboxane A2 in responses of cerebral arterioles during chronic hypertension.* American Journal of Physiology-Heart and Circulatory Physiology, 1992. **262**(2): p. H539-H543.

26.   Ungvari, Z. and A. Koller, *Endothelin and prostaglandin H2/thromboxane A2 enhance myogenic constriction in hypertension by increasing Ca2+ sensitivity of arteriolar smooth muscle.* Hypertension, 2000. **36**(5): p. 856-861.

27.   Homma, K., et al., *Rho-kinase Contributes to Pressure-induced Constriction ofRenal Microvessels.* The Keio journal of medicine, 2013.

28.   Uehata, M., et al., *Calcium sensitization of smooth muscle mediated by a Rho-associated protein kinase in hypertension.* Nature, 1997. **389**(6654): p. 990.

29.   Lesniewski, L.A., et al., *Decreased NO signaling leads to enhanced vasoconstrictor responsiveness in skeletal muscle arterioles of the ZDF rat prior to overt diabetes and hypertension.* Am J Physiol Heart Circ Physiol, 2008. **294**(4): p. H1840-50.

30.   Schini, V., *The L-Arginine-Nitric Oxide Pathway in the Vascular Smooth Muscle: Regulation and Pathophysiological Significance*, in *Vascular Endothelium*. 1996, Springer. p. 320-320.

31.   Jeremy, J.Y., et al., *Nitric oxide and the proliferation of vascular smooth muscle cells.* Cardiovascular research, 1999. **43**(3): p. 580-594.

32.   Butler, A.R., F.W. Flitney, and D.L.H. Williams, *NO, nitrosonium ions, nitroxide ions, nitrosothiols and iron-nitrosyls in biology: a chemist's perspective.* Trends in pharmacological sciences, 1995. **16**(1): p. 18-22.

33.   Darley-Usmar, V., H. Wiseman, and B. Halliwell, *Nitric oxide and oxygen radicals: a question of balance.* FEBS letters, 1995. **369**(2-3): p. 131-135.

34.   Carlisle, R.E., et al., *Endoplasmic reticulum stress inhibition reduces hypertension through the preservation of resistance blood vessel structure and function.* J Hypertens, 2016. **34**(8): p. 1556-69.

35.   Bagi, Z., Z. Ungvari, and A. Koller, *Xanthine oxidase–derived reactive oxygen species convert flow-induced arteriolar dilation to constriction in hyperhomocysteinemia: possible role of peroxynitrite.* Arteriosclerosis, thrombosis, and vascular biology, 2002. **22**(1): p. 28-33.

36.   Hu, D., et al., *Thyroid hormone exacerbates vasoconstriction in insulin resistance: The role of ONOO−.* European journal of pharmacology, 2014. **730**: p. 41-50.

37.   Ren, Y., et al., *Enhanced myogenic response in the afferent arteriole of spontaneously hypertensive rats.* American Journal of Physiology-Heart and Circulatory Physiology, 2010. **298**(6): p. H1769-H1775.

38.   Hong, K., et al., *Angiotensin II Type 1 Receptor Mechanoactivation Involves RGS5 (Regulator of G Protein Signaling 5) in Skeletal Muscle Arteries: Impaired Trafficking of RGS5 in Hypertension.* Hypertension, 2017. **70**(6): p. 1264-1272.

39.   Imig, J.D., et al., *Elevated renovascular tone in young spontaneously hypertensive rats. Role of cytochrome P-450.* Hypertension, 1993. **22**(3): p. 357-364.

40.   Imig, J.D., et al., *Cytochrome P-450 inhibitors alter afferent arteriolar responses to elevations in pressure.* American Journal of Physiology-Heart and Circulatory Physiology, 1994. **266**(5): p. H1879-H1885.

41.   Szarka, N., et al., *Hypertension-induced enhanced myogenic constriction of cerebral arteries is preserved after traumatic brain injury.* Journal of neurotrauma, 2017. **34**(14): p. 2315-2319.

42.   Juncos, L.A., et al., *Flow modulates myogenic responses in isolated microperfused rabbit afferent arterioles via endothelium-derived nitric oxide.* The Journal of clinical investigation, 1995. **95**(6): p. 2741-2748.

43.   Molina, R., A. Hidalgo, and M.J. de Boto García, *Influence of mechanical endothelium removal techniques and conservation conditions on rat aorta responses.* Methods and findings in experimental and clinical pharmacology, 1992. **14**(2): p. 91-96.

44.   Ralevic, V., et al., *A new protocol for removal of the endothelium from the perfused rat hind-limb preparation.* Circulation research, 1989. **64**(6): p. 1190-1196.

45.   Harder, D.R., *Pressure-induced myogenic activation of cat cerebral arteries is dependent on intact endothelium.* Circ Res, 1987. **60**(1): p. 102-7.

46.   Hughes, J.M. and S.J. Bund, *Arterial myogenic properties of the spontaneously hypertensive rat.* Experimental physiology, 2002. **87**(5): p. 527-534.

47.   Katusic, Z.S., J.T. Shepherd, and P.M. Vanhoutte, *Endothelium-dependent contraction to stretch in canine basilar arteries.* Am J Physiol, 1987. **252**(3 Pt 2): p. H671-3.

48.   Rubanyi, G.M., *Endothelium-dependent pressure-induced contraction of isolated canine carotid arteries.* American Journal of Physiology-Heart and Circulatory Physiology, 1988. **255**(4): p. H783-H788.

49.   Kuo, L., M.J. Davis, and W.M. Chilian, *Endothelium-dependent, flow-induced dilation of isolated coronary arterioles.* American Journal of Physiology-Heart and Circulatory Physiology, 1990. **259**(4): p. H1063-H1070.

50.   Juncos, L.A., et al., *Flow modulates myogenic responses in isolated microperfused rabbit afferent arterioles via endothelium-derived nitric oxide.* J Clin Invest, 1995. **95**(6): p. 2741-8.

51.   Garcia-Roldan, J.-L. and J.A. Bevan, *Flow-induced constriction and dilation of cerebral resistance arteries.* Circulation research, 1990. **66**(5): p. 1445-1448.

52.   Huang, A., et al., *Contribution of 20-HETE to augmented myogenic constriction in coronary arteries of endothelial NO synthase knockout mice.* Hypertension, 2005. **46**(3): p. 607-13.

53.   Gschwend, S., et al., *Myogenic constriction is increased in mesenteric resistance arteries from rats with chronic heart failure: instantaneous counteraction by acute AT1 receptor blockade.* British journal of pharmacology, 2003. **139**(7): p. 1317-1325.

54.   Scotland, R.S., et al., *An Endothelium-Derived Hyperpolarizing Factor–Like Factor Moderates Myogenic Constriction of Mesenteric Resistance Arteries in the Absence of Endothelial Nitric Oxide Synthase–Derived Nitric Oxide.* Hypertension, 2001. **38**(4): p. 833-839.

55.   Chaston, D.J., et al., *Polymorphism in endothelial connexin40 enhances sensitivity to intraluminal pressure and increases arterial stiffness.* Arterioscler Thromb Vasc Biol, 2013. **33**(5): p. 962-70.

56.   Daneshtalab, N. and J.S. Smeda, *Alterations in the modulation of cerebrovascular tone and blood flow by nitric oxide synthases in SHRsp with stroke.* Cardiovascular research, 2010. **86**(1): p. 160-168.

57.   Hwa, J.J. and J.A. Bevan, *Stretch-dependent (myogenic) tone in rabbit ear resistance arteries.* American Journal of Physiology-Heart and Circulatory Physiology, 1986. **250**(1): p. H87-H95.

58.   Falcone, J.C., M.J. Davis, and G.A. Meininger, *Endothelial independence of myogenic response in isolated skeletal muscle arterioles.* American Journal of Physiology-Heart and Circulatory Physiology, 1991. **260**(1): p. H130-H135.

59.   Earley, S. and B.R. Walker, *Endothelium-dependent blunting of myogenic responsiveness after chronic hypoxia.* American Journal of Physiology-Heart and Circulatory Physiology, 2002. **283**(6): p. H2202-H2209.

60.   Hörl, W.H., *Nonsteroidal anti-inflammatory drugs and the kidney.* Pharmaceuticals, 2010. **3**(7): p. 2291-2321.

61.   Kadowaki, D., et al., *Effect of acetaminophen on the progression of renal damage in adenine induced renal failure model rats.* Life sciences, 2012. **91**(25-26): p. 1304-1308.

62.   Sandhu, G.K. and C.A. Heyneman, *Nephrotoxic potential of selective cyclooxygenase-2 inhibitors.* Annals of Pharmacotherapy, 2004. **38**(4): p. 700-704.
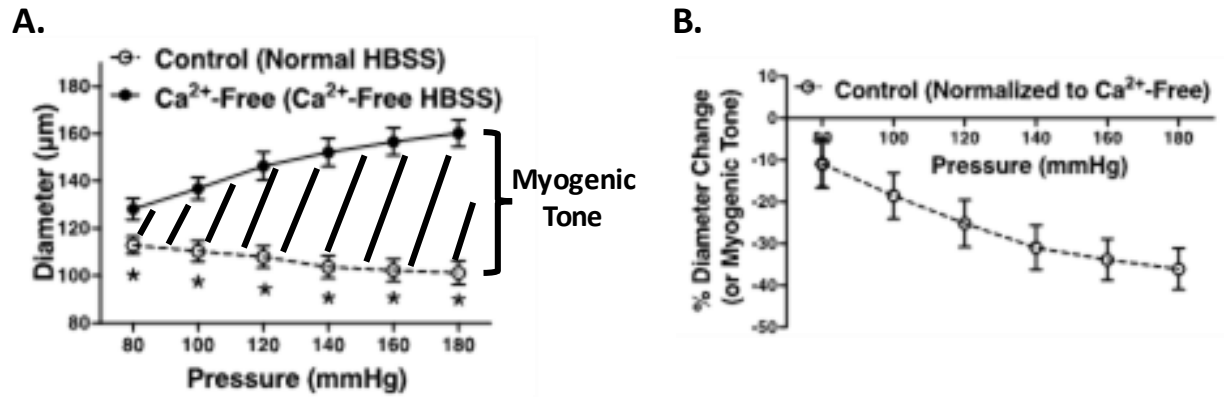
Figure 1.

Figure 1. Demonstration of how figures in this manuscript were generated. A) Vessel diameters were recorded at different intraluminal pressures (P80 to P180 mmHg) in the presence of normal HBSS (control) or calcium (Ca^{2+})-free HBSS. The area in between the two graphs (graph of normal HBSS and Ca^{2+}-free HBSS) represents myogenic tone. **B)** Myogenic tone was calculated as percent diameter change by subtracting lumen diameter at each pressure point in Ca^{2+}-free HBSS ($D_{n\,(Ca2+\,free)}$) from the lumen diameter at the same pressure point in normal HBSS (D_n), divided by the diameter in Ca^{2+}-free HBSS ($D_{n\,(Ca2+\,free)}$), and multiplied by 100 (% Diameter Change $= \left(\frac{D_n - D_{n\,(Ca-Free)}}{D_{n\,(Ca-Free)}}\right) * 100$). Two-way ANOVA and Holm-Sidak post-hoc test were used to assess significance between two population means at each pressure point; denoted by "*", $P \leq 0.05$. Graphs were made using WKY arcuate arteries. $N_{WKY} = 5$, $n_{WKY} = 5$ ("N": number of vessels, "n": number of animals).
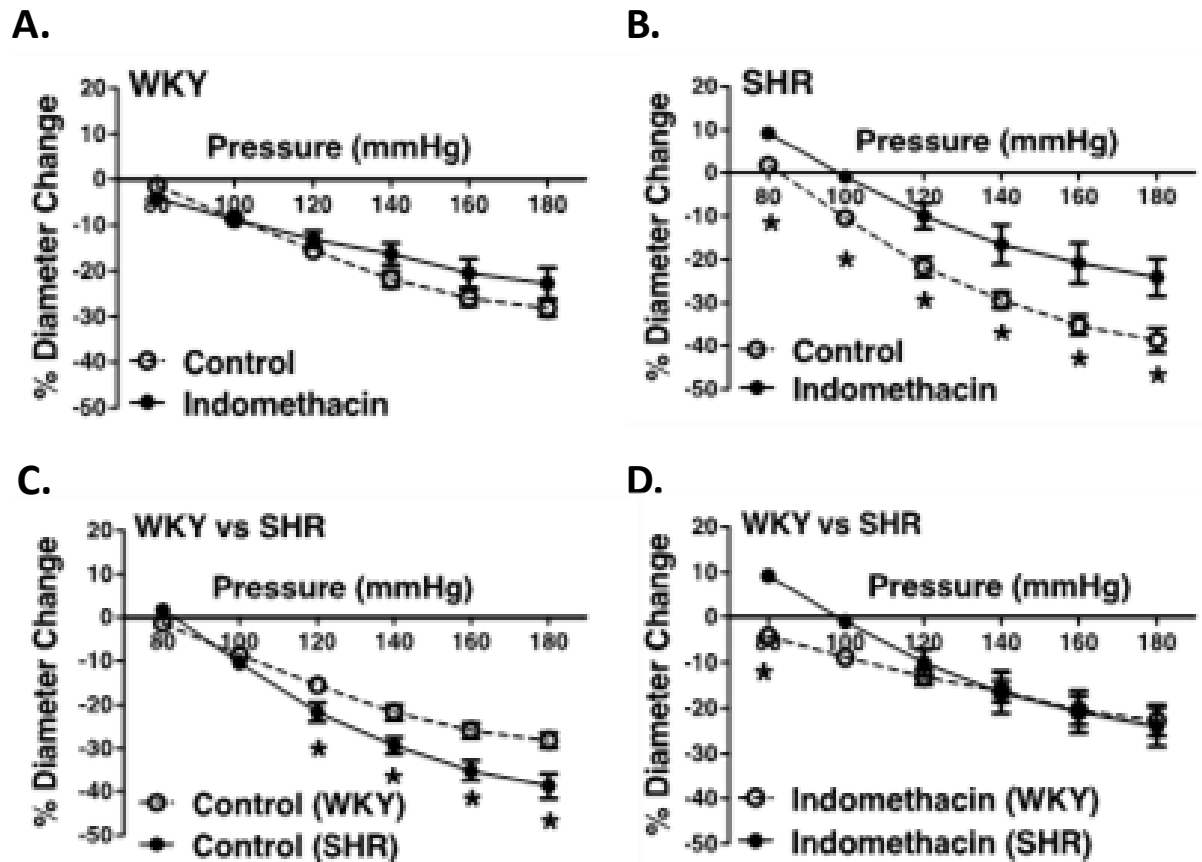
Figure 2.

Figure 2. Effects of inhibiting cyclooxygenase 1 and 2 (prostaglandin H2 synthesis) in WKY and SHR preglomerular arteries (30-40 weeks-old rats). A) Effect of indomethacin (10 µM) on WKY arcuate artery myogenic constriction (MC). **B)** Effect of indomethacin (10 µM)   on SHR arcuate artery MC. **C)** Comparison of MC between WKY and SHR arcuate arteries. **D)** Comparison of MC between WKY and SHR arcuate arteries that were treated with 10 µM indomethacin. Two-way ANOVA and Holm-Sidak post-hoc test were used to assess significance; denoted by "*", $P \leq 0.05$. $N_{WKY} = 9$, $N_{SHR} = 5$, $n_{WKY} = 7$, $n_{SHR} = 5$ ("N": number of vessels, "n": number of animals).
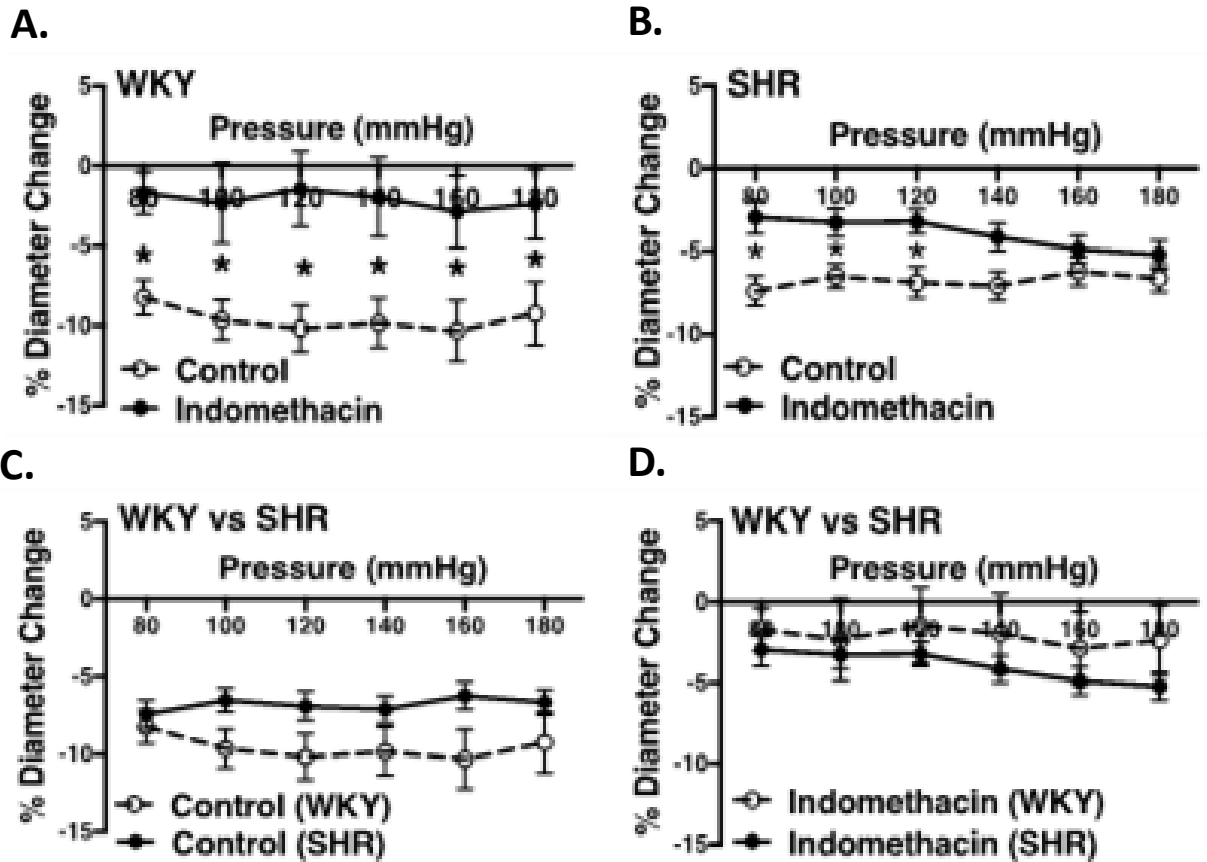
Figure 3.

Figure 3. Effects of inhibiting cyclooxygenase 1 and 2 (prostaglandin H2 synthesis) in WKY and SHR mesenteric arteries (30-40 weeks-old rats). **A)** Effect of indomethacin (10 μM) on WKY mesenteric artery myogenic constriction (MC). **B)** Effect of indomethacin (10 μM) on SHR mesenteric artery MC. **C)** Comparison of MC between WKY and SHR mesenteric arteries. **D)** Comparison of MC between WKY and SHR mesenteric arteries that were treated with 10 μM indomethacin. Two-way ANOVA and Holm-Sidak post-hoc test were used to assess significance; denoted by "*", $P \leq 0.05$. $N_{WKY} = 8$, $N_{SHR} = 17$, $n_{WKY} = 5$, $n_{SHR} = 6$ ("N": number of vessels, "n": number of animals).
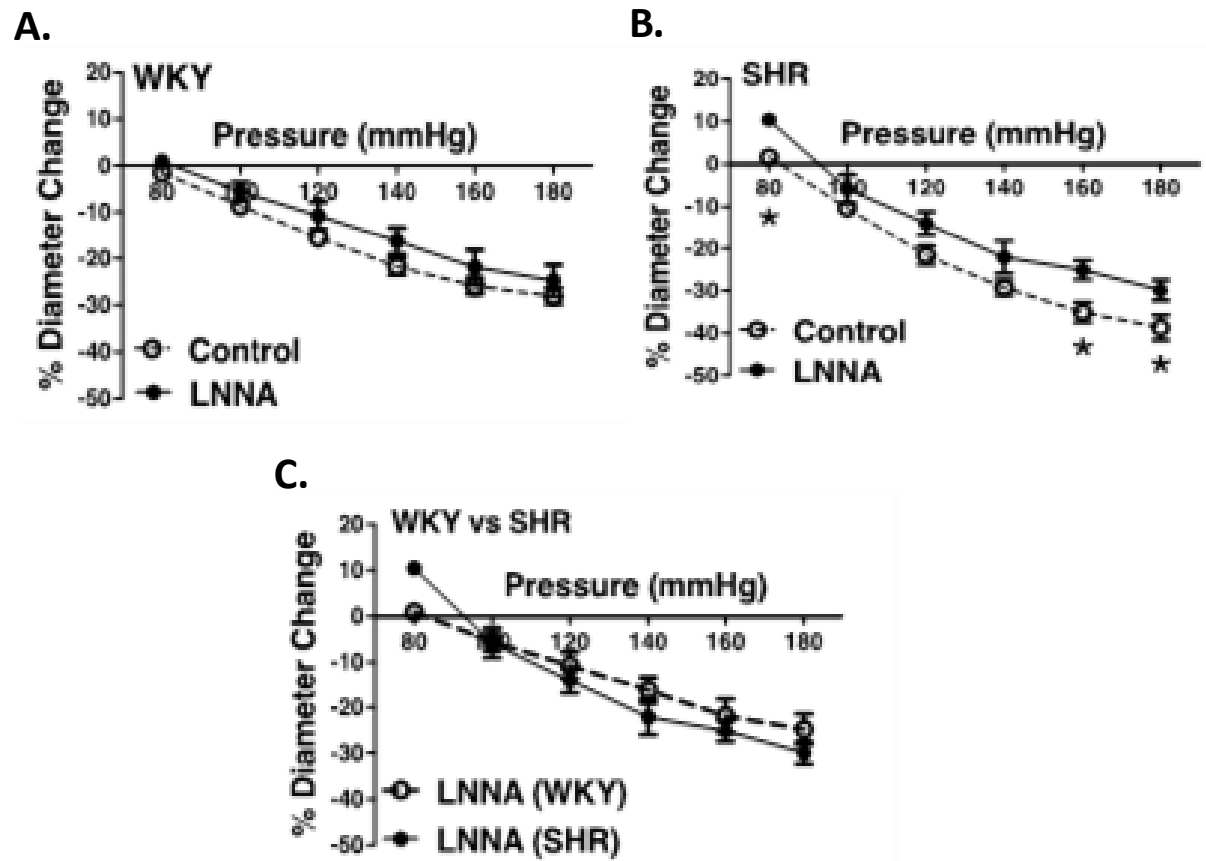
Figure 4.

Figure 4. Effects of nitric oxide synthase inhibition on MC of preglomerular arteries in WKY and SHR rats (30-40 weeks-old rats). A) Effect of N omega-nitro-L-arginine (LNNA, 100 µM) on myogenic constriction (MC) of WKY arcuate arteries. **B)** Effect of LNNA (100 µM) on MC of SHR arcuate arteries. **C)** Comparing MC in WKY and SHR arcuate arteries that were treated with LNNA (100 µM). Two-way ANOVA and Holm-Sidak post-hoc test were used to assess significance; denoted by "*", $P \leq 0.05$. $N_{WKY} = 7$, $N_{SHR} = 6$, $n_{WKY} = 7$, $n_{SHR} = 6$ ("N": number of vessels, "n": number of animals).
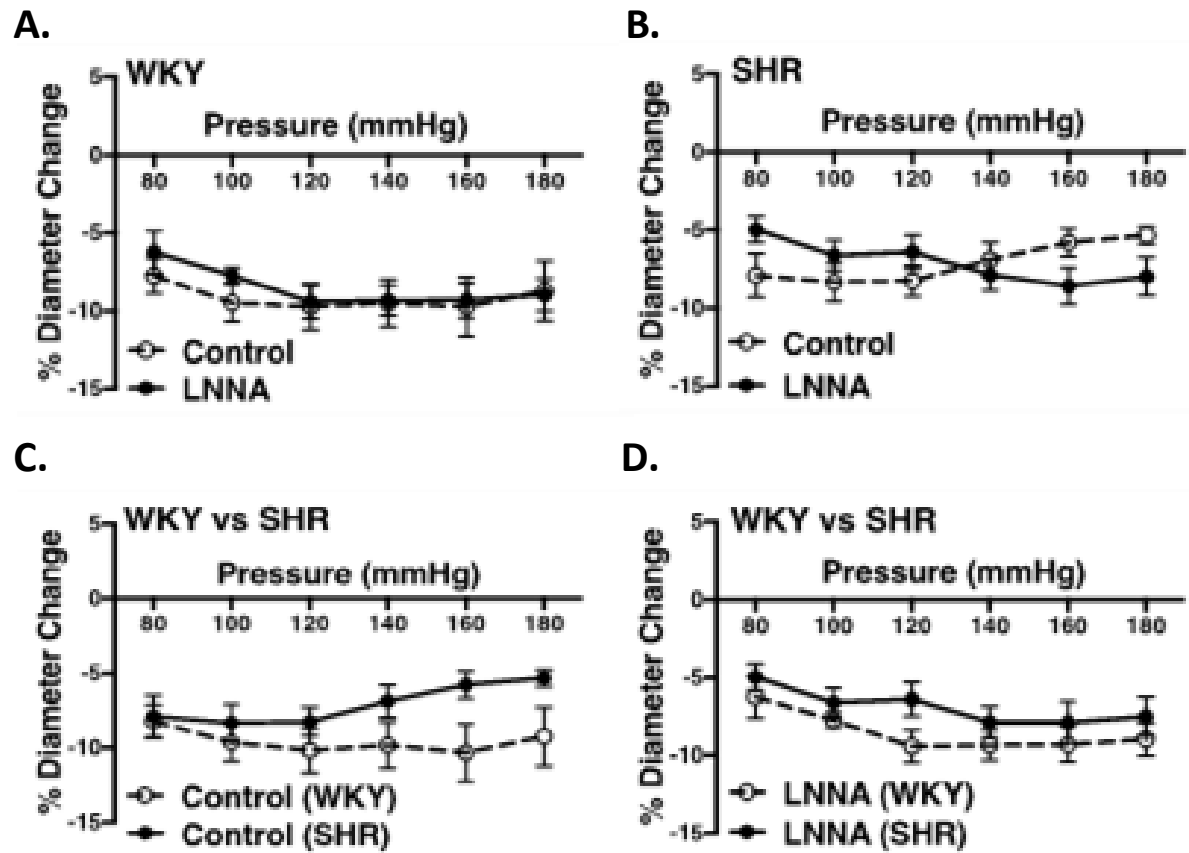
Figure 5.

Figure 5. Effects of nitric oxide synthase inhibition on MC of mesenteric arteries in WKY and SHR rats (30-40 weeks-old rats). A) Effect of N omega-nitro-L-arginine (LNNA, 100 µM) on myogenic constriction (MC) of WKY mesenteric arteries. **B)** Effect of LNNA (100 µM) on MC of SHR mesenteric arteries. **C)** Comparison of MC between WKY and SHR mesenteric arteries. **D)** Comparing MC in WKY and SHR mesenteric arteries that were treated with LNNA (100 µM). Two-way ANOVA and Holm-Sidak post-hoc test were used to assess significance; denoted by "*", $P \leq 0.05$. $N_{WKY} = 7$, $N_{SHR} = 6$, $n_{WKY} = 5$, $n_{SHR} = 6$ ("N": number of vessels, "n": number of animals).

Figure 6.

Figure 6. Effects of L-type calcium channel blockade on arcuate arteries of WKY and SHR older rats (30-40 weeks-old). A) Effect of nifedipine (10 μM) on myogenic constriction (MC) of WKY arcuate arteries. **B)** Effect of nifedipine (10 μM) on MC of SHR arcuate arteries. **C)** Comparing MC in WKY and SHR preglomerular arteries that were treated with nifedipine (10 μM). Two-way ANOVA and Holm-Sidak post-hoc test were used to assess significance; denoted by "*", $P \leq 0.05$. $N_{WKY} = 7$, $N_{SHR} = 5$, $n_{WKY} = 4$, $n_{SHR} = 4$ ("N": number of vessels, "n": number of animals).
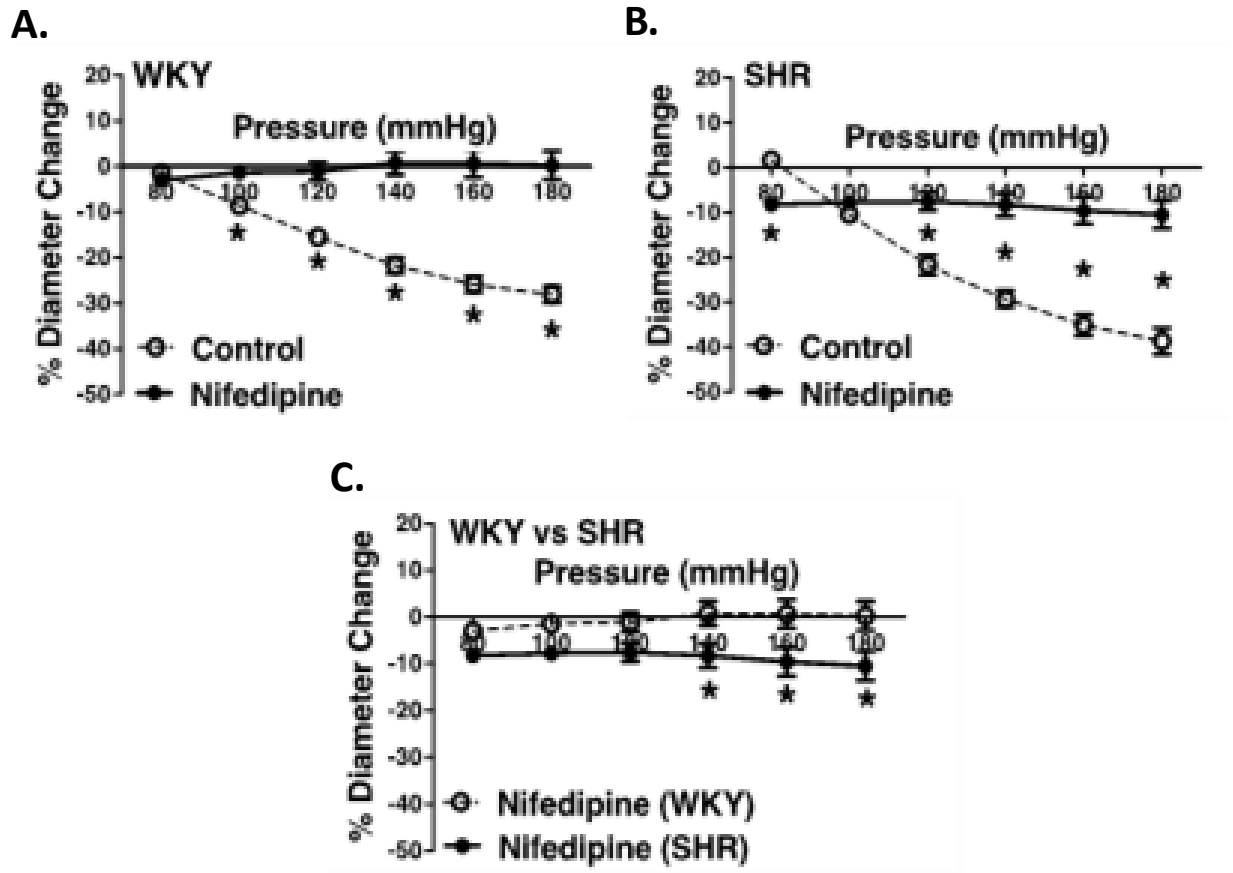
Figure 7.

Figure 7. Effects of L-type calcium channel blockade on mesenteric arteries of WKY and SHR older rats (30-40 weeks-old). A) Effect of nifedipine (1 µM) on myogenic constriction (MC) of WKY mesenteric arteries. **B)** Effect of nifedipine (1 µM) on MC of SHR mesenteric arteries. **C)** Comparing MC in WKY and SHR mesenteric arteries that were treated with nifedipine (1 µM). Two-way ANOVA and Holm-Sidak post-hoc test were used to assess significance; denoted by "*", $P \leq 0.05$. $N_{WKY} = 9$, $N_{SHR} = 8$, $n_{WKY} = 5$, $n_{SHR} = 4$ ("N": number of vessels, "n": number of animals).

Figure 8.
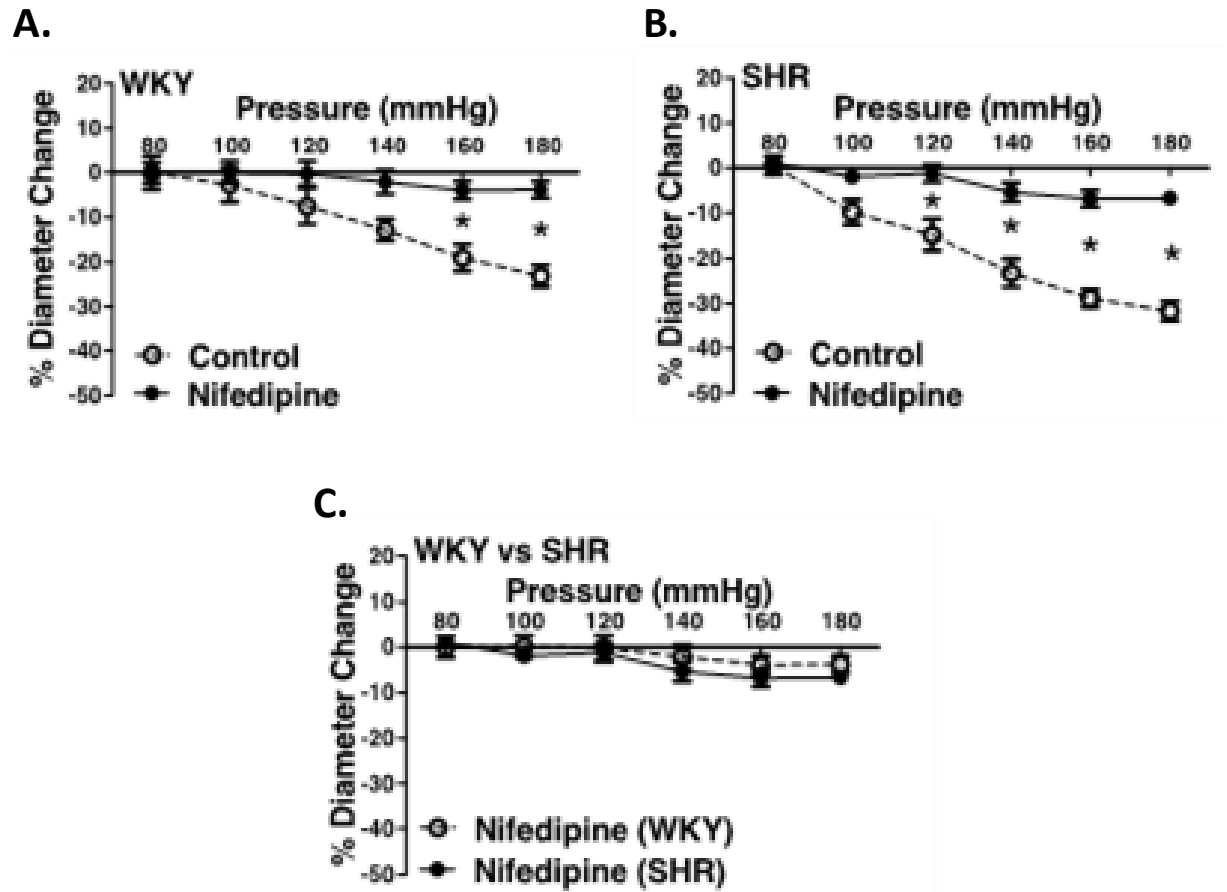
Figure 8. Effects of L-type calcium channel blockade on arcuate arteries of WKY and SHR younger rats (12-16 weeks-old). A) Effect of nifedipine (10 µM) on myogenic constriction (MC) of WKY arcuate arteries. **B)** Effect of nifedipine (10 µM) on MC of SHR arcuate arteries. **C)** Comparing MC in WKY and SHR arcuate arteries that were treated with nifedipine (10 µM). Two-way ANOVA and Holm-Sidak post-hoc test were used to assess significance; denoted by "*", $P \leq 0.05$. $N_{WKY} = 5$, $N_{SHR} = 5$, $n_{WKY} = 5$, $n_{SHR} = 5$ ("N": number of vessels, "n": number of animals).
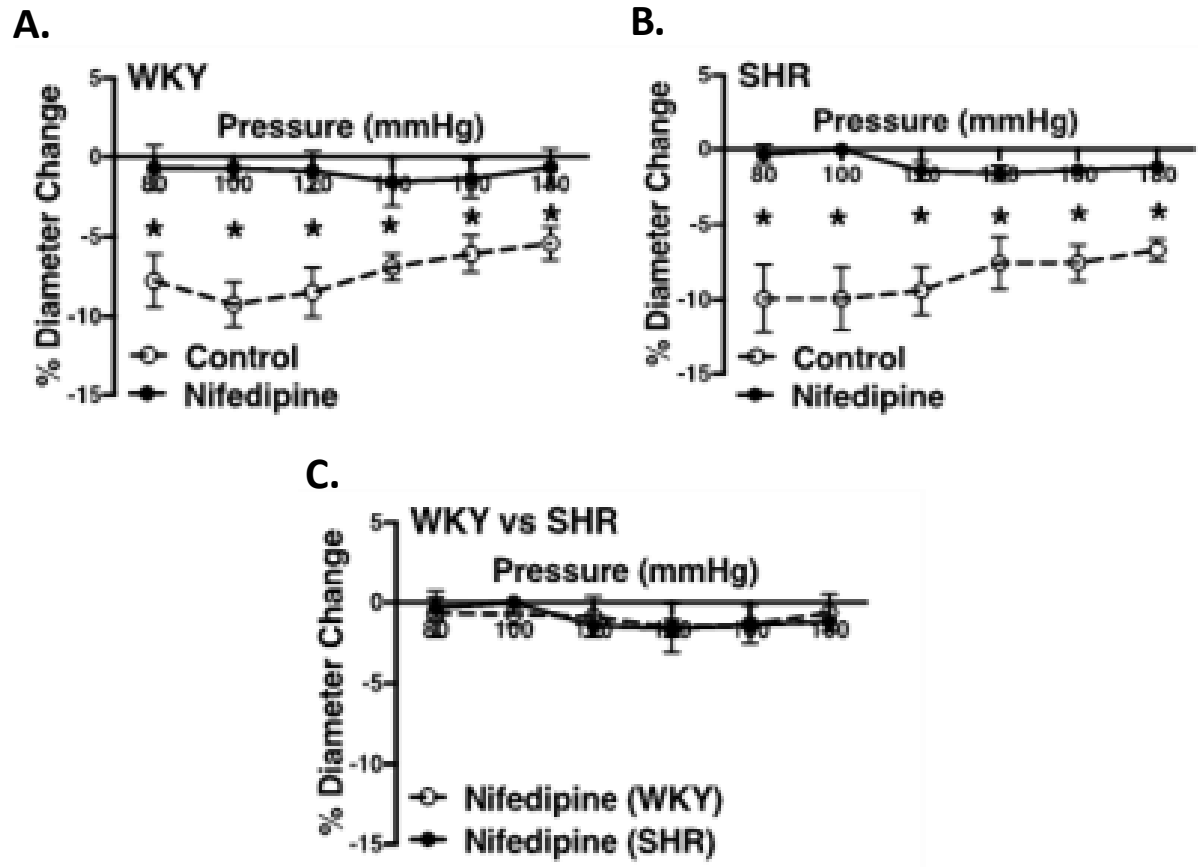
Figure 9.

A.
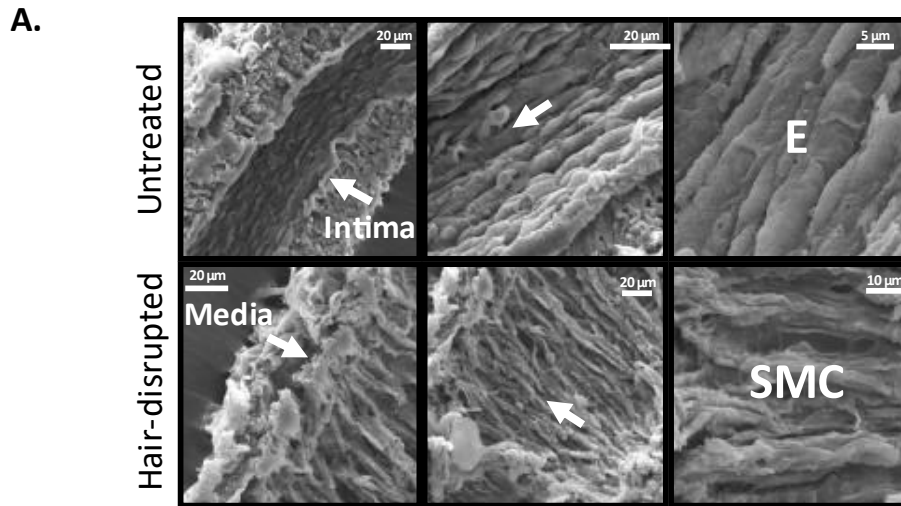
B. Arcuate Arteries:
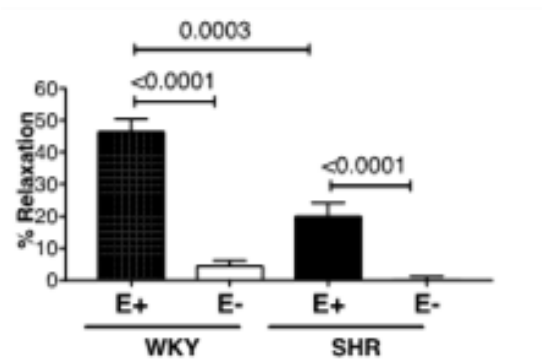
C. Mesenteric Arteries:
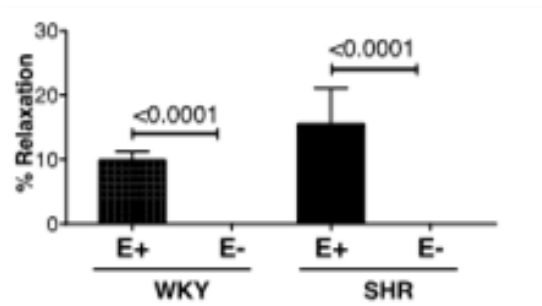
Figure 9. Scanning Electron Micrographs and carbachol treatments demonstrating physical and functional removal of endothelium. A) Scanning Electron Microscopy (SEM) showing intact tunica intima (consisting of endothelium, E) and media (consisting of smooth muscle cells) in untreated, but only tunica media in hair-disrupted WKY arcuate arteries. Micrographs were magnified between 700 to 15000 times. **B)** Percent carbachol-induced relaxation (10 μM) in WKY and SHR arcuate arteries that were pre-constricted with 3 μM phenylephrine at P80 mmHg. **C)** Percent carbachol-induced relaxation (10 μM) in WKY and SHR mesenteric arteries that were pre-constricted with 3 μM phenylephrine at P80 mmHg. Paired t-test was used to compare endothelium-intact (E+) and endothelium-removed (E-) arteries in the same animal strain. Unpaired t-test was used to compare E+ and E- arteries in different animal strains. "*", $P \leq 0.05$; for arcuate arteries: $N_{WKY} = 10$, $N_{SHR} = 10$, $n_{WKY} = 5$, $n_{SHR} = 4$; for mesenteric arteries: $N_{WKY} = 11$, $N_{SHR} = 5$, $n_{WKY} = 5$, $n_{SHR} = 4$; ("N": number of vessels; "n": number of animals).

Figure 10.
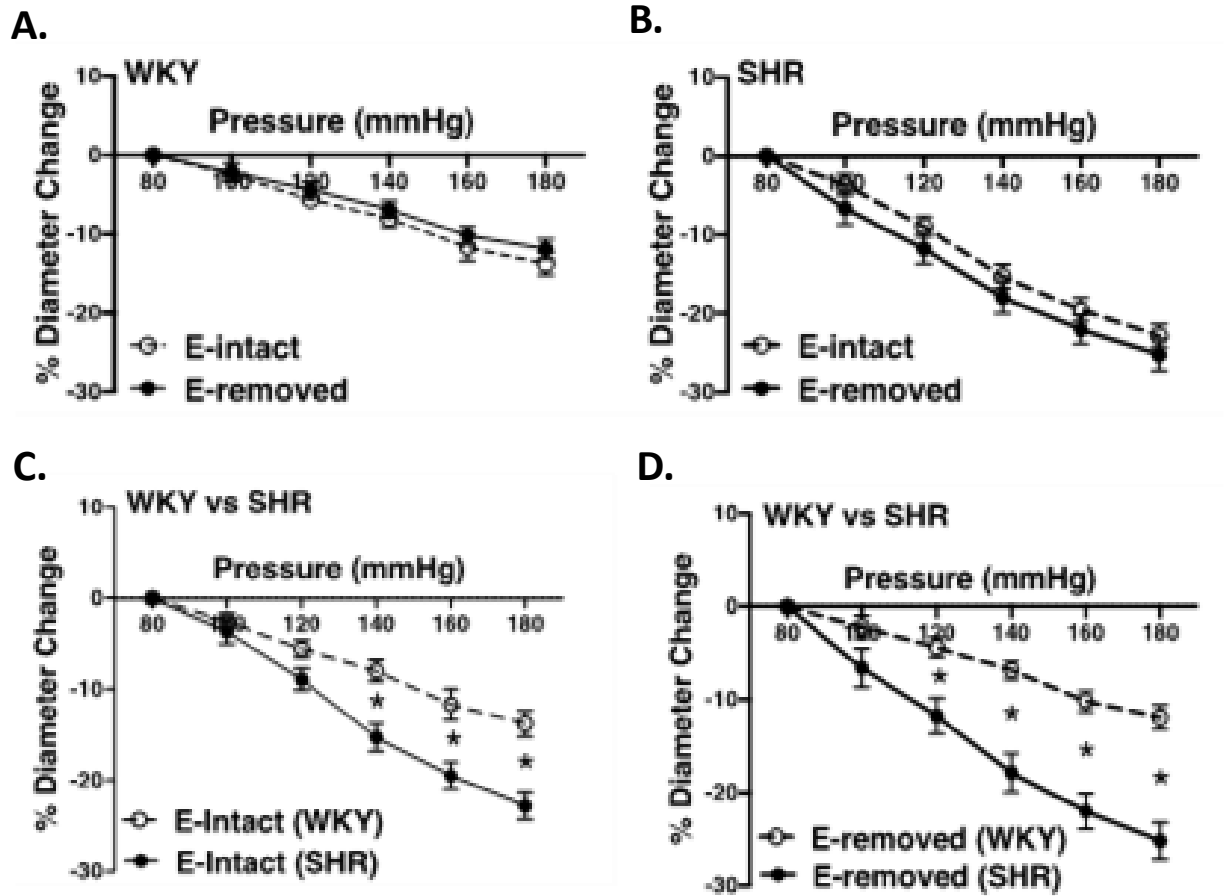
Figure 10. Effects of removing endothelium from WKY and SHR preglomerular arteries using human hair (30-40 weeks-old rats). A) Effect of removing endothelium in WKY arcuate arteries. **B)** Effect of removing endothelium in SHR arcuate arteries. **C)** Comparison of myogenic constriction (MC) in endothelium-intact (E-intact) WKY and SHR arcuate arteries. **D)** Comparison of MC in endothelium-removed (E-removed) WKY and SHR arcuate arteries. Two-way ANOVA and Holm-Sidak post-hoc test was used to assess significance; denoted by "*", $P \leq 0.05$. $N_{WKY} = 10$, $N_{SHR} = 10$, $n_{WKY} = 5$, $n_{SHR} = 4$; ("N": number of vessels; "n": number of animals).

Figure 11.
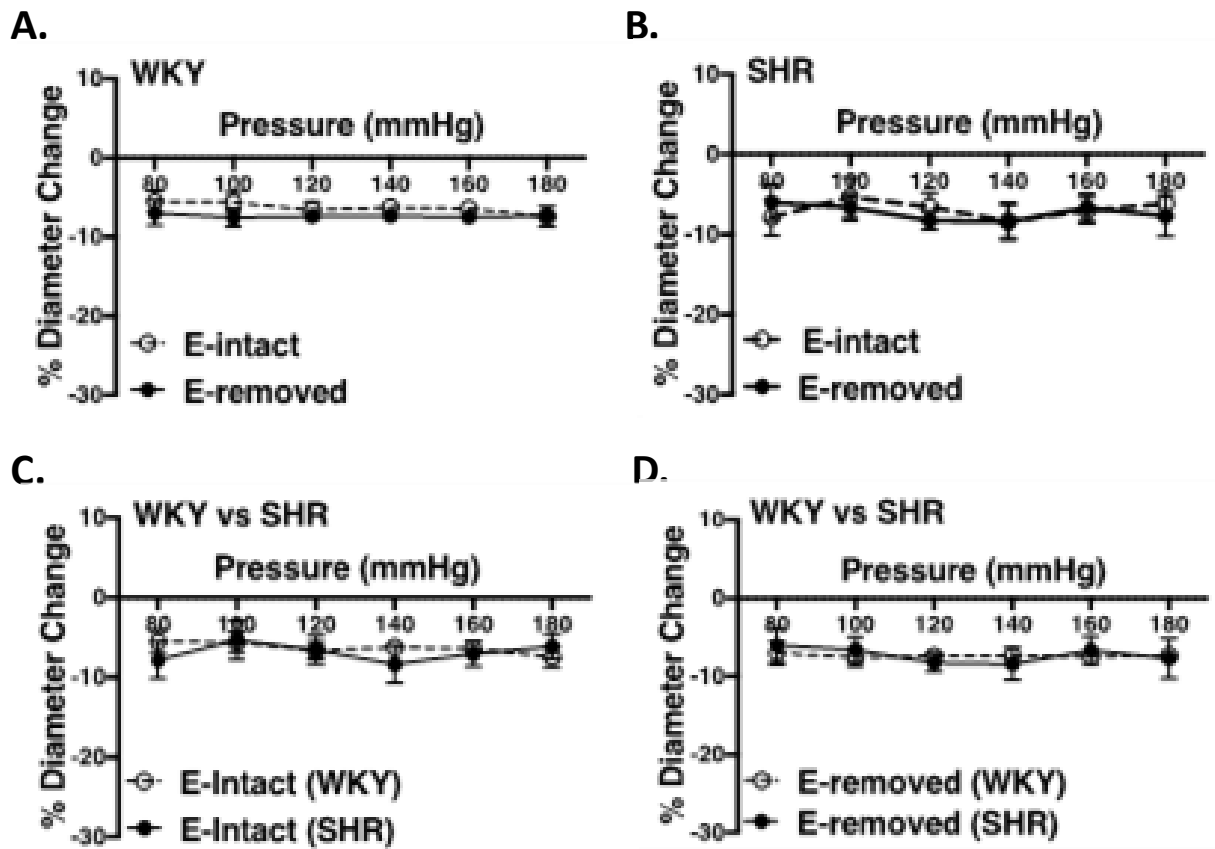
Figure 11. Effects of removing endothelium from WKY and SHR mesenteric arteries using human hair (30-40 weeks-old rats). A) Effect of removing endothelium in WKY mesenteric arteries. **B)** Effect of removing endothelium in SHR mesenteric arteries. **C)** Comparison of myogenic constriction (MC) in endothelium-intact (E-intact) WKY and SHR mesenteric arteries. **D)** Comparison of MC in endothelium-removed (E-removed) WKY and SHR mesenteric arteries. Two-way ANOVA and Holm-Sidak post-hoc test was used to assess significance; denoted by "*", $P \leq 0.05$. $N_{WKY} = 11$, $N_{SHR} = 5$, $n_{WKY} = 6$, $n_{SHR} = 4$; ("N": number of vessels; "n": number of animals).

Figure 12.

**Figure 12. Effects of inhibiting cyclooxygenase 1 and 2 (prostaglandin H2 synthesis) and thromboxane synthetase on arcuate arteries of young WKY and SHR rats (12-16 weeks-old). A)** Myogenic constriction (MC) comparison between endothelium-intact (E-intact) WKY and SHR arcuate arteries. **B and C)** Comparing WKY and SHR arcuate arteries with E-intact, endothelium-removed (E-removed), and E-removed that were treated with indomethacin (prostaglandin H2 synthesis inhibitor, 10 μM). Star,"*", depicts significant differences between indomethacin-treated vessels with when they had their E-removed and E-intact ($P \leq 0.05$). **D and E)** Comparing WKY and SHR arcuate arteries with E-intact, E-removed, and E-removed that were treated with furegrelate (thromboxane A2 synthesis inhibitor, 100 μM). Star,"*", depicts significant differences between furegrelate-treated vessels with when they had their E-removed and E-intact ($P \leq$ 0.05). **F and G)** Comparing WKY and SHR E-removed arcuate arteries that were treated with either indomethacin or furegrelate. Two-way ANOVA and Holm-Sidak post-hoc test was used to assess significance. $N_{WKY} = 9$, $N_{SHR} = 10$, $n_{WKY} = 6$, $n_{SHR} = 9$; ("N": number of vessels; "n": number of animals).

Figure 13.
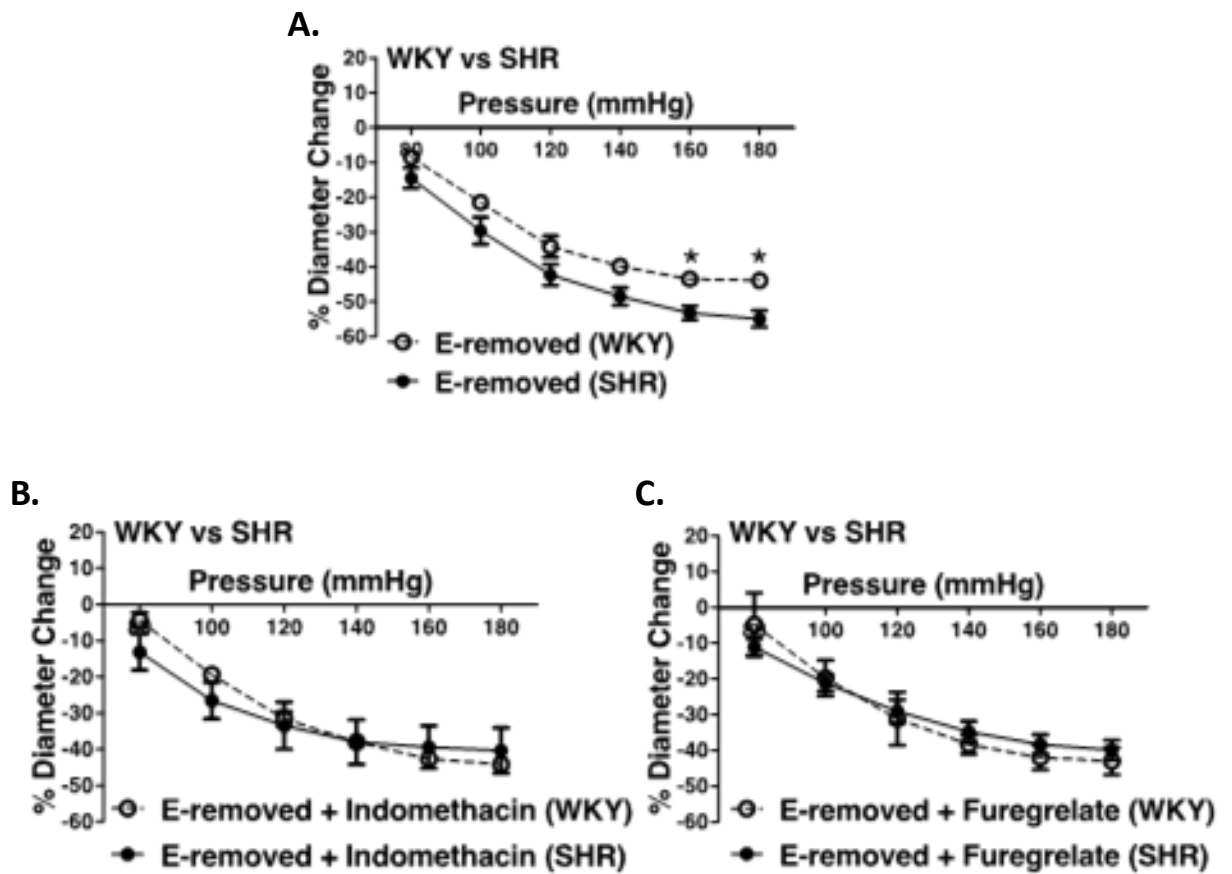
Figure 13. Enhanced myogenic constriction (MC) in the young SHR arcuate arteries, compared to the WKY, was abolished with inhibiting prostaglandin H2 synthesis (by indomethacin) and thromboxane A2 synthesis (by furegrelate) independent from endothelium. A) MC is enhanced in the endothelium-removed (E-removed) SHR arcuate arteries compared with E-removed WKY arcuate arteries at high intraluminal pressures. **B)** Treating E-removed SHR arcuate arteries with 10 μM indomethacin abolished the enhanced MC compared to the WKY arcuate arteries. **C)** Treating E-removed SHR arcuate arteries with 100 μM furegrelate abolished the enhanced MC compared to the WKY arcuate arteries. Two-way ANOVA and Holm-Sidak post-hoc test was used to assess significance; denoted by "*", $P \leq 0.05$. $N_{WKY} = 9$, $N_{SHR} = 10$, $n_{WKY} = 6$, $n_{SHR} = 9$; ("N": number of vessels; "n": number of animals).
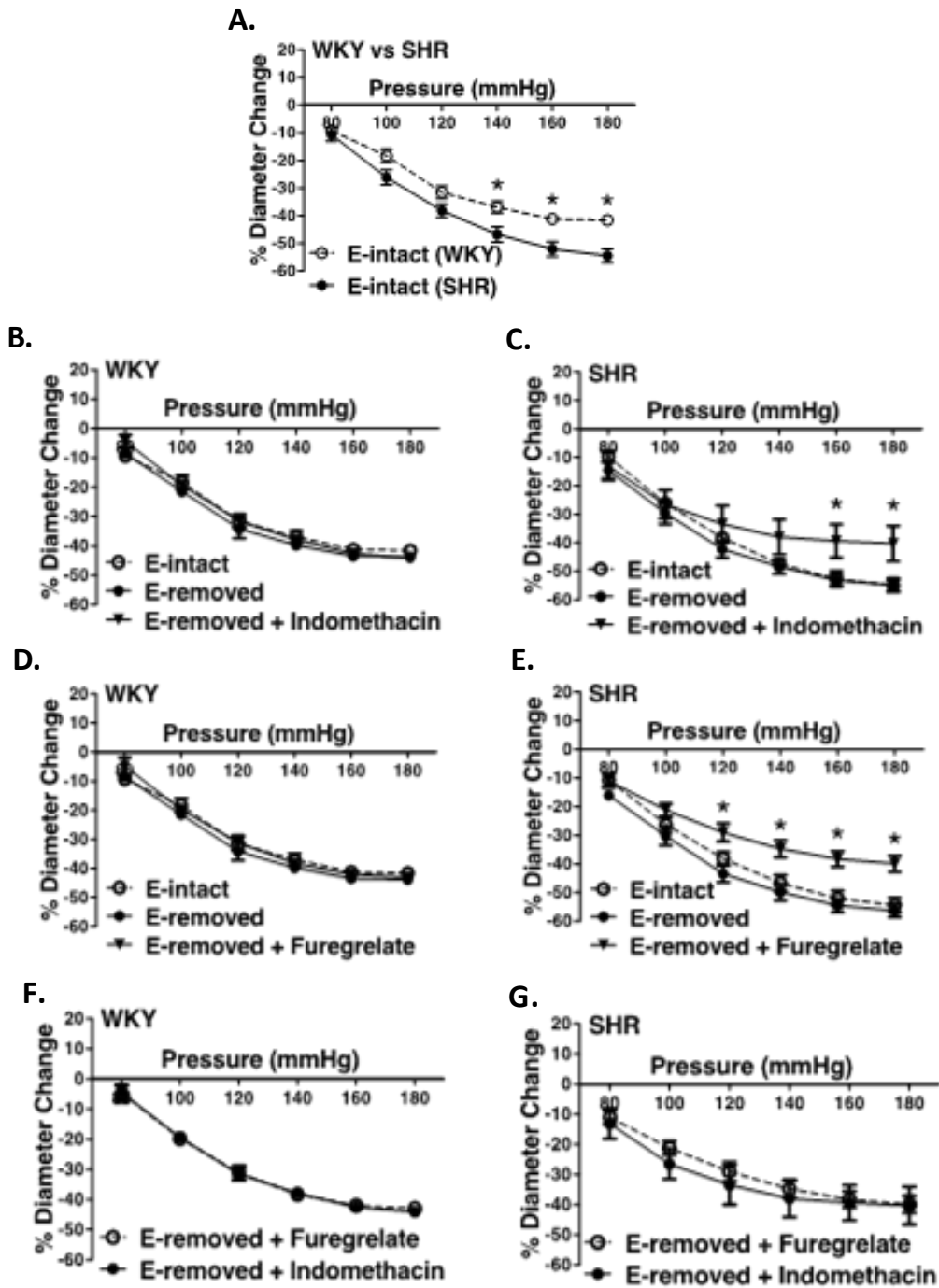
Figure 14.

Tunica Adventitia

Tunica Media

Tunica Intima

Arterial Lumen

Either or both produce Thromboxane A2, leading to an enhanced myogenic constriction in the SHR arcuate arteries.
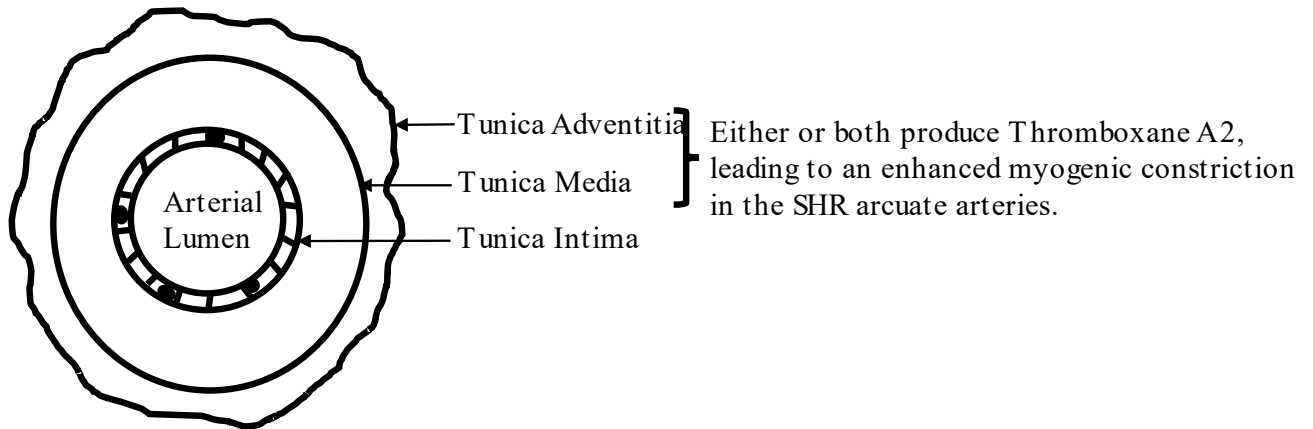
Figure 14. Proposed mechanism for the enhanced myogenic constriction in the SHR arcuate arteries. Tunica intima, Tunica media, and tunica adventitia are composed of endothelial cells, smooth muscle cells, and connective tissue respectively.

CHAPTER 3

Nifedipine Prevented from Salt-Induced Renal Injury in Older Spontaneously Hypertensive Rats

Authors: Samera Nademi[1], Chao Lu[2], Rushank Patel[3], and Jeffrey G. Dickhout[1,2]

Chapter Summary:

The purpose of this study was to address a gap in the literature regarding the effects of nifedipine on blood pressure and chronic kidney disease (CKD) development in an older hypertensive animal model. Nifedipine is an L-type calcium channel blocker that is commonly used as a first line therapy for the treatment of hypertension. Nifedipine has been known to reduce the blood pressure and myogenic constriction (MC) in hypertensive individuals. MC is contraction of small arterioles in response to increasing intraluminal pressure. We successfully attempted to induce CKD in older spontaneously hypertensive rats (SHR) through high dietary sodium feeding. We administered normal salt (NS, 0.4% NaCl), high salt (HS, 8% NaCl), or high salt plus nifedipine (HSN, 25 mg/kg body weight/day) to 43-46 weeks-old SHR and their age-matched normotensive controls, WKY, for 8 weeks until they were 51-54 weeks old. We then assessed blood pressure progression, CKD characteristics, and renal functioning in these rats. To our knowledge, this is the first evidence to show that nifedipine prevented HS-induced elevations in serum creatinine, renal protein casts, and urinary uromodulin (UMOD) excretion levels in older SHR rodents. UMOD is a kidney-specific glycoprotein that has the strongest association to CKD based on a genome-wide association study. We demonstrated that nifedipine may be an appropriate first line therapy for the treatment of hypertension in older CKD patients.

Author's Contribution:

S. Nademi and J.G. Dickhout designed the study. S. Nademi, C. Lu, and R. Patel performed the experiments and analyzed the data. S. Nademi and J.G. Dickhout interpreted the results. S. Nademi prepared the figures and drafted the manuscript. S. Nademi and J.G. Dickhout edited and revised the manuscript. All authors approved the final version of the manuscript.

Title: Nifedipine Prevented Salt-Induced Renal Injury in Older Spontaneously Hypertensive Rats

Authors: Samera Nademi[1], Chao Lu[2], Rushank Patel[3], and Jeffrey G. Dickhout[1,2]

[1] Department of Medicine, Division of Nephrology, McMaster University, Hamilton, ON, Canada, [2] St. Joseph's Healthcare Hamilton, Hamilton, ON, Canada, [3] Michael G. DeGroote School of Medicine, McMaster University, Hamilton, ON, Canada

Address Correspondence to:

Jeffrey G. Dickhout, Ph.D.

Department of Medicine, Division of Nephrology

McMaster University and St. Joseph's Healthcare Hamilton

50 Charlton Avenue East, T-3312

Hamilton, ON, Canada, L8N 4A6

Tel: 905-522-1155 ext. 35334

Fax: 905-540-6589

Email: jdickhou@stjosham.on.ca

ABSTRACT

   Background. Myogenic constriction (MC) is contraction of arteries in response to increasing intraluminal pressure. Nifedipine, an L-type calcium channel antagonist, has been shown to inhibit MC and to reduce blood pressure. Nevertheless, the effects of nifedipine on preventing chronic kidney disease (CKD) progression is controversial. There is also a paucity of studies concerning the effects of nifedipine in older hypertensive animal models with salt-induced CKD. **Methods.** We placed older (43-46 weeks old) spontaneously hypertensive rat (SHR) and Wistar-Kyoto (WKY) rats on either: 1) normal salt (NS, 0.4% NaCl), 2) high salt (HS, 8% NaCl), or 3) HS and nifedipine (HSN, 25 mg/day/kg) for 8 weeks. **Results.** HS did not change the blood pressure in either WKY or SHR, but induced CKD characteristics in the SHR-HS compared to the SHR-NS rats. SHR-HS suffered from proteinuria, albuminuria, increased urinary uromodulin (UMOD) excretion, decreased glomerular filtration rate (GFR), increased serum creatinine, protein casts, renal and cardiac hypertrophy, and interstitial fibrosis. Co-treatment of HS with nifedipine significantly reduced the blood pressure in WKY (last 3 weeks) and SHR (week 1-8); and prevented the development of CKD in older SHR-HSN versus SHR-HS rats. Nifedipine reduced both UMOD concentration (mg/ml urine) and 24-hour total excretion (mg/24 hour). UMOD is a kidney-specific glycoprotein that has a strong association with CKD. Nifedipine also significantly attenuated the protective enhanced MC in the SHR preglomerular arterioles, but this reduction was associated with improved renal outcomes. Interestingly unlike younger SHR, the MC in older SHR-NS preglomerular arteries was not augmented. **Conclusions.**

The present study demonstrated that nifedipine effectively prevented CKD progression in older hypertensive SHR rats. The renoprotective effects of nifedipine appear to be mediated through a reduction in blood pressure, UMOD, and albumin excretion.

INTRODUCTION

Chronic kidney disease (CKD) is a chronic loss of renal function, resulting in significant morbidity and mortality globally as well as a large financial burden on health care systems world-wide (1). Genetic studies have shown that variants in the non-coding uromodulin (UMOD) locus have the strongest association with incident CKD (2). These variants were also associated with increased UMOD excretion (3). Another study based on mendelian randomization has established a causal link between UMOD and CKD (4). UMOD, also called Tamm-Horsfall protein, is a kidney-specific glycoprotein that is the most abundant in normal urine (5). Other important risk factors and predictors of CKD include high dietary salt (HS) intake (6) as well as older ages (7). HS diet has been shown to induce CKD characteristic such as proteinuria, albuminuria (8), UMOD overexcretion (9, 10), renal tissue injury, glomerular filtration rate (GFR) decline (6), and hypertension (11). Hypertension occurs in about 60-90% of CKD patients, making it the most common comorbidity that results in the progression of CKD and eventually end stage renal disease (ESRD) (12, 13). Treatment of hypertension often requires multiple medications or large doses of antihypertensive agents (14). First line of therapy include calcium channel blockers, thiazide-type diuretics, angiotensin-converting enzyme inhibitors, or angiotensin receptor blockers; with dihydropyridine calcium channel blockers being one of the most commonly used antihypertensive drugs (15). One type of dihydropyridine calcium channel blocker commonly used for hypertension treatment is nifedipine (16). As an L-type calcium channel antagonist, nifedipine prevents calcium influx into smooth and cardiac muscle cells, thus dilating arteries and relaxing the heart. This leads to a reduction

in peripheral vascular resistance as well as cardiac output, resulting in a decrease in systematic blood pressure (17). In addition, nifedipine dose-dependently impairs myogenic constriction (MC) in renal preglomerular arterioles *in-vivo* (18) and *ex-vivo* (19). MC is contraction of arterioles' smooth muscle cells in response to elevations in transluminal pressure in order to autoregulate blood flow (20). This process is particularly important in hypertensive individuals as people and animal models with essential hypertension may have enhanced MC in preglomerular vessels protecting the kidney from hyperfiltration and thus maintaining a constant blood flow and GFR (20). In this way, enhanced MC in preglomerular arterioles may help prevent CKD development (20). Nifedipine blocks MC, but the effects of nifedipine on older hypertensive animals with CKD has never been investigated. We hypothesized that nifedipine impairs MC in preglomerular vessels since it is a vasodilator, hence worsens renal pathology despite reducing the blood pressure. To test this, we induced CKD in older hypertensive rodents via HS diet and co-administered nifedipine to a subset of the rats for 8 weeks, then measured CKD characteristics, MC, and UMOD excretion levels.

METHODS

   Animal Studies. Older (43-46 weeks old) male Wistar-Kyoto (WKY) and spontaneously hypertensive rat (SHR) were placed on either normal salt (**NS**, %0.4 NaCl; AIN-76A), high salt (**HS**, %8 NaCl; AIN-76A), or HS plus nifedipine (**HSN**) for 8 weeks until they reached 51-54 weeks of age. Nifedipine in our study (Sigma Aldrich, N7634) was dissolved in dimethylsulfoxide (DMSO), placed in 2ml-Jell-O cubes (1:2 ratio of

flavored jelly powder and water), and orally given to the animals based on a 25 mg/kg body weight dose daily for 8 weeks. At the end of the study period, animals were anesthetized with isoflurane (4% to induce and 2-2.5% to maintain) and 1.5 L/min oxygen; their endpoint GFR was measured; and their left-ventricle blood was collected for plasma creatinine measurements. The rodents were then perfused with Hank's basic salt solution (HBSS) and their kidneys were collected for staining and vessel studies. All rats were bred at McMaster University Central Animal Facility, maintained at St Joseph's Healthcare Hamilton Animal Facility, and housed with a 12-hour light-dark cycle and had free access to food and drinking water. All animal works were approved by McMaster University Animal Research Ethics Board and performed in accordance with their guidelines.

Blood Pressure. In order to determine the effects of HS and nifedipine on blood pressure, SBP and diastolic blood pressure (DBP) were measured weekly at baseline (prior to diet consumption) and during the 8-week study period using radiotelemetry. Radiotelemetry catheter was surgically implanted into the rodent's abdominal aorta caudal to the left renal vein as previously described (21). At weeks 0, 1, 2, 3, 4, 5, 6, 7, and 8, the transmitter was activated with a strong magnet and the rodents' cages were placed on a telemetry receiver. An acquisition system software was used to record the blood pressure every 10 minutes for 2 hours.

Glomerular Filtration Rate (GFR). Baseline (before commencing the diets) and endpoint GFR were measured to assess renal function. Briefly, blood was collected through rats' saphenous veins using heparinized hematocrit tubes (baseline blood). Then a mixture of heparin (500 µl of 500 USP sterilized heparin) and fluorescein isothiocyanate inulin (FITC-inulin, 50 mg/ml dose, dialyzed, and sterilized) was injected to the rats through their tail vein (2 µl/g body weight). Blood was re-collected from the saphenous veins 3, 7, 10, 15, 20, 40, and 60 minutes following the FITC-inulin injection. The blood was then centrifuged, and plasma FITC-inulin levels were measured using a fluorescent spectrophotometer. GFR was calculated based on the plasma FITC-inulin levels and a two-component model of two-phase exponential decay.

Proteinuria and Albuminuria. To further assess the effects of HS and nifedipine on renal function at endpoint, the rats were placed in metabolic cages and their 24-hour (hr)-urine samples were collected for urinalysis studies. Total 24hr-urine protein was measured using Bio-Rad Bradford Protein Assay (5000006, Bio-Rad; Mississauga, Canada) with Rat Bovine Serum Albumin (BSA) standards based on the manufacturer's instructions. Total 24hr-urine albumin was also determined using enzyme-linked immunosorbent assay (ELISA) according to the kit's (E111-125, Bethyl Laboratories Inc; Burlington, Canada) specifications. Briefly, ELISA plates were coated with primary antibody; blocked for an hr; incubated with samples and standards for an hr; treated with horseradish peroxidase (HRP) detection antibody and tetramethylbenzdine (TMB) substrate solution (Sigma Aldrich); stopped the reaction with 0.18 M H2SO4; and read

absorbances at 450 nm using a plate reader (Molecular Devices Spectra Max Plus384 Absorbance Microplate Reader).

Extracting Urinary UMOD to Use as Standards. To make a standard curve for western blot analysis, UMOD was extracted from the urine of 30-week-old male WKY using a Trichloroacetic (TCA) acid-acetone precipitation method in order to make 4 serially diluted UMOD standards. To remove sediments, the 24-hour collected urine was centrifuged at 3000 relative centrifugal force (RCF) for 15 mins. The supernatant was then concentrated in a 30000 molecular weight cutoff (MW) Amicon® Ultra-15 Centrifugal Filter (Sigma Aldrich) for 15 mins and centrifuged again at 3000 RCF for 25 mins at 25^0C. Next, 1 ml urine was collected from the upper chamber and incubated at 4^0C for 1 hour and centrifuged at 14000 RPM for 25 mins. Subsequently, 850 µl of the concentrated urine was mixed with 150 µl of 100% TCA. This mixture was incubated at $4\ ^0$C for 1 hour, and centrifuged at 14000 RCF for 10 mins. Then the bottom pellet containing the precipitated UMOD was incubated with ice-cold acetone for 5 mins, centrifuged at 14000 g for 10 mins, and this process was repeated twice to wash. After discarding the supernatant and air-drying the pellet, 1ml 15 mM Tris buffer (pH 8.8) was added and mixed well until the UMOD was completely dissolved. The resulting mixture was the purified UMOD suspended in Tris buffer. BioRad DC Protein Assay (BioRad; Mississauga, Canada) was used to determine UMOD stock concentration. UMOD standards were serially diluted from this UMOD stock to 5, 2.5, 1, and 0.5 mg/ml. These 4 serial dilutions were used in western blot gels to construct a standard curve from which samples' concentrations were calculated.

Urinary UMOD Detection. Total (mg/24 hours) and concentration (mg/ml) of urinary UMOD was measured in order to investigate the effects of HS and nifedipine on UMOD excretion. Samples and standards were diluted 1:2 in loading buffer containing protease and phosphatase inhibitor cocktails (Roche) and were separated in SDS-PAGE electrophoresis (BioRad; Mississauga, Canada). Recombinant anti-UMOD primary antibodies (1:10000, Abcam ab207170) were detected by anti-rabbit horseradish peroxidase-conjugated secondary antibodies (1:25000, 170-6515, BioRad; Mississauga, Canada) and enhanced chemiluminescence (ECL) Western Blotting Detection Reagents (Amersham, RPN3244), as previously reported [21]. To analyze the results, ChemiDoc Imaging Systems (BioRad; Mississauga, Canada) and Image Lab software were used. An equation of the fitted standard curve was obtained from the 4 serially diluted standards of known concentrations. Samples' band volumes were plotted into this equation and urinary UMOD concentration (mg/ml urine) was calculated. To calculate the total 24-hr urinary UMOD (mg/24hr), UMOD concentration (mg/ml urine) was multiplied by the 24-hr urine volume.

Measuring Myogenic Constriction (MC). To determine the effects of HS and nifedipine on preglomerular arteries' pressure induced constriction, we measured MC of arcuate arteries after 8 weeks of diet consumption. Upon sacrifice, arcuate arteries were dissected out of the kidneys and transferred into a pressure myograph chamber filled with oxygenated Hank's balanced salt solution (HBSS) at 37^0C. The vessels were mounted on

a glass micropipette and tied off at branches to create a blind sac. Pressure was set to 80 mmHg (P80) and 80 mM KCl was added to produce a contractile response to ensure vessels' viability. Only arteries that demonstrated a viable KCl contraction were utilized. The chamber was then washed with HBSS and the vessels were allowed 30 minutes to equilibrate. After equilibration, lumen diameter was recorded and intraluminal pressure was increased in 20 mmHg increments until 180 mmHg, allowing 5-minute-intervals between each pressure change for the vessel to adjust its diameter. The diameter changes corresponding to each pressure point between 80 to 180 mmHg were recorded. Lumen diameter changes were also recorded in calcium (Ca^{2+})-Free HBSS (containing a 5mM Ca^{2+} chelator called ethylene glycol-bis(β-aminoethyl ether)-N,N,N′,N′-tetraacetic acid), – or EGTA in short. The HBSS inside the vessel and tubing systems were replaced by cutting off the end of the artery, changing the normal-HBSS pumping source to Ca^{2+}-Free HBSS, and allowing the normal-HBSS to run out of the vessel for 5 minutes before re-cannulating the end. The artery was then allowed to equilibrate in oxygenated Ca^{2+}-Free HBSS at 37^0C for 30 minutes, and lumen diameter was recorded with increasing pressure as previously described. Percent Diameter Change was calculated by subtracting the artery's diameter (D) at a given pressure (Pn, n = 80-180 mmHg) in Ca^{2+}-Free HBSS (D Pn, Ca^{2+} free HBSS) from the diameter of the same artery (D) at the same given pressure (Pn, n = 80-180 mmHg) in normal HBSS (D Pn, normal HBSS), divided by the [D Pn, Ca^{2+} free HBSS], multiplied by 100%, as follows:

$$\left(\frac{D_{(Pn,\ normal\ HBSS)} - D_{(Pn,\ Ca2+\ Free\ HBSS)}}{D_{(Pn,\ Ca2+Free\ HBSS)}}\right) * 100\%.$$

Vascular and Renal Tissue Preparation for Histology Assessments. After sacrificing the rats, their kidneys were dissected out and fixed in 4% paraformaldehyde. The tissues were processed (by St Joseph's Hospital Histology lab), embedded in paraffin blocks, sectioned 4 μm-thick using a microtome, and mounted on charged Superfrost™ Plus slides. The tissue slides were then deparaffinized by xylene and graded ethanol solutions and the respective staining was carried out.

Measuring Protein Cast Areas by Periodic Acid-Schiff (PAS) Staining. After deparaffinization, the kidney sections were oxidized with 1% aqueous periodic acid, treated with Schiff reagent, counterstained with haematoxylin, dehydrated through graded ethanol and xylene solutions, and mounted. The kidney section slides were imaged using Olympus BX41 microscope and 20X objective lens. For each animal, 10 images per cortex and 10 per medulla were obtained and analyzed using the Image-J software. Percent protein cast area was calculated by the sum of protein cast areas in each image, divided by area of the entire image, multiplied by 100%, as follow: (= $\left(\frac{\sum \text{Protein cast areas per image}}{\text{Image area}}\right) * 100\%$).

Measuring Interstitial Fibrosis by Masson's Trichrome. After deparaffinization, the kidney sections were mordanted in pre-heated (37^0C) Zenker's solution. Samples were then stained in hematoxylin (30 sec), Biebrich Scarlet-Acid Fuchsin solution (5 mins), phosphotungstic solution (5 mins), and aniline blue solution (5 mins). The sections were treated with 1% glacial acetic acid (2 mins), dehydrated in

graded ethanol solutions, incubated in xylene, and mounted. The slides were imaged using Olympus BX41 microscope and 20x objective lens. For each animal, 10 images per cortex and 10 per medulla were obtained and analyzed using the Metamorph software by color thresholding (RGB color model). The percent threshold area (percent interstitial fibrosis) was directly read by the software after thresholding. Percent interstitial fibrosis area was calculated by the sum of the fibrosis areas in each image, divided by area of the entire image, multiplied by 100%, as follow: $\left(= \left(\frac{\sum \text{Interestitial fibrosis areas per image}}{\text{Image area}}\right) * 100\%\right)$.

Hypertrophy Assessments. In order to investigate whether HS and/or nifedipine treatments affected renal and cardiac weights, when sacrificing, the kidneys and heart weights for each rat were recorded and normalized to the rat's body weight.

Correlation Studies. Simple linear regression tests were performed to determine the degree of contribution to renal pathology, which was represented by % medullary protein casts area. Datapoints from WKY and SHR rats in all diet groups (NS, HS, and HSN) were used for the correlation studies. Proteinuria, total 24-hr urinary UMOD, albuminuria, % medullary fibrosis area, and systolic blood pressure (SBP) were correlated with % medullary protein casts area using the GraphPad Prism software. Coefficient of determination (R^2) was calculated to determine the degree the above predictive variables accounted for variation in renal pathology.

Statistical Analysis. One-way Analysis of Variance (ANOVA) was used to assess significant differences between three or more dependent variables. Regular two-way ANOVA was used to evaluate statistical significance between two independent variables. Both tests were corrected by Holm-Sidak posthoc test. Significant differences were evaluated using 95% confidence intervals. P ≤ 0.05 was deemed statistically significant.

RESULTS

Blood Pressure. Co-treatment of HS and nifedipine in WKY (WKY-HSN) significantly reduced SBP and DBP compared to WKY-HS rats during the last 3 weeks (weeks 6, 7, 8). At week 7, WKY-HSN DBP was also lower than WKY-NS DBP (**Figure 1B**). In the SHR, nifedipine reduced SBP and DBP in SHR-HSN compared to both SHR-HS and SHR-NS during the entire 8-week study period except for week 3 of the SBP (**Figure 1C, 1D**).

Proteinuria and Albuminuria. Eight weeks of HS consumption significantly increased proteinuria and albuminuria in the SHR-HS compared to the SHR-NS. Nifedipine treatment decreased proteinuria and albuminuria in the SHR-HSN to the same level as the SHR-NS, significantly less than the SHR-HS (**Figure 2A, 2B**). When comparing SHR with WKY, only SHR-HS showed significantly higher proteinuria and albuminuria than WKY-HS (**Figure 2A, 2B**).

Uromodulin. Nifedipine significantly reduced UMOD concentration (mg/ml) in the SHR-HSN compared to the SHR-HS and SHR-NS (**Figure 3A**). Compared to the WKY of the same diets, SHR-NS and SHR-HSN demonstrated lower UMOD concentration (mg/ml) (**Figure 3A**). Expectedly, urine volume was increased to the same levels with HS intake in both WKY and SHR rats (**Figure 3B**). HS increased total UMOD levels (mg/24 hours) in the SHR-HS, but nifedipine reduced it in the SHR-HSN versus SHR-HS (**Figure 3C**). Markedly, this HS-induced elevation in total UMOD excretion (mg/24 hours) was not the result of increased urinary UMOD concentration (mg/ml urine) in the SHR-HS but the result of increased urinary volume flows (**Figure 3A, 3C**). In the WKY, 24-hour UMOD (mg/24 hours) excretion was also elevated with HS but nifedipine did not significantly reduce it (**Figure 3C**).

Glomerular Filtration Rate and Creatinine Levels. SHR-HS showed lower GFR compared to the WKY-HS. HS decreased the GFR in the SHR-HS rats versus SHR-NS, however co-treatment of HS with nifedipine did not improve GFR (**Figure 4A**). Conversely, HS increased serum creatinine in the SHR-HS versus SHR-NS, but co-treatment of HS with nifedipine restored serum creatinine levels in the SHR-HSN to that of SHR-NS (**Figure 4B**).

Myogenic Constriction. MC was attenuated in WKY-HSN versus WKY-NS between P120 to P180 mmHg. HS diet also reduced MC in WKY-HS versus WKY-NS between P140 to P180 mmHg (**Figure 5A**, * compared to NS). Moreover, nifedipine

reduced MC in the SHR-HSN compared to both SHR-HS and SHR-NS between P120-180 mmHg (**Figure 5B**, * compared to NS, # compared to HS). Furthermore, MC in preglomerular arteries of older (51-54 weeks old) SHR was not augmented compared to the WKY (**Figure 5C**).

Protein Cast Areas. HS increased cortex and medullary % protein casts area in the SHR-HS compared to SHR-NS. However, HS plus nifedipine significantly reduced the elevated protein cast levels in the SHR-HSN to NS levels in both cortex and medulla. Moreover, SHR-NS and SHR-HS demonstrated higher protein casts than WKY-NS and WKY-HS respectively (**Figure 6A, 6B, 6C**).

Interstitial Fibrosis Areas. Nifedipine co-administered with HS diet reduced medullary % interstitial fibrosis in the SHR-HSN versus SHR-HS (**Figure 7A, 7C**). There seems to be an increasing trend in the medullary % interstitial fibrosis with HS diet in the SHR, but this elevation was not statistically significant (**Figure 7C**). Additionally, SHR rats showed significantly more cortical and medullary interstitial fibrosis compared to the WKY rats (**Figure 7A, 7B, 7C**).

Heart and Kidneys Weight Measurements. SHR-HS suffered from left kidney and cardiac weights (**Figure 8A, 8C**). Nifedipine co-administered with HS diet did not significantly reverse these effects (**Figure 8A, 8C**).

Correlation Comparisons. In order to determine whether a given parameter contributed to the % protein casts area (as a measure of renal pathology), coefficient of determination (R-squared) was calculated. R-squared of % protein casts area versus 24-hour proteinuria (0.92), 24-hour total urinary UMOD (0.89), 24-hour albuminuria (0.77), % medullary fibrosis area (0.58), and SBP (0.53) were statistically significant ($P \leq 0.05$) (**Figure 9**).

DISCUSSION

The purpose of this study was to address a gap in the literature regarding the effects of nifedipine on blood pressure and CKD progression in older hypertensive animal models. To our knowledge, we were the first to investigate the effects of nifedipine on salt-induced serum creatinine, protein casts, and urinary UMOD concentration in older SHR rats. UMOD is a kidney-specific protein that has the strongest association with CKD in GWAS studies (22). In order to induce CKD in our older hypertensive SHR (43-46 weeks old), we fed the rodents HS diet for 8 weeks until they reached 51-54 weeks of age.

Effects of High Salt on Blood Pressure and CKD Characteristics. High dietary salt did not change the blood pressure in either WKY or SHR in our study. Other studies in the literature found that 8 weeks of HS diet (8% NaCl) increased BP in both WKY and SHR (8 weeks old) (23); and increased mean arterial pressure (MAP) in the SHR but not the age-matched WKY (5-6 weeks old) (24). The observed discrepancy could be due to

age-related differences in sodium handling due to differential expression, activity, or localization of Na^+/H^+ antiporter 3 (NHE3), found on epithelial cells of the proximal tubules in the kidneys and enterocytes in the intestines, in younger versus older SHR (25). This exchanger is responsible for reabsorbing sodium in exchange for secreting one hydrogen ion (26). Yip et al. showed that NHE3 was localized on the brush borders of the proximal tubules of 5-weeks-old SHR, while they were located in the base of microvilli in 12-weeks-old SHR. As such, the authors predicted a differential sodium handling between these two age groups (27). Similarly, Crajoinas et al. reported that NHE3 activity was increased in the proximal tubules of 5 vs 14 weeks-old SHR leading to more sodium excretion in the older SHR rats (28). Nevertheless, high dietary salt has been found to cause several renal abnormalities. Similar to our findings, Berger et al. showed that HS induced glomerular hypertension, reduced nephrin expression, damaged podocytes, increased proteinuria, and elevated albuminuria in SHR rats (29). Henry et al. also discovered that HS induced fibrosis in the kidneys and heart in both WKY and SHR (30). Our study however did not find considerable renal interstitial fibrosis in the WKY rats (**Figure 7**). SHR in our study indeed developed CKD characteristics such as proteinuria, albuminuria, reduced GFR, increased serum creatinine, renal protein casts, and medullary interstitial fibrosis. However, WKY showed minimal renal injury after 8 weeks of salt feeding. High dietary salt has been shown to reduce nephrin expression (a critical component of glomerular filtration barrier structure), resulting in damage to podocyte foot processes and slit diaphragms (31). This leads to the observed proteinuria and albuminuria that are associated with salt loading (31). We co-administered HS and

nifedipine (HSN) to a subset of our hypertensive animals in order to investigate the effects of nifedipine on hypertensive CKD progression.

Effects of Nifedipine on Blood Pressure and CKD Characteristics. Although this and other studies (32-34) in the literature consistently have shown nifedipine to be effective at reducing the blood pressure, the effects of nifedipine on renal function and structure in CKD is controversial (32, 35-39). In addition, there is a lack of studies about the effects of nifedipine in elderly animal models that suffer from hypertensive CKD. We found that nifedipine prevented salt-induced proteinuria and albuminuria in older (51-54 weeks old) SHR rats. Prior studies examining the effects of nifedipine on proteinuria and albuminuria have yielded contradicting results (35, 37, 38). Reams et al. suggested that nifedipine improved GFR in SHR rats but it did not change albuminuria (35). Lin et al. found that nifedipine exacerbated doxorubicin-induced lipogenesis in the kidneys (37). Bellinghieri et al. showed that nifedipine (60 mg/daily) did not change plasma and urine creatinine levels but increased proteinuria in hypertensive CKD patients (38). Inconsistently, Marin et al. found that nifedipine reduced proteinuria in patients with primary renal disease after 3 years of follow-up (40).

Effects of Nifedipine on UMOD Excretion. To our knowledge, this is the first evidence to demonstrate that: 1) 24-hr total urinary UMOD increased upon HS (8% NaCl for 8 weeks) feeding in older SHR-HS vs SHR-NS rats (**Figure 3C**); and 2) co-administration of HS with nifedipine reduced urinary UMOD concentration (mg/ml) in

older SHR-HSN vs SHR-HS rats (**Figure 3A**). Consistent with our results, Mary et al. reported that co-administration of HS (1% NaCl for 3 weeks) with nifedipine decreased 24-hr total urinary UMOD in 12-week-old Stroke-Prone-SHR (SPSHR)-HSN vs SPSHR-HS rats (41). However contrary to our study, Mary et al. showed that HS reduced 24-hr total urinary UMOD in the SPSHR-HS versus SPSHR-NS rats (41). The contradictory results could be because the SPSHR is markedly more salt-sensitive than the SHR rats (42). Additionally, the differences in animal ages (youth vs elderly in our study), HS contents (1% vs 8 % in our study), and/or treatment durations (3 weeks vs 8 weeks in our study) could also play a role in the differing results. Also inconsistent with our findings, another study by Mary et al. (43) detected only 1 band for UMOD in their western blot analysis of nifedipine-treated pregnant SPSHR at gestational days (GD) 12 and 18 (these rats also showed elevated urinary UMOD levels). These results were inconsistent with our findings of 2 UMOD bands corresponding to approximately 60 to 75 kDa. Mary et al. and his colleagues suggested that their nifedipine-treated rats displayed altered peptidomic profile for UMOD likely due to the pregnancy (43).

Effects of Nifedipine on Myogenic Constriction (MC). As a vasodilator, nifedipine inhibits MC in preglomerular arteries and arterioles (44). We hypothesized that attenuating MC through nifedipine treatment along with inducing renal injury with HS would exacerbates salt-induced renal disease in older SHR rats. Nifedipine indeed attenuated MC in SHR-HSN vs SHR-HS (**Figure 5B**); however, this inhibition was associated with improved renal function and structure in the SHR-HSN vs SHR-HS. This

could be because nifedipine significantly decreased both SBP and DBP in the SHR-HSN vs SHR-HS (**Figure 1C, 1D**), and blood pressure reduction has been shown to be important in the control of CKD (45). Moreover, MC has been shown to be augmented in chronically hypertensive human (i.e., essential hypertensives) and animal models (i.e., SHR) (19, 20). However, our results showed that unlike younger SHRs, MC was not augmented in older (51-54 weeks old) SHR-NS rats compared to WKY-NS (**Figure 5C**). This finding is consistent with literature reports that older SHRs lack the protective augmented MC and exhibit reduced responsiveness in their afferent arterioles (46, 47). Unlike younger SHRs, the older animals demonstrated reduced afferent arteriole resistance (R_A) resulting in increased glomerular capillary hydrostatic pressure (P_{GC}) despite exhibiting the same systematic blood pressure. Paradoxically, older SHR rats showed a reduction in glomerular capillary ultrafiltration coefficient (K_f). These findings suggested a loss of responsiveness in the afferent arteriolar of older SHR rats (46).

Effects of Nifedipine on Renal Function and Histopathology. Our findings showed that serum creatinine was increased with HS feeding, but co-treatment of HS and nifedipine significantly reduced it in older hypertensive rats (**Figure 4B**). Similarly, Fujiwara et al. showed that 8 weeks of co-administration of HS and nifedipine reduced serum creatinine levels in 6-week-old SHR rats, but the authors did not report creatinine levels for HS-fed SHR rats (48). Moreover, GFR in our study was reduced with salt feeding. These findings were consistent with most reports in the literature (49, 50).

Nifedipine treatment in the SHR also affected salt-induced renal pathology since protein casts formation in older HS-fed SHR rats was significantly reduced with the nifedipine treatment. (**Figure 6**). Protein casts are mainly composed of UMOD and albumin (51). Thus, an increase or a decrease in the excretion of these proteins may lead to an increase or a decrease in protein cast formation, respectively, in the renal tubules. So it appears that the effect of nifedipine to reduce both UMOD and albumin excretion may have contributed to reduced cast formation. Moreover, consistent with other literature reports, we showed that HS increased medullary interstitial fibrosis (23, 29) while nifedipine decreased it (52) (**Figure 7**). Unlike past studies that reported HS-induced renal and cardiac hypertrophy in both WKY and SHR rats (23, 30, 53), we observed elevated cardiac and left renal weights only in the SHR-HS, which were improved by nifedipine treatment (**Figure 8**). The hypertrophy has been reported to be both blood pressure dependent (53) and independent (54, 55). High systolic blood pressure in the SHR was shown to induce left ventricular and renal hypertrophy (53), while salt overload may activate cardiac angiotensin II type 1 receptor independent of blood pressure (54, 55).

Effects of Nifedipine on Renal Interstitial Fibrosis. Nifedipine inhibits L-type calcium channels which are found in excitable cells such as muscle cells (cardiac, smooth, and skeletal), neurons, endocrine cells of adrenal cortex (produce aldosterone), and myofibroblasts (56, 57). Renal myofibroblasts are fibroblast cells that have been activated to deposit extracellular matrix, and serve as the major contributors to renal

interstitial fibrosis (57, 58). Nifedipine was shown to prevent bleomycin-induced pulmonary fibrosis in mice through interfering with calcium oscillations in pulmonary fibroblasts (59). In the kidneys, nifedipine was shown to reduce cyclosporin-induced renal fibrosis in kidney allografts that were obtained from patients (52). Nifedipine was also shown to reduce renal perivascular fibrosis in a transgenic rat model of severe angiotensin II-dependent hypertension (36). This is because free intracellular calcium acts as a secondary messenger that stimulates fibroblasts' migration, proliferation, differentiation, and secretion (60). These literature findings are consistent with the results of our study that showed nifedipine to reduce high salt-induced medullary interstitial fibrosis in the SHR-HSN versus SHR-HS rats (**Figure 7C**). As such, the fibrosis reduction in our study could have been mediated through the inhibition of L-type calcium channels in renal myofibroblasts.

Correlation Studies. The present study illustrated that medullary protein casts area as a measure of renal pathology was significantly correlated with proteinuria ($R^2 =$ 0.92), total UMOD excretion ($R^2 = 0.89$), albuminuria ($R^2 = 0.77$), medullary fibrosis ($R^2 = 0.58$), and SBP ($R^2 = 0.53$) (**Figure 9**). These results suggest that variations in these factors strongly and positively account for incidents of protein casts in the medulla as a measure of renal injury. A study conducted in 1962 by McQueen showed that albumin, even at low concentrations, was very effective at precipitating UMOD in the urine of patients with albuminuria and UMOD over-excretion; but not the urine of healthy individuals (61). Given that this study found both total UMOD and albumin excretion to

increase upon salt feeding and to decrease with nifedipine treatment in the SHR, it seems plausible that UMOD and albumin aggregate together to form protein casts in the nephron tubules. This may explain the elevated protein casts levels in the SHR-HS, while this level was reduced in the SHR-HSN. This may also be the reason that WKY-HS rats did not suffer from elevated protein casts incidents even though they showed increased total UMOD excretion (because both UMOD and albumin overexcretion may be needed for the protein cast formations in the nephron tubules).

CONCLUSIONS

In this study, we demonstrated that 8 weeks of HS feeding induced CKD characteristics in older hypertensive rats while co-administration of HS with nifedipine prevented salt-induced renal injury in these rodents, in addition to reducing their blood pressure. Although nifedipine significantly diminished the MC in the SHR, this was associated with an improvement in renal function and structure. The renoprotective effects of nifedipine may be mediated through a reduction in blood pressure, UMOD, and albumin excretion, but not through its effects on MC.

AUTHOR CONTRIBUTIONS

SN and JD designed the study. SN, CL, and RP performed the experiments and analyzed the data. SN and JD interpreted the results. SN prepared the figures and drafted the manuscript. SN and JD edited and revised the manuscript. All authors approved the final version of the manuscript.

FUNDING

CONFLICT OF INTEREST

The authors declare that the research was conducted in the absence of any commercial or financial relationships that could be construed as a potential conflict of interest.

REFERENCES

1.   Luyckx VA, Tonelli M, Stanifer JW. The global burden of kidney disease and the sustainable development goals. Bulletin of the World Health Organization. 2018;96(6):414.

2.   Kottgen A, Glazer NL, Dehghan A, Hwang SJ, Katz R, Li M, et al. Multiple loci associated with indices of renal function and chronic kidney disease. Nat Genet. 2009;41(6):712-7.

3.   Olden M, Corre T, Hayward C, Toniolo D, Ulivi S, Gasparini P, et al. Common variants in UMOD associate with urinary uromodulin levels: a meta-analysis. J Am Soc Nephrol. 2014;25(8):1869-82.

4.   Sjaarda J, Gerstein HC, Yusuf S, Treleaven D, Walsh M, Mann JFE, et al. Blood HER2 and Uromodulin as Causal Mediators of CKD. J Am Soc Nephrol. 2018;29(4):1326-35.

5.   Devuyst O, Olinger E, Rampoldi L. Uromodulin: from physiology to rare and complex kidney disorders. Nature Reviews Nephrology. 2017;13(9):525-44.

6.   Sugiura T, Takase H, Ohte N, Dohi Y. Dietary salt intake is a significant determinant of impaired kidney function in the general population. Kidney and Blood Pressure Research. 2018;43(4):1245-54.

7.   Mallappallil M, Friedman EA, Delano BG, McFarlane SI, Salifu MO. Chronic kidney disease in the elderly: evaluation and management. Clinical practice (London, England). 2014;11(5):525.

8.   Jones-Burton C, Mishra SI, Fink JC, Brown J, Gossa W, Bakris GL, et al. An in-depth review of the evidence linking dietary salt intake and progression of chronic kidney disease. American journal of nephrology. 2006;26(3):268-75.

9.   Devuyst O, Olinger E, Rampoldi L. Uromodulin: from physiology to rare and complex kidney disorders. Nat Rev Nephrol. 2017;13(9):525-44.

10.   Mount DB. Thick ascending limb of the loop of Henle. Clin J Am Soc Nephrol. 2014;9(11):1974-86.

11.   McMahon EJ, Bauer JD, Hawley CM, Isbel NM, Stowasser M, Johnson DW, et al. A randomized trial of dietary sodium restriction in CKD. Journal of the American Society of Nephrology. 2013;24(12):2096-103.

12.   Tozawa M, Iseki K, Iseki C, Kinjo K, Ikemiya Y, Takishita S. Blood pressure predicts risk of developing end-stage renal disease in men and women. Hypertension. 2003;41(6):1341-5.

13.   Muntner P, Anderson A, Charleston J, Chen Z, Ford V, Makos G, et al. Hypertension awareness, treatment, and control in adults with CKD: results from the Chronic Renal Insufficiency Cohort (CRIC) Study. American Journal of Kidney Diseases. 2010;55(3):441-51.

14.   Becker GJ, Wheeler DC, De Zeeuw D, Fujita T, Furth SL, Holdaas H, et al. Kidney disease: Improving global outcomes (KDIGO) blood pressure work group. KDIGO clinical practice guideline for the management of blood pressure in chronic kidney disease. Kidney International Supplements. 2012;2(5):337-414.

15.   Armstrong C. JNC8 guidelines for the management of hypertension in adults. American family physician. 2014;90(7):503-4.

16.   Khalil H, Zeltser R. Antihypertensive Medications. StatPearls [Internet]. 2020.

17.   Abrams J, Schroeder J, Frishman WH, Freedman J. Pharmacologic options for treatment of ischemic disease. Cardiovascular Therapeutics: Elsevier; 2007. p. 77-120.

18.   Frandsen RH, Salomonsson M, Hansen PB, Jensen LJ, Braunstein TH, Holstein-Rathlou N-H, et al. No apparent role for T-type Ca 2+ channels in renal autoregulation. Pflügers Archiv-European Journal of Physiology. 2016;468(4):541-50.

19.   Nademi S, Lu C, Dickhout JG. Enhanced Myogenic Constriction in the SHR Preglomerular Vessels Is Mediated by Thromboxane A2 Synthesis. Frontiers in Physiology. 2020;11:853.

20.   Burke M, R Pabbidi M, Farley J, J Roman R. Molecular mechanisms of renal blood flow autoregulation. Current vascular pharmacology. 2014;12(6):845-58.

21.   Naiel S. The Role of Endoplasmic Reticulum Stress in the Development of Essential Hypertension 2017.

22.   Devuyst O, Pattaro C. The UMOD locus: insights into the pathogenesis and prognosis of kidney disease. Journal of the American Society of Nephrology. 2018;29(3):713-26.

23.   Yu HC, Burrell LM, Black MJ, Wu LL, Dilley RJ, Cooper ME, et al. Salt induces myocardial and renal fibrosis in normotensive and hypertensive rats. Circulation. 1998;98(23):2621-8.

24.   Huang BS, Van Vliet BN, Leenen FH. Increases in CSF [Na+] precede the increases in blood pressure in Dahl S rats and SHR on a high-salt diet. American Journal of Physiology-Heart and Circulatory Physiology. 2004;287(3):H1160-H6.

25.   He P, Yun CC. Mechanisms of the Regulation of the Intestinal Exchanger NHE3. Journal of Biomedicine and Biotechnology. 2010;2010.

26.   Bobulescu IA, Moe OW. Luminal Na+/H+ exchange in the proximal tubule. Pflügers Archiv-European Journal of Physiology. 2009;458(1):5-21.

27.   Yip K-P, Tse C-M, McDonough AA, Marsh DJ. Redistribution of Na+/H+ exchanger isoform NHE3 in proximal tubules induced by acute and chronic hypertension. American Journal of Physiology-Renal Physiology. 1998;275(4):F565-F75.

28.   Crajoinas RO, Lessa LM, Carraro-Lacroix LR, Davel APC, Pacheco BP, Rossoni LV, et al. Posttranslational mechanisms associated with reduced NHE3 activity in adult vs. young prehypertensive SHR. American Journal of Physiology-Renal Physiology. 2010;299(4):F872-F81.

29.   Berger RC, Vassallo PF, Crajoinas Rde O, Oliveira ML, Martins FL, Nogueira BV, et al. Renal Effects and Underlying Molecular Mechanisms of Long-Term Salt Content Diets in Spontaneously Hypertensive Rats. PLoS One. 2015;10(10):e0141288.

30.   Henry C, Burrell LM, Black MJ, Wu LL, Dilley RJ, Cooper ME, et al. Salt induces myocardial and renal fibrosis in normotensive and hypertensive rats. Circulation. 1998;98(23):2621-8.

31.   Berger RCM, Vassallo PF, Crajoinas RdO, Oliveira ML, Martins FL, Nogueira BV, et al. Renal effects and underlying molecular mechanisms of long-term salt content diets in spontaneously hypertensive rats. PLoS One. 2015;10(10):e0141288.

32.   Dworkin LD, Benstein JA, Parker M, Tolbert E, Feiner HD. Calcium antagonists and converting enzyme inhibitors reduce renal injury by different mechanisms. Kidney international. 1993;43(4):808-14.

33.   Ishimitsu T, Ohno E, Nakano N, Furukata S, Akashiba A, Minami J, et al. Combination of angiotensin II receptor antagonist with calcium channel blocker or diuretic as antihypertensive therapy for patients with chronic kidney disease. Clinical and experimental hypertension. 2011;33(6):366-72.

34.   Lv R, Chen J, Wang H, Wang J, Cheng H, Li R, et al. Effectiveness and Tolerability of Nifedipine GITS in Patients with Chronic Kidney Disease and Uncontrolled Hypertension: A Prospective, Multicenter, Observational Study (ADRENAL). Advances in therapy. 2021;38(9):4771-85.

35.   Reams GP, Hamory A, Lau A, Bauer JH. Effect of nifedipine on renal function in patients with essential hypertension. Hypertension. 1988;11(5):452-6.

36.   Seccia TM, Maniero C, Belloni AS, Guidolin D, Pothen P, Pessina AC, et al. Role of angiotensin II, endothelin-1 and L-type calcium channel in the development of glomerular, tubulointerstitial and perivascular fibrosis. Journal of hypertension. 2008;26(10):2022-9.

37.   Lin Y-C, Wang J-C, Wu M-S, Lin Y-F, Chen C-R, Chen C-Y, et al. Nifedipine Exacerbates Lipogenesis in the Kidney via KIM-1, CD36, and SREBP Upregulation:

Implications from an Animal Model for Human Study. International journal of molecular sciences. 2020;21(12):4359.

38.   Bellinghieri G, Mazzaglia G, Savica V, Santoro D. Effects of manidipine and nifedipine on blood pressure and renal function in patients with chronic renal failure: a multicenter randomized controlled trial. Renal failure. 2003;25(5):681-9.

39.   Dhaun N, MacIntyre IM, Kerr D, Melville V, Johnston NR, Haughie S, et al. Selective endothelin-A receptor antagonism reduces proteinuria, blood pressure, and arterial stiffness in chronic proteinuric kidney disease. Hypertension. 2011;57(4):772-9.

40.   Marin R, Ruilope LM, Aljama P, Aranda P, Segura J, Diez J. A random comparison of fosinopril and nifedipine GITS in patients with primary renal disease. Journal of hypertension. 2001;19(10):1871-6.

41.   Mary S, Boder P, Rossitto G, Graham L, Scott K, Flynn A, et al. Salt loading decreases urinary excretion and increases intracellular accumulation of uromodulin in stroke-prone spontaneously hypertensive rats. Clinical Science. 2021;135(24):2749-61.

42.   Griffin KA, Churchill PC, Picken M, Webb RC, Kurtz TW, Bidani AK. Differential salt-sensitivity in the pathogenesis of renal damage in SHR and stroke prone SHR. American journal of hypertension. 2001;14(4):311-20.

43.   Mary S, Small HY, Siwy J, Mullen W, Giri A, Delles C. Polymerization-incompetent uromodulin in the pregnant stroke-prone spontaneously hypertensive rat. Hypertension. 2017;69(5):910-8.

44.   MacGregor GA. Nifedipine and hypertension: Roles of vasodilation and sodium balance. Cardiovascular drugs and therapy. 1989;3(1):295-301.

45.   Ravera M, Re M, Deferrari L, Vettoretti S, Deferrari G. Importance of blood pressure control in chronic kidney disease. Journal of the American Society of Nephrology. 2006;17(4 suppl 2):S98-S103.

46.   Tolbert EM, Weisstuch J, Feiner HD, Dworkin LD. Onset of glomerular hypertension with aging precedes injury in the spontaneously hypertensive rat. American Journal of Physiology-Renal Physiology. 2000;278(5):F839-F46.

47.   Weinstein JR, Anderson S. The aging kidney: physiological changes. Advances in chronic kidney disease. 2010;17(4):302-7.

48.   Fujiwara K, Kanno Y, Hayashi K, Takenaka T, Saruta T. Renal protective effects of efonidipine in partially nephrectomized spontaneously hypertensive rats. Clinical and experimental hypertension. 1998;20(3):295-312.

49.   Matavelli LC, Zhou X, Varagic J, Susic D, Frohlich ED. Salt loading produces severe renal hemodynamic dysfunction independent of arterial pressure in spontaneously hypertensive rats. American Journal of Physiology-Heart and Circulatory Physiology. 2007;292(2):H814-H9.

50.   Ishizawa K, Yamaguchi K, Horinouchi Y, Fukuhara Y, Tajima S, Hamano S, et al. Drug discovery for overcoming chronic kidney disease (CKD): development of drugs on endothelial cell protection for overcoming CKD. Journal of pharmacological sciences. 2009;109(1):14-9.

51.   Sanders PW, Booker BB, Bishop JB, Cheung HC. Mechanisms of intranephronal proteinaceous cast formation by low molecular weight proteins. The Journal of clinical investigation. 1990;85(2):570-6.

52.   McCulloch T, Harper S, Donnelly P, Moorhouse J, Bell P, Walls J, et al. Influence of nifedipine on interstitial fibrosis in renal transplant allografts treated with cyclosporin A. Journal of clinical pathology. 1994;47(9):839-42.

53.   Hayakawa Y, Aoyama T, Yokoyama C, Okamoto C, Komaki H, Minatoguchi S, et al. High salt intake damages the heart through activation of cardiac (pro) renin receptors even at an early stage of hypertension. PloS one. 2015;10(3):e0120453.

54.   Ferreira DN, Katayama IA, Oliveira IB, Rosa KT, Furukawa LN, Coelho MS, et al. Salt-induced cardiac hypertrophy and interstitial fibrosis are due to a blood pressure–Independent mechanism in wistar rats. The Journal of nutrition. 2010;140(10):1742-51.

55.   Katayama IA, Pereira RC, Dopona EP, Shimizu MH, Furukawa LN, Oliveira IB, et al. High-salt intake induces cardiomyocyte hypertrophy in rats in response to local angiotensin II type 1 receptor activation. The Journal of Nutrition. 2014;144(10):1571-8.

56.   Yang S, Huang X-Y. Ca2+ influx through L-type Ca2+ channels controls the trailing tail contraction in growth factor-induced fibroblast cell migration. Journal of Biological Chemistry. 2005;280(29):27130-7.

57.   Qi W, Chen X, Poronnik P, Pollock CA. The renal cortical fibroblast in renal tubulointerstitial fibrosis. The international journal of biochemistry & cell biology. 2006;38(1):1-5.

58.   Lin S-L, Kisseleva T, Brenner DA, Duffield JS. Pericytes and perivascular fibroblasts are the primary source of collagen-producing cells in obstructive fibrosis of the kidney. The American journal of pathology. 2008;173(6):1617-27.

59.   Mukherjee S, A. Ayaub E, Murphy J, Lu C, Kolb M, Ask K, et al. Disruption of

calcium signaling in fibroblasts and attenuation of bleomycin-induced fibrosis by

nifedipine. American journal of respiratory cell and molecular biology. 2015;53(4):450-8.

60.   Roach KM, Bradding P. Ca2+ signalling in fibroblasts and the therapeutic

potential of KCa3. 1 channel blockers in fibrotic diseases. British journal of

pharmacology. 2020;177(5):1003-24.

61.   McQueen E. The nature of urinary casts. Journal of Clinical Pathology.
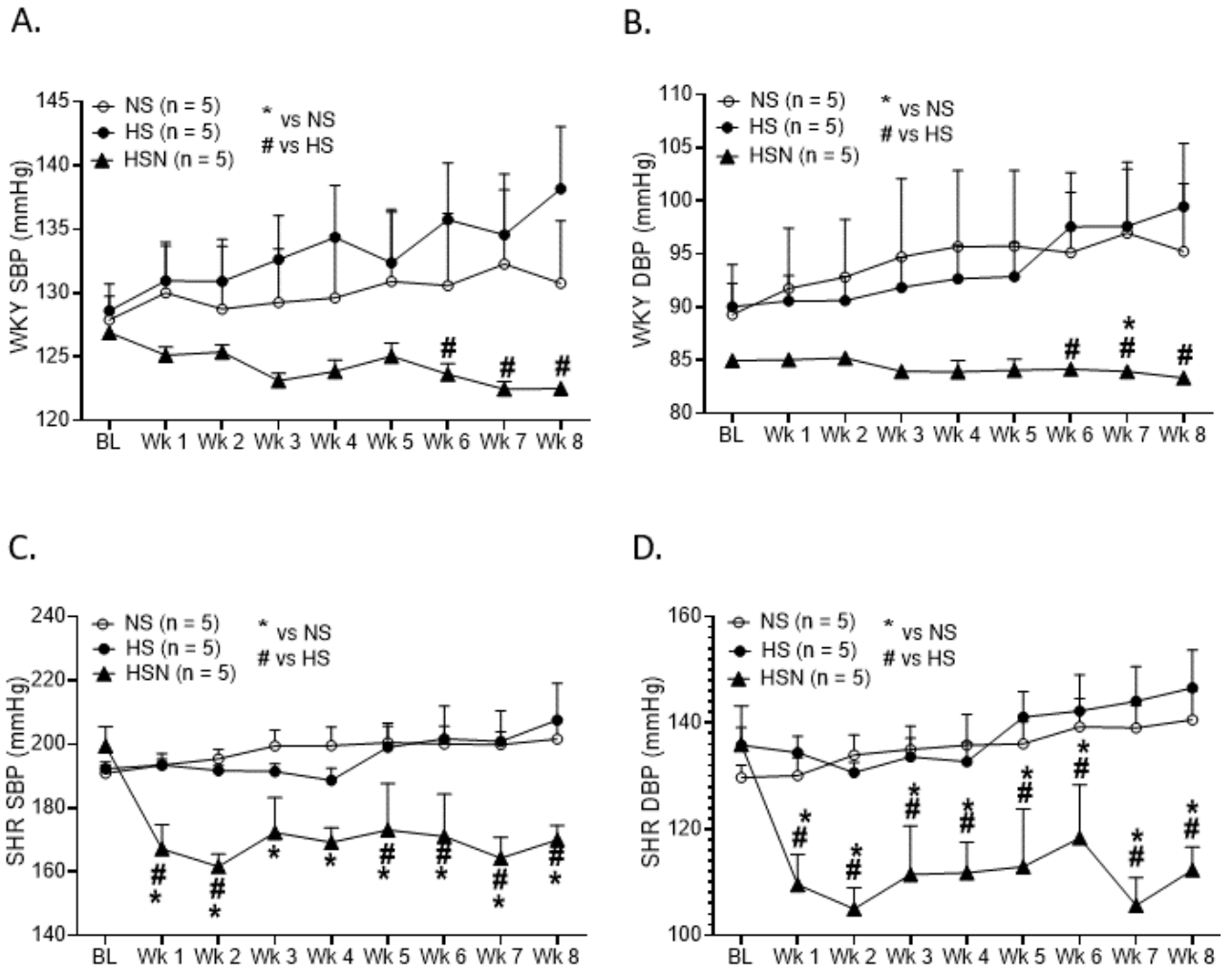
1962;15(4):367-73.

Figure 1.

FIGURE 1 | Blood pressure comparison throughout the 8 weeks of normal salt (NS), high salt (HS), or HS plus nifedipine (HSN) feeding. A and B) Systolic (SBP) and diastolic blood pressure (DBP) in WKY rats after 8 weeks of diet consumption. **C and D)** SBP and DBP in the SHR rats after 8 weeks of diet consumption. $P \leq 0.05$ was statistically significant, demonstrated by * or #. Star (*) compares to NS diet (same strain). Hash (#) compares to HS diet (same strain). N (WKY-NS) = 5, N (WKY-HS) = 5, N (WKY-HSN) = 5, N (SHR-NS) = 5, N (SHR-HS) = 5, N (SHR-HSN) = 5. NS = normal salt, HS = high salt, HSN = HS plus nifedipine.
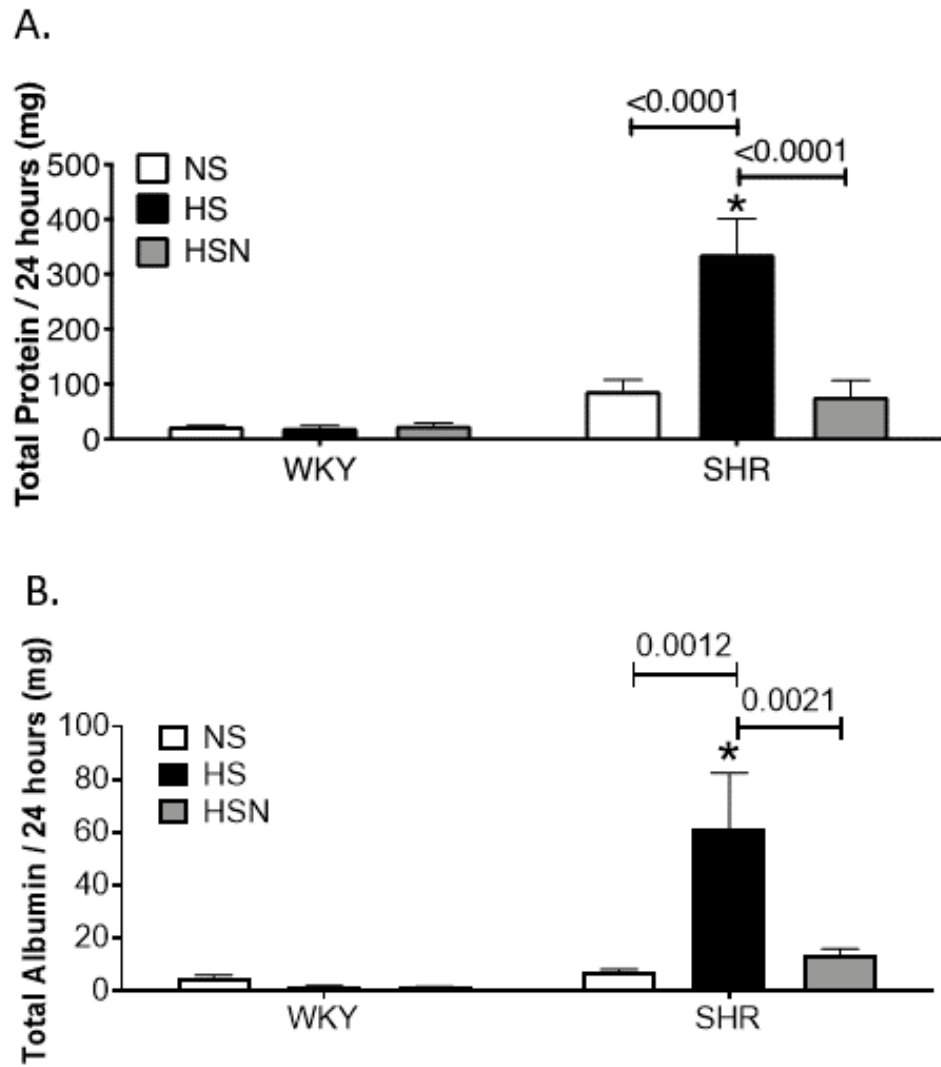
Figure 2.

FIGURE 2 | 24-hr proteinuria and albuminuria at endpoint. A) 24-hr proteinuria after 8 weeks of salt feeding. **B)** 24-hr albuminuria after 8 weeks of salt feeding. $P \leq 0.05$ was statistically significant, demonstrated by * or P-value. Star (*) compares to WKY (same diet). For proteinuria: N (WKY-NS) = 4, N (WKY-HS) = 4, N (WKY-HSN) = 4, N (SHR-NS) = 4, N (SHR-HS) = 4, N (SHR-HSN) = 4. For albuminuria: N (WKY-NS) = 4, N (WKY-HS) = 4, N (WKY-HSN) = 4, N (SHR-NS) = 4, N (SHR-HS) = 4, N (SHR-HSN) = 5. NS = normal salt, HS = high salt, HSN = HS plus nifedipine.
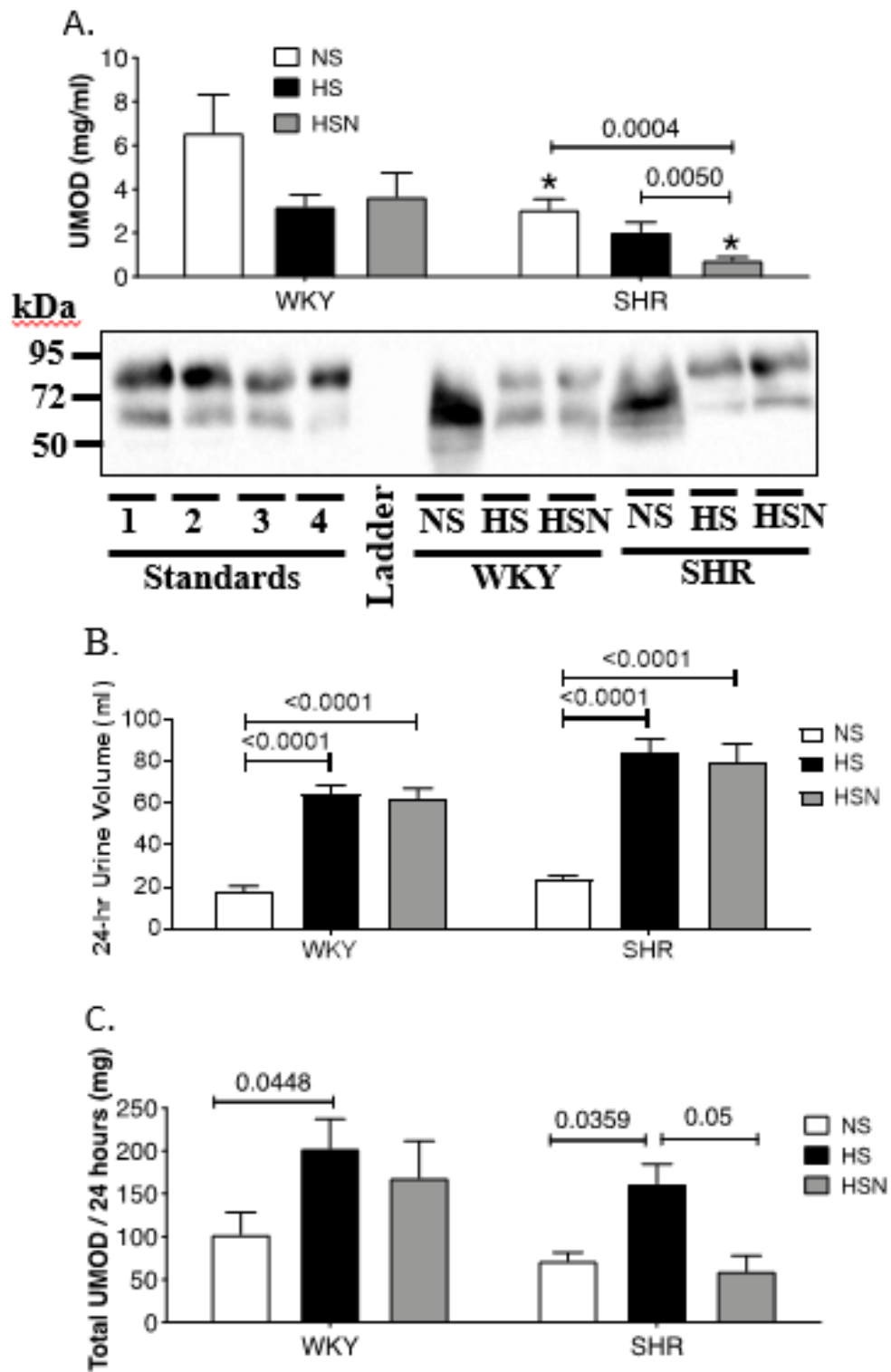
Figure 3.

FIGURE 3 | 24-hr urinary uromodulin (UMOD) measurements at endpoint. A) Urinary UMOD concentration (mg/ml) comparison. **B)** 24-hr urine volume comparison. **C)** 24-hr total urinary UMOD comparison. Urinary UMOD concentration (mg/ml) and 24-hr urine volume were used to determine 24-hr total urinary UMOD. $P \leq 0.05$ was statistically significant, demonstrated by * or P-value. Star (*) compares to the WKY of the same diet. N (WKY-NS) = 6, N (WKY-HS) = 6, N (WKY-HSN) = 5, N (SHR-NS) = 9, N (SHR-HS) = 5, N (SHR-HSN) = 9. NS = normal salt, HS = high salt, HSN = HS plus nifedipine.
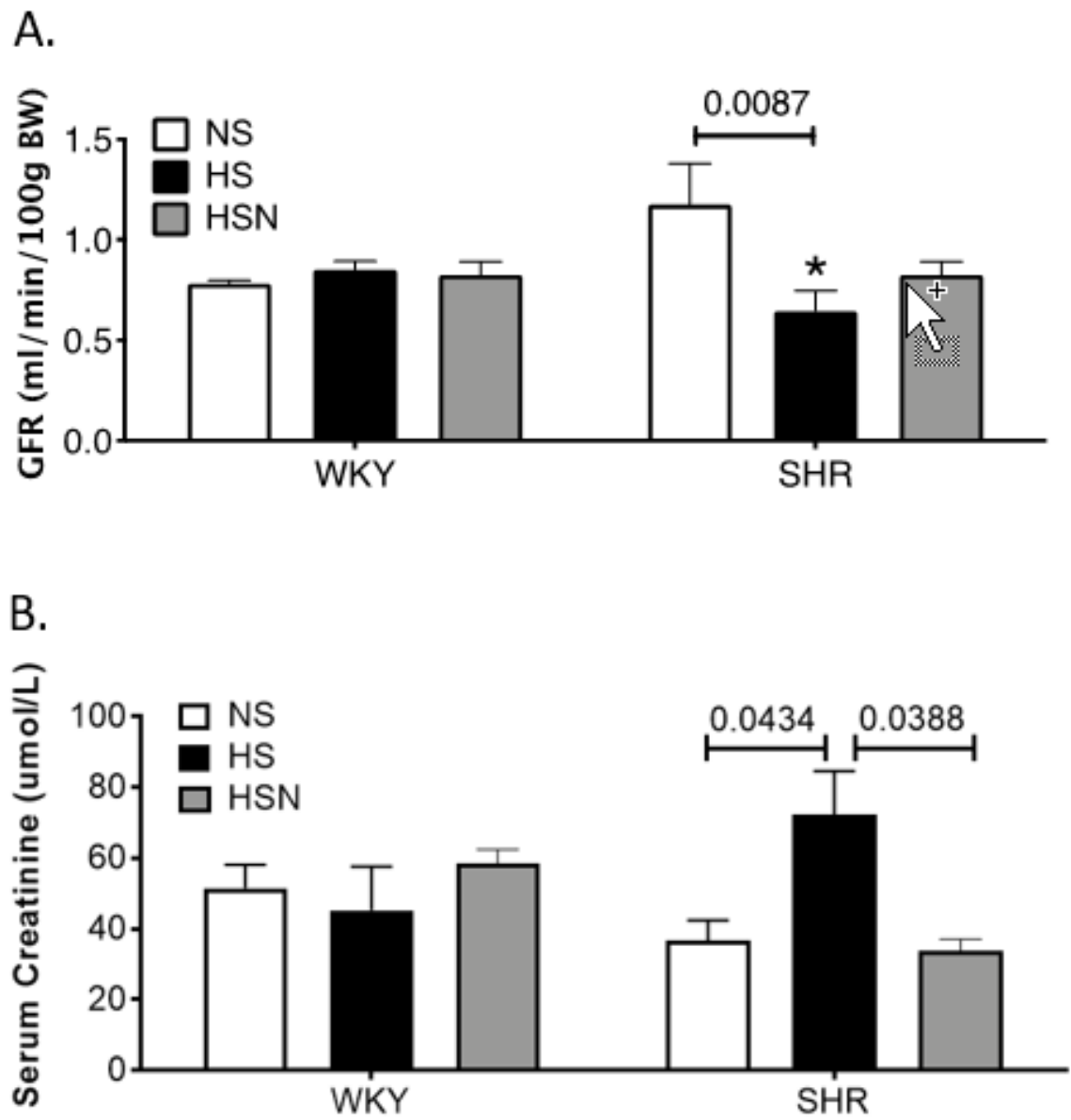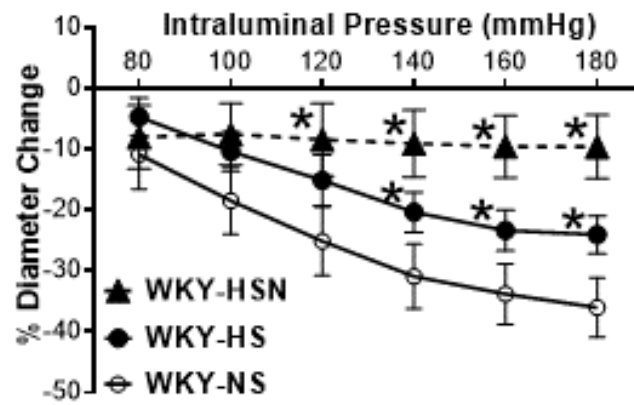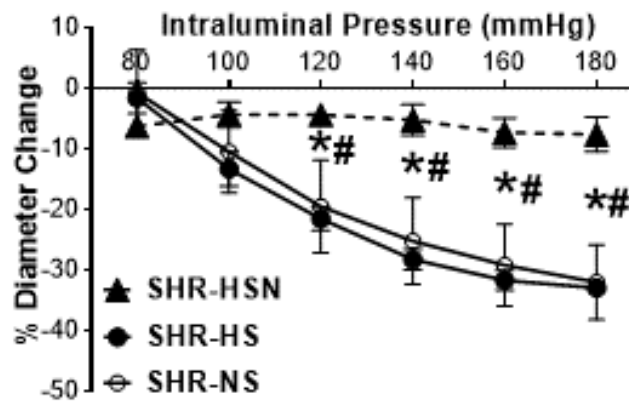
Figure 4.

FIGURE 4 | Renal functional assessments through glomerular filtration rate (GFR) and serum creatinine measurements. A) GFR (ml/min/100 g body weight) comparison at endpoint. **B)** Serum creatinine (umol/L) comparison at endpoint. $P \leq 0.05$ was statistically significant, demonstrated by * or P-value. Star (*) compares to WKY of the same diet. For GFR: N (WKY-NS) = 5, N (WKY-HS) = 4, N (WKY-HSN) = 5, N (SHR-NS) = 5, N (SHR-HS) = 5, N (SHR-HSN) = 5. For creatinine: N (WKY-NS) = 9, N (WKY-HS) = 5, N (WKY-HSN) = 7, N (SHR-NS) = 5, N (SHR-HS) = 7, N (SHR-HSN) = 5. NS = normal salt, HS = high salt, HSN = HS plus nifedipine.
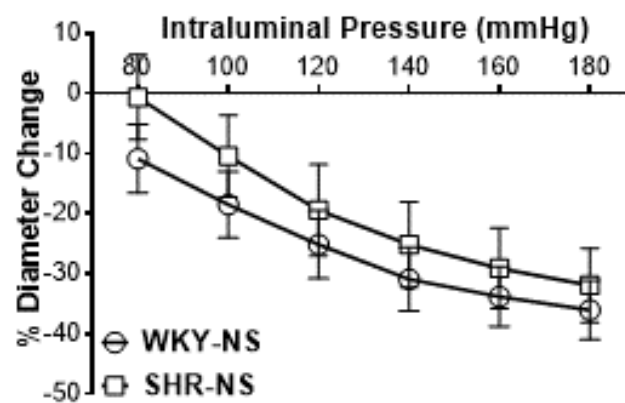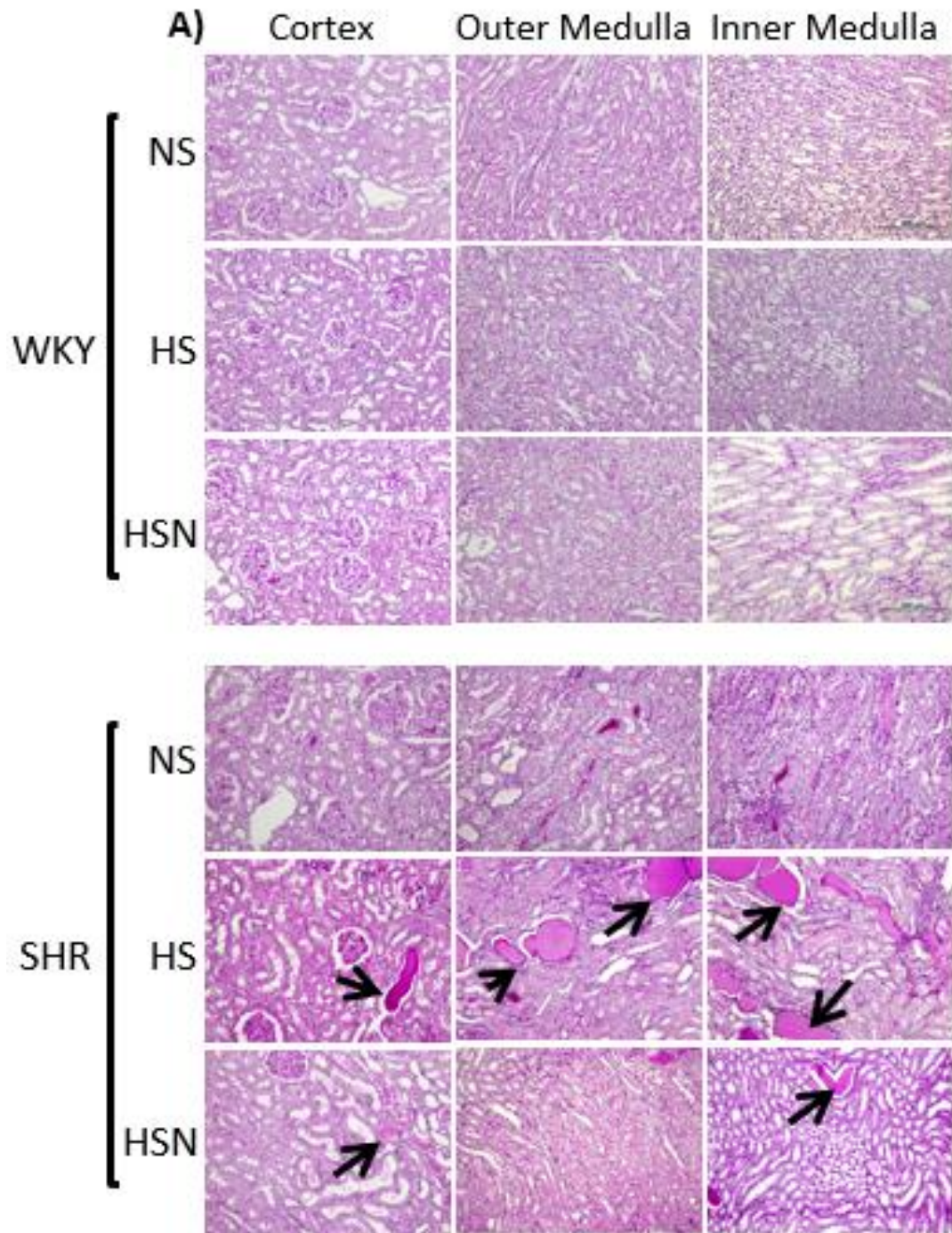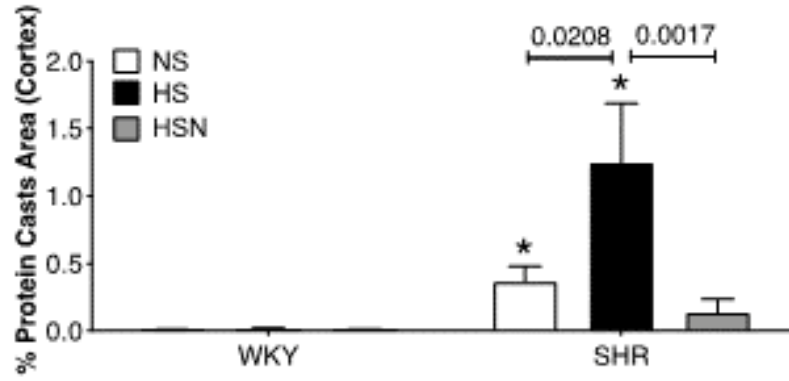
Figure 5.

FIGURE 5 | Myogenic constriction (MC) in arcuate arteries after 8 weeks of diet consumption. A) MC comparison in the WKY. **B)** MC comparison in the SHR. **C)** MC comparison between WKY and SHR. The % Diameter Change was normalized to the vessel's diameter in calcium-free buffer as was explained in the methods. $P \leq 0.05$ deemed statistically significant, shown by * or #. Star (*) compares to NS. Hash (#) compares to HS. Regular 2-way ANOVA was used to compare each treatment group with either the NS or HS groups at a given pressure. Holm-Sidak post-hoc test with 95% confidence interval was used to correct for the differences. When "N" is the number of vessels, "n" is the number of animals: N (WKY-NS) = 4, N (WKY-HS) = 5, N (WKY-HSN) = 5, N (SHR-NS) = 5, N (SHR-HS) = 5, N (SHR-HSN) = 6. N (WKY-NS) = 6, n (WKY-HS) = 5, n (WKY-HSN) = 6, n (SHR-NS) = 6, n (SHR-HS) = 5, n (SHR-HSN) = 8. NS = normal salt, HS = high salt, HSN = HS plus nifedipine.

Figure 6.

B) Protein Cast in Cortex

C) Protein Cast in Medulla
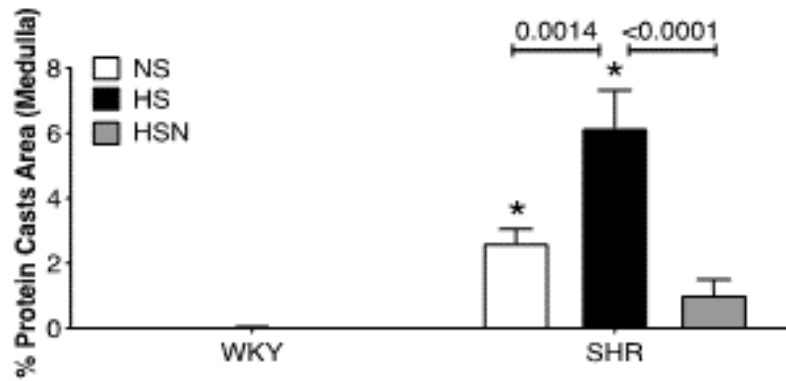
FIGURE 6 | Percent cortical and medullary protein casts area measured by Periodic Acid-Schiff (PAS) staining. A) PAS-stained micrographs comparing protein casts between WKY and SHR in renal cortex and medulla. **B)** Cortical % protein casts area comparisons. **C)** Medullary % protein casts area comparisons. $P \leq 0.05$ was statistically significant, shown by P-value or *. Star (*) compares to WKY of the same diet. N (WKY-NS) = 4, N (WKY-HS) = 4, N (WKY-HSN) = 4, N (SHR-NS) = 4, N (SHR-HS) = 4, N (SHR-HSN) = 5. NS = normal salt, HS = high salt, HSN = HS plus nifedipine.

Figure 7.
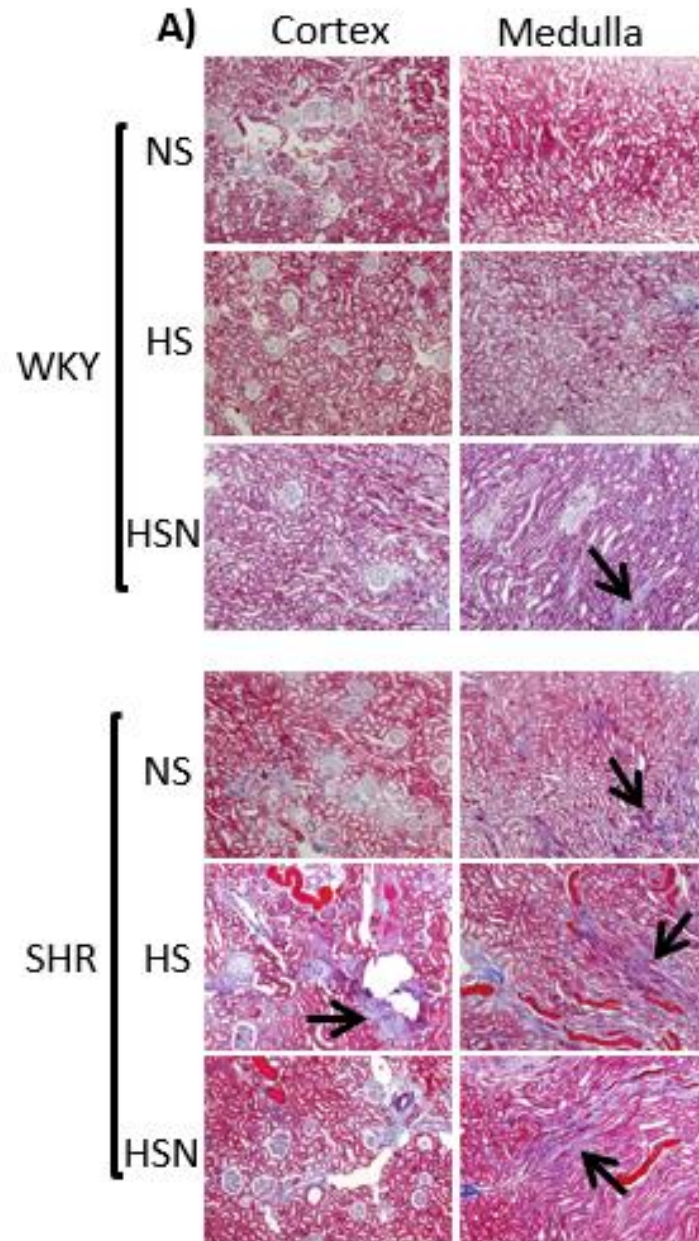
B) Interstitial Fibrosis in Cortex

C) Interstitial Fibrosis in Medulla

FIGURE 7 | Percent cortical and medullary interstitial fibrosis area measured by masson's trichrome staining. A) Trichrome-stained micrographs comparing interstitial fibrosis between WKY and SHR in renal cortex and medulla. **B)** Cortical % interstitial fibrosis comparisons. **C)** Medullary % interstitial fibrosis comparisons. $P \leq 0.05$ was statistically significant, shown by P-value or *. Star (*) compares to WKY of the same diet. N (WKY-NS) = 3, N (WKY-HS) = 4, N (WKY-HSN) = 4, N (SHR-NS) = 3, N (SHR-HS) = 4, N (SHR-HSN) = 5. NS = normal salt, HS = high salt, HSN = HS plus nifedipine.

Figure 8.

A) Left Kidney

B) Right Kidney

C) Heart
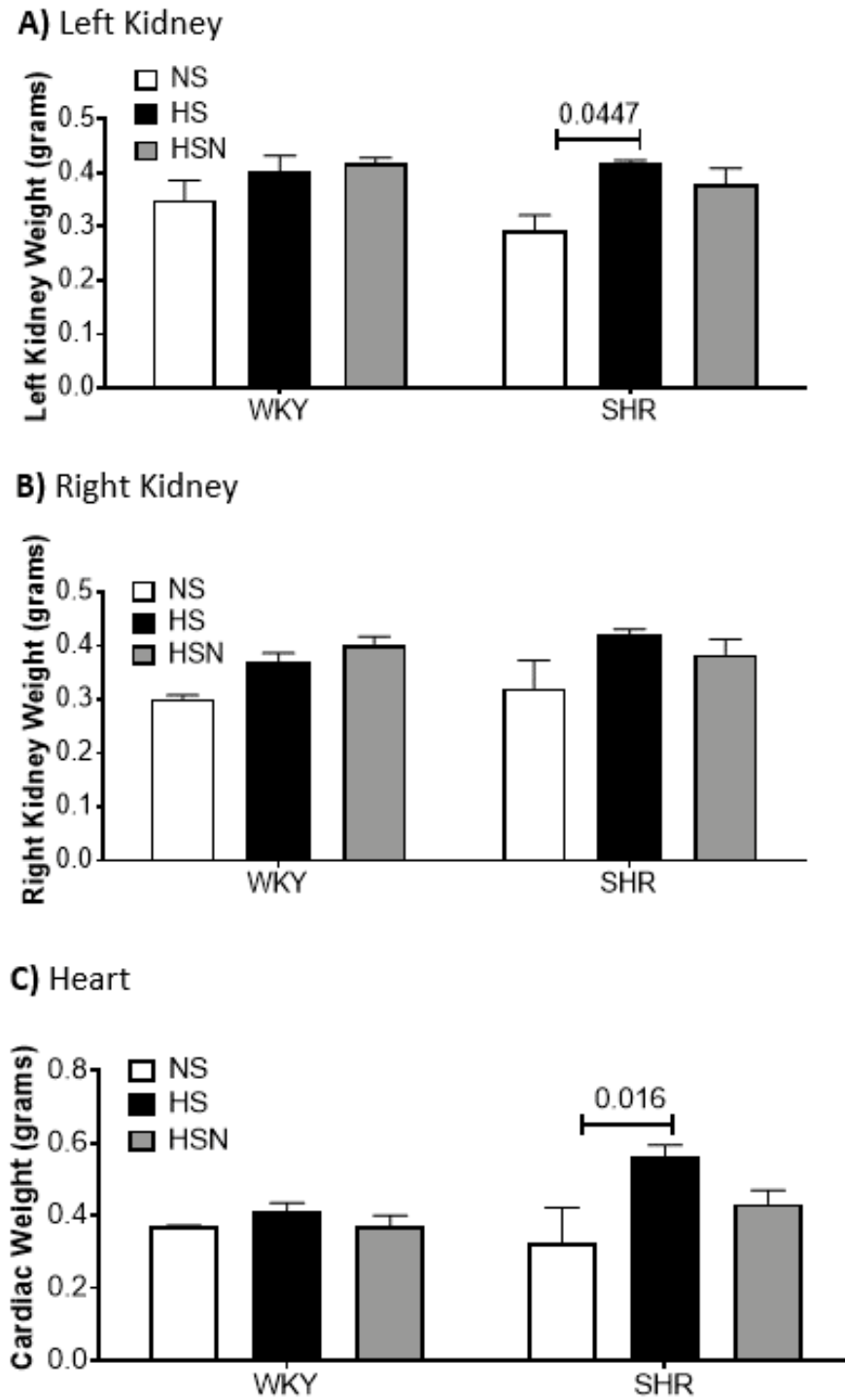
FIGURE 8 | Cardiac and kidney weight assessments at endpoint. A and B) left and right kidney weight (grams) measurements. **C)** Cardiac weight measurements. $P \leq 0.05$ was statistically significant, demonstrated by P-value. N (WKY-NS) = 3, N (WKY-HS) = 4, N (WKY-HSN) = 4, N (SHR-NS) = 3, N (SHR-HS) = 3, N (SHR-HSN) = 5. NS = normal salt, HS = high salt, HSN = high salt plus nifedipine.
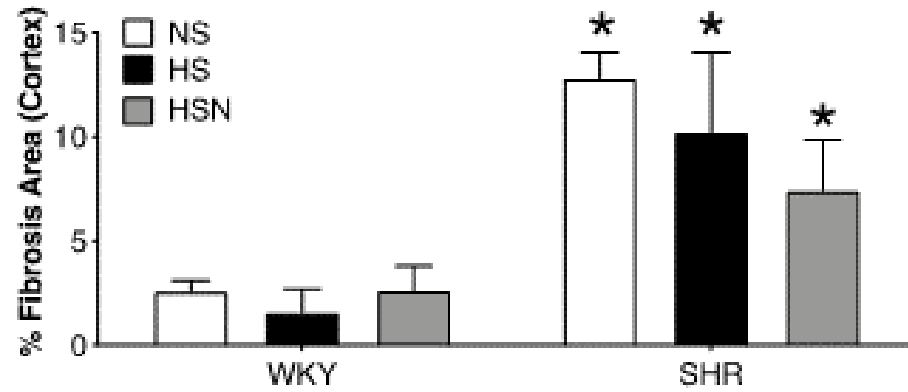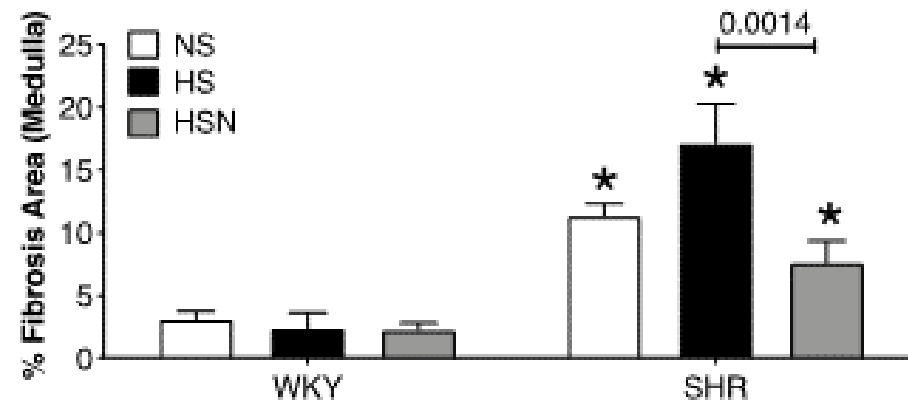
Figure 9.
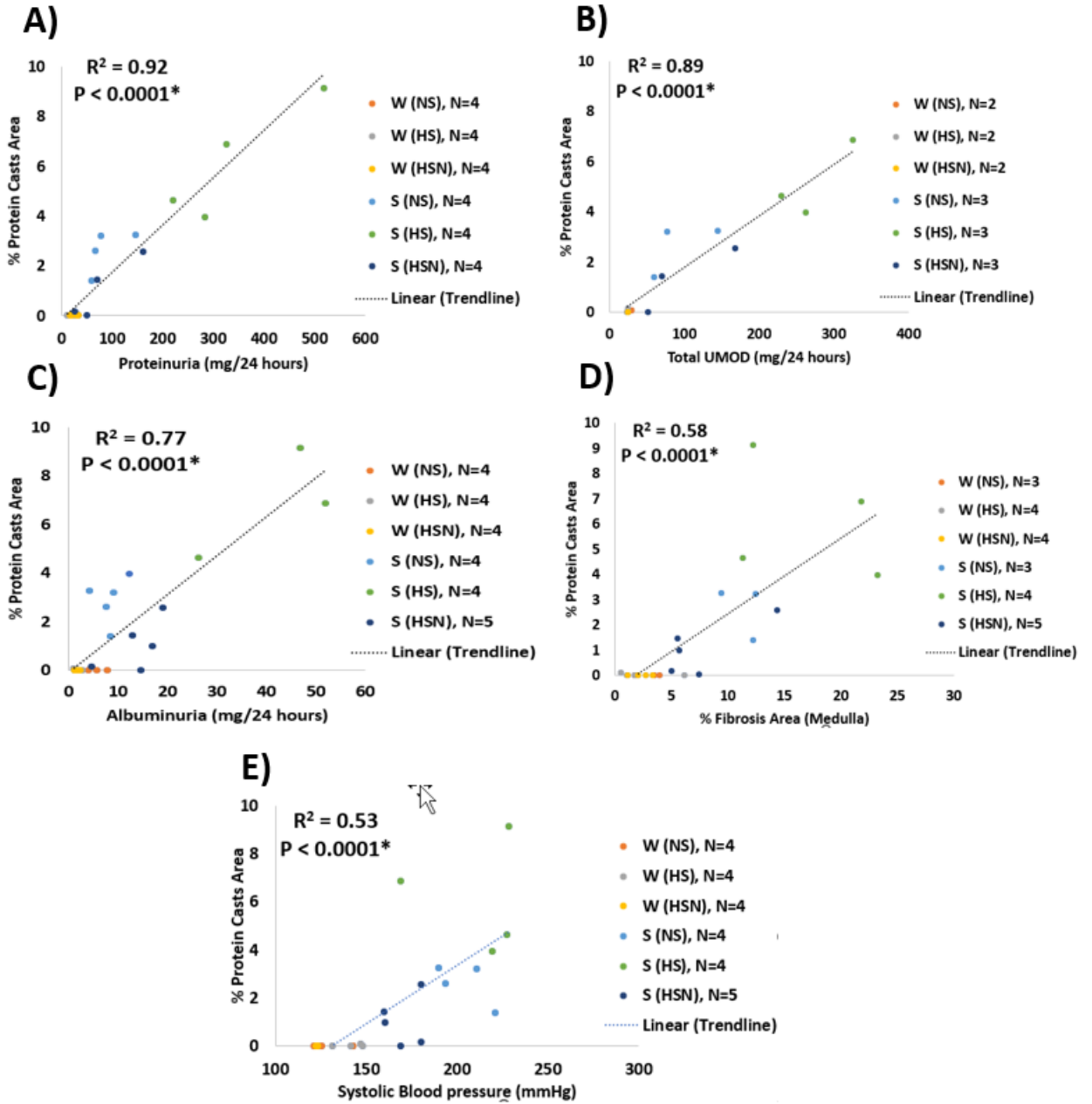
FIGURE 9 | Correlation Studies. Correlation between % protein casts area and **(A)** proteinuria, **(B)** total 24-hour uromodulin (UMOD, mg/24hs), **(C)** 24- hour albuminuria, **(D)** % medullary fibrosis area, and **(C)** systolic blood pressure**.** $P \leq 0.05$ was statistically significant, denoted by a star (*). NS = normal salt, HS = high salt, HSN = high salt plus nifedipine.

CHAPTER 4

Renal Disease in the Dahl Salt Sensitive (DSS) is Associated with

Excessive Uromodulin Excretion

Samera Nademi[1], Victoria Yum[1], Chao Lu[2], and Jeffrey G. Dickhout[1,2]

Public Library of Science

Chapter Summary:

One in three adults in the United States suffers from hypertension but the prevalence of hypertension is substantially higher amongst Chronic Kidney Disease (CKD) patients [1, 2]. CKD is a gradual loss of kidney function. Approximately 50-90% of CKD patients also suffer from hypertension in the United States, making hypertension the second leading cause of CKD [3]. Two animal models commonly used in hypertension and CKD research are the Spontaneously Hypertensive Rats (SHR) and Dahl Salt Sensitive (DSS) rats. SHR is resistant but DSS is susceptible to developing kidney disease particularly upon high salt feeding, even though SHR are more hypertensive than the DSS rats. This paper for the first time compared these two commonly used animal models in terms of blood pressure, myogenic constriction (MC), and urinary uromodulin (UMOD) excretion to elucidate the pathogenesis of CKD in the DSS. MC is contraction of arteries in response to increasing intraluminal pressure, while UMOD is the most abundant protein that is excreted in normal urine. We were the first to measure UMOD excretion levels in the DSS and SHR rats; as well as to compare the urinary UMOD levels between the DSS and SHR rats. We have concluded in this paper that UMOD overexcretion may play a critical role in the pathogenesis of the DSS, potentially through coagulation of kidney tubules, leading to nephron loss and eventually CKD.

Author's Contribution:

S. Nademi and J.G. Dickhout designed the study. S. Nademi, V. Yum, and C. Lu performed the experiments. S. Nademi and V. Yum analyzed the data. S. Nademi and J.G. Dickhout interpreted the results. S. Nademi prepared the figures and drafted the manuscript. S. Nademi and J.G. Dickhout edited and revised the manuscript. All authors approved the final version of the manuscript.

Title: Renal Disease in the Dahl Salt Sensitive (DSS) is Associated with Excessive

Uromodulin Excretion

Authors: Samera Nademi[1], Victoria Yum[1], Chao Lu[2], and Jeffrey G. Dickhout[1,2]

[1] Department of Medicine, Division of Nephrology, McMaster University, Hamilton,

ON, Canada, [2] St. Joseph's Healthcare Hamilton, Hamilton, ON, Canada

Address Correspondence to:

Jeffrey G. Dickhout, PhD

Department of Medicine, Division of Nephrology

McMaster University and St. Joseph's Healthcare Hamilton

50 Charlton Avenue East, T-3312

Hamilton, ON, Canada, L8N 4A6

Tel: 905-522-1155 ext. 35334

Fax: 905-540-6589

Email: jdickhou@stjosham.on.ca

Keywords: Chronic Kidney Disease, Hypertensive, DSS, SHR, WKY, BN13, Salt

Sensitivity, Uromodulin, Proteinuria, Albuminuria, Myogenic Constriction

ABSTRACT

Background: Dahl Salt Sensitive (DSS) and Spontaneously Hypertensive Rats (SHR) are two commonly used animal models of hypertension and chronic kidney disease (CKD). Nevertheless, the development of kidney disease in these animal models in the context of a normal salt (NS) or a high salt (HS) diet is not fully understood. The purpose of this study was to investigate the relationship between blood pressure, sodium chloride loading, myogenic constriction (MC), and protein excretion including uromodulin (UMOD) on the development of CKD in these models. UMOD is the most abundant protein in normal urine; MC is contraction of small arterioles with increasing intraluminal pressure and may provide protection for the glomerulus in the context of high blood pressure. This study compared DSS with SHR to investigate the role of hypertension, urinary UMOD, and MC in renal pathology and CKD progression. **Methods:** DSS, SHR, and their age-matched normotensive controls, Consomic Brown Norway chromosome 13 DSS (BN13) and Wistar Kyoto Rats (WKY), were placed on either HS (8% NaCl) or NS (0.4% NaCl) diet for 4 weeks. **Results:** At endpoint, SHR was significantly more hypertensive than the DSS regardless of salt feeding but showed minimal renal pathology. DSS showed renal injury regardless of salt feeding, but HS diet worsened the pathology. HS diet also attenuated or abolished MC in all rats, except for BN13-HS. MC was augmented in the SHR versus WKY controls; but MC was similar between SHR and DSS regardless of salt diet. DSS excreted more 24-hr urinary UMOD compared to the SHR regardless of salt feeding, but HS exacerbated this. Urinary UMOD levels had the strongest correlation with protein casts in the tubular lumen of SHR and

DSS kidneys. **Conclusions:** These results suggest that the observed CKD in the DSS may be mediated through increased UMOD excretion in response to salt loading. UMOD appears to be polymerizing in nephron tubules, forming protein casts, and obstructing the tubules leading to nephron loss**.**

INTRODUCTION

Chronic Kidney Disease (CKD) is a gradual and persistent loss of kidney function that often progresses to end-stage renal disease (ESRD), requiring dialysis or renal transplantation [4]. CKD characteristics in human includes proteinuria, albuminuria, renal interstitial fibrosis, increased serum creatinine, increased blood urea nitrogen (BUN), glomerular damage, renal inflammation, and hypertension. Approximately 85% to 95% of stage 3-5 CKD patients suffer from hypertension [5], the second leading cause of renal disease world-wide [6]. Hypertension and CKD often go hand-in-hand with one exacerbating the other [7, 8]. On one hand, hypertension often results in CKD and is associated with a faster CKD progression [9]; on the other, CKD exacerbates hypertension through volume expansion and increased systemic vascular resistance [10]. Hypertension is sometimes accompanied by salt sensitivity which worsens the hypertension and CKD, commonly resulting in ESRD [11]. About 50% of hypertensive individuals and 25% of normotensive people are also salt-sensitive [12]. Two hypertensive animal models that are commonly used in hypertension and renal research are Dahl Salt Sensitive (DSS) and Spontaneously Hypertensive Rats (SHR) [13]. Even though both are hypertensive, high salt (HS) diet induces severe renal disease in the DSS while it minimally affects the SHR [14, 15]. One reason that SHR shows resistance to developing CKD in spite of its hypertension may be the existence of an enhanced myogenic constriction (MC) in its renal arterioles compared to its normotensive control, Wistar Kyoto Rats (WKY) [16]. MC is defined as contraction of small arterioles in response to increasing intraluminal pressure (vessels contract with increasing pressure

instead of dilating) [17]. Impaired MC in patients and animal models has been associated with progressive albuminuria, proteinuria, glomerulosclerosis, and fibrosis in the kidneys [18-23]. It has been shown that MC is impaired in the DSS rats that were fed HS diet and this was associated with extensive renal damage [15]. We hypothesized that HS diet impairs MC in DSS rats but not age-matched SHR rats, leading to an extensive renal damage in the DSS-HS but not the SHR-HS rats. We also examined the role of uromodulin (UMOD) in the pathogenesis of CKD in the DSS and the SHR. UMOD, also called Tamm-Horsfall protein, is the most abundant protein in normal urine and is expressed exclusively by epithelial cells of the thick ascending limb (TAL) of the loop of Henle and distal convoluted tubules (DCT, 10% of TAL expression) of the kidneys [24]. Genome-wide association studies have shown common variants in UMOD coding region to have the strongest association with CKD in human populations [25]. New research by Sjaard et al. used a Mendelian randomization to demonstrate that UMOD is a causal mediator of CKD [26]. A meta-analysis study also showed that the UMOD promoter and non-coding variants induce overexpression and overexcretion of UMOD and are associated with CKD in the general population [27]. Therefore, we hypothesized that renal disease in the DSS is mediated by excessive UMOD excretion in addition to impaired MC. To investigate these hypotheses, we gave HS diet to 12 weeks-old DSS, SHR, and their respective controls, Consomic Brown Norway chromosome 13 DSS (BN13) and WKY, for 4 weeks and measured their preglomerular MC, UMOD excretion, and renal pathology. To our knowledge this is the first study that measured UMOD excretion levels in the DSS and SHR; and compared the two animal models in terms of

blood pressure, MC, and urinary UMOD to elucidate the pathogenesis of CKD in the DSS.

METHODS

Animal Studies.

Twelve-weeks old male DSS and SHR, and their respective age-matched controls, male BN13 and WKY, were divided equally into two diet groups: either HS (8% NaCl; AIN-76A) or normal salt (NS, 0.4% NaCl; AIN-76A) and consumed the diets for 4 weeks until the rats were 16 weeks old. At endpoint, animals were placed in metabolic cages and their 24hr-urine samples were collected for urinalysis studies. At the end of the study period, animals were anesthetized with isoflurane, perfused *with* Hank's basic salt solution (HBSS), and their kidneys were collected for staining and vessel studies. Blood was also collected in heparinized tubes by puncturing the left ventricle to measure plasma creatinine and BUN levels. All rats were bred at McMaster University Central Animal Facility, maintained at St Joseph's Healthcare Hamilton Animal Facility, and housed with a 12-hour light-dark cycle and had free access to food and drinking water. All animal work was approved by McMaster University Animal Research Ethics Board and performed in accordance with their guidelines.

Blood Pressure Measurements

After 4 weeks of diet consumption, blood pressure was measured using tail cuff plethysmography (Kent Scientific, CODA system). Rats were restrained in a holder tube,

occlusion tail cuffs were placed at the base of the tails, and a volume pressure recording (*VPR*) sensor cuff was used to measure heart rate, systolic (SBP) and diastolic blood pressure (DBP).

Urinalysis

Proteinuria. Total 24hr-urine protein was measured using Bio-Rad Bradford Protein Assay (5000006, BioRad; Mississauga, Canada) with Rat Bovine Serum Albumin (BSA) standards based on the manufacturer's instructions.

Albuminuria. Total 24hr-urine albumin was measured using a rat enzyme-linked immunosorbent assay (ELISA) kit (E111-125, Bethyl Laboratories Inc; Burlington, Canada) according to supplier's specifications. Briefly, 96-well plates were coated with primary antibody in coating buffer overnight, blocked for 1 hour, incubated with samples and standards for an hour, followed by horseradish peroxidase (HRP) detection antibody treatment. After the wells were washed, tetramethylbenzidine (TMB) substrate solution (Sigma Aldrich) was added and the reaction was stopped with 0.18 M H_2SO_4. Absorbance was then measured at 450 nm using a plate reader (Molecular Devices Spectra Max Plus384 Absorbance Microplate Reader).

Extracting Urinary UMOD to Use as Standards. To construct a standard curve for western blot analysis, UMOD was extracted from 30-week-old WKY rats (on normal chow diet). UMOD was extracted using Trichloroacetic (TCA) acid-acetone precipitation

method [28]. To extract, the 24-hour collected urine was centrifuged at 3000 relative centrifugal force (RCF) for 15 mins to remove any sediment, then the supernatant was concentrated by 30000 molecular weight cutoff (MW) Amicon® Ultra-15 Centrifugal Filter (Sigma Aldrich) for 15 mins at 3000 RCF at 25 ^{0}C, 1 mL of the concentrated urine was collected from the upper chamber. Subsequently, 850 μl of the concentrated urine was mixed with 150 μl of 100% TCA. This mixture was incubated at 4 ^{0}C for 1 hour, and centrifuged at 14000 RCF for 10 mins. Then the bottom pellet containing the precipitated UMOD was incubated with ice-cold acetone for 5 mins, centrifuged at 14000 g for 10 mins, and this process was repeated twice to wash. After discarding the supernatant and air-drying the pellet, 1ml 15 mM Tris buffer (pH 8.8) was added and mixed well until the UMOD was completely dissolved. The resulting mixture was the purified UMOD suspended in Tris buffer and was evaluated using western blotting and UMOD antibodies (1:10000, ab207170) as described in the next section. Supplementary **Figure 1** illustrates that almost all collected proteins were identified by the UMOD antibody. UMOD concentration was determined using BioRad DC Protein Assay (BioRad; Mississauga, Canada) and was diluted serially to 5, 2.5, 1, and 0.5 mg/ml. These 4 serial dilutions were used to construct a standard curve from which samples' concentrations were calculated.

Urinary UMOD Detection. Standards and samples were diluted 1:2 in 4X SDS lysis buffer that contained protease inhibitor cocktail (Roche) and phosphatase inhibitor cocktail (Roche) and separated in SDS-PAGE electrophoresis (BioRad; Mississauga, Canada). The primary antibody for UMOD, Abcam ab207170 (1:10000 dilution), was

detected using appropriate horseradish peroxidase-conjugated secondary antibodies (1:25000, 170-6515, BioRad; Mississauga, Canada) and ECL Western Blotting Detection Reagents (Amersham, RPN3244), as previously reported [29]. Results were analyzed using the ChemiDoc Imaging Systems (BioRad; Mississauga, Canada) and Image Lab software. To quantify urinary UMOD concentration (mg/ml), equation of the fitted standard curve was obtained from the 4 serially diluted standards. Band volumes of the samples were plotted into this equation and UMOD concentration (mg/ml urine) was calculated. To quantify total urinary UMOD excretion, UMOD concentration (mg/ml) was multiplied by the 24-hour urine volume from which the concentration was measured.

Myogenic Constriction Measurements

Arcuate arteries were dissected out of the kidneys and transferred into a myogenic chamber containing oxygenated HBSS at 37^0C. Arteries were mounted and sutured onto a micropipette, and blind-sacs were created as previously described [30]. The vessel's viability was tested by 80 mM potassium chloride (KCl) treatment followed by a 30 min equilibration time. Only vessels that showed a viable KCl constriction response were utilized. Subsequently, the vessels were subjected to 80 mmHg pressure and allowed 30 min to equilibrate. To measure MC, lumen diameter was then recorded at 80, 100, 120, 140, 160, and 180 mmHg pressures, allowing a 5 min-interval between each pressure change. Percent Diameter Change (normalized to P80) was calculated by subtracting lumen diameter at P80 mmHg ($D_{P80\ mmHg}$) from the lumen diameter at the current

pressure point (D_n), divided by the diameter at ($D_{P80\ mmHg}$), and multiplied by 100 (%

Diameter Change (normalized to P80) $= \left(\dfrac{D_n - D_{P80\ mmHg}}{D_{P80\ mmHg}} \right) * 100$).

Histological Assessments

After sacrificing the rats, their kidneys were fixed in 4% paraformaldehyde, embedded in paraffin blocks, sectioned 4 μm-thick using a microtome, and mounted on charged Superfrost™ Plus slides.

Periodic Acid-Schiff (PAS) Staining. Sections were deparaffinized by Xylene and graded ethanol solutions, oxidized with 1% aqueous periodic acid, treated with Schiff reagent, counterstained with hematoxylin, dehydrated through graded ethanol and Xylene solutions, and mounted. All section slides were imaged using Olympus BX41 microscope with 20x objective lens. To quantify protein cast areas, 10 PAS-stained images per animal were analyzed. The hand tool in the Image J software was used to draw and calculate protein cast areas per image. The values for each image were then summed, divided by the area of the entire image, and multiplied by 100 to provide the % protein casts area for each image.

Pico Sirius Red (PSR) Staining. Sections were deparaffinized by Xylene and graded ethanol solutions, incubated with saturated picric acid solution, and then treated with Sirius red F3B (Colour Index 35782). All section slides were imaged using Olympus BX41 microscope with 20x objective lens. To quantify interstitial fibrosis, 10 PSR-

stained images per animal were analyzed. Image J software was used to color threshold each image detecting PSR positive stained areas. These areas were then summed and divided by total image area, and multiplied by 100% to provide the % interstitial fibrosis area for each image.

Glomerular Damage Scoring. Five images for each animal per diet group were randomly taken from the PAS-stained section cortex. Two trained and experienced researchers (SN and JD) scored the glomeruli either 0 (0% damage), 1 (25% damage), 2 (50% damage), 3 (75% damage), or 4 (100% damage) based on a scale described by El Nahas in 1987 [31]. The researchers were blinded to the strain and diet of the animals. An average of 26 glomeruli per animal was scored. The total glomeruli scored per group (N) were as following: N (SHR-NS) = 123, N (SHR-HS) = 134, N (DSS-NS) = 139, N (DSS-HS) = 146, N (WKY-NS) = 102, N (WKY-HS) = 122, N (BN13-NS) = 133, and N (BN13-HS) = 143.

Serum Analysis

Plasma creatinine levels were determined using an enzymatic assay (c7548-120, Pointe Scientific) based on the manufacturer's instructions. Briefly, plasma samples and standards were placed in 96-well plate, incubated with 'reagent 1' at 37 °C for 5 min, read absorbance at 550 nm (A1), incubated with 'reagent 2' at 37 °C for 5 min, and read absorbance at 550 nm again (A2). The change in the absorbance values (A2-A1) were interpolated into the standard curve and creatinine values were calculated. Serum BUN

levels were also measured using spectrophotometry according to the supplier's specifications (EIABUN, ThermoFisher Scientific).

Correlation studies

SHR-NS, SHR-HS, DSS-NS, and DSS-HS were used for the correlation studies. Urinary UMOD, proteinuria, albuminuria, % fibrosis area, systolic blood pressure, and glomerular damage score were correlated with % medullary protein casts area values as a measure of renal pathology using the GraphPad Prism software. R-squared values were calculated to determine the degree that the above predictive variables accounted for variations in renal pathology measured by protein casts levels.

Statistical analysis

Significant differences were evaluated using the GraphPad prism and 95% confidence intervals. P-values less than or equal to 0.05 were deemed statistically significant. When there were more than 2 groups with 1 or 2 independent variables, one-way or two-way Analysis of Variance (ANOVA) were used respectively, followed by Holm-Sidak post-hoc test to determine significant differences between the groups. The results are reported as mean ± standard error of the mean (SEM).

RESULTS

Blood pressure

SHR showed significantly higher SBP than the DSS irrespective of salt consumption (**Figure 1A**). Additionally, SHR-NS had a higher DBP compared to DSS-NS (**Figure 1B**). Both SHR and DSS were hypertensive compared to their normotensive controls, WKY and BN13 respectively, regardless of salt feeding. Nevertheless, HS diet increased SBP and DBP in the DSS. SHR blood pressure was not changed as a result of HS feeding (**Figure 1A, 1B**).

Urinalysis.

Regardless of salt intake, 24-hr proteinuria and albuminuria were higher in the DSS compared to the SHR (**Figure 2A, 2B**). Nevertheless, 4 weeks of HS consumption increased the 24-hr proteinuria and albuminuria in the DSS rats, but not the SHR (**Figure 2A, 2B**). Also, DSS-HS showed elevated proteinuria and albuminuria compared to BN13-HS (**Figure 2A, 2B**). Urinary UMOD concentration (mg/ml) was increased in the DSS-HS versus SHR-HS (**Figure 3A**). Nevertheless, 4 weeks of HS feeding did not change urinary UMOD concentration (mg/ml) in the DSS but decreased it in the SHR (**Figure 3A**). HS feeding increased 24-hr urine volume, but there were no strain-related differences (**Figure 3B**). Similar to proteinuria and albuminuria, total UMOD excretion (mg/24 hours) was higher in the DSS versus SHR regardless of salt intake. Further, 4 weeks of salt consumption increased the 24-hr total UMOD excretion in the DSS rats (**Figure 3C**).

Myogenic Constriction in Renal Arcuate Arteries.

Between P140-180 mmHg intraluminal pressure, HS feeding decreased MC in both WKY and SHR (WKY-HS and SHR-HS demonstrated by elevated % diameter change compared to WKY-NS and SHR-NS respectively) (**Figure 4A**, illustrated by #). SHR-NS demonstrated an augmented MC (decreased % diameter change) compared to the WKY-NS at P100 and P140-180 mmHg (**Figure 4A**, shown by *). SHR-HS also showed an enhanced MC (decreased % diameter change) versus the WKY-HS at 160 and 180-mmHg intraluminal pressure (**Figure 4A**, shown by *). Similarly, HS feeding significantly decreased MC in the DSS-HS compared to the DSS-NS (higher % diameter change) between P120-180 mmHg (**Figure 4B**, shown by #). MC in the DSS-HS was also significantly reduced compared to its control, BN13-HS, between P120-180 mmHg (**Figure 4B**, shown by *). There were no differences between DSS and SHR MC in the same diet group, even though HS feeding decreased MC in both DSS and SHR rats compared to NS feeding (**Figure 4C**, shown by #).

Renal Histological Assessment.

DSS rats showed significantly more cortical and medullary % protein casts area than SHR rats, regardless of salt feeding. However, HS diet further increased the % protein casts area in the DSS in both cortex and medulla compared to NS diet. Additionally, DSS-HS exhibited higher % protein casts area than BN13-HS (**Figure 5A, 5B**). Likewise, glomerular damage score was higher in the DSS compared to the SHR

regardless of salt feeding. DSS rats also showed significantly higher glomerular damage than BN13 rats irrespective of the diets (**Figure 5C**).

PSR staining (**Figure 6A**) revealed that cortical % fibrosis area was only elevated in the DSS-HS versus SHR-HS; and DSS-NS versus BN13-NS (**Figure 6B**). Medullary % fibrosis area was higher in the DSS compared to both SHR and BN13 regardless of salt diets. Though, HS worsened the observed medullary fibrosis in the DSS and BN13 rats (**Figure 6C**).

Serum Analysis.

Plasma creatinine levels were higher in the DSS compared to the SHR and BN13 regardless of salt feeding. (**Figure 7A**). BUN levels were also elevated in the DSS-HS and SHR-HS versus their respective controls, BN13-HS and WKY-HS. Nonetheless, DSS-HS showed increased BUN levels compared to SHR-HS (**Figure 7B**).

Correlation Comparisons.

In order to determine the degree that the parameters in the x-axis accounted for variations in % protein casts area (as a measure of renal pathology), coefficient of determinations (R-squared) were calculated (**Figure 8**). R-squared of % protein casts area versus % medullary fibrosis area (0.89), 24-hr urinary UMOD (0.82), proteinuria (0.76), and albuminuria (0.74) were positive and statistically significant (**Figure 8, A-D**).

Conversely, correlation coefficient of % protein casts area versus SBP (0.1) and glomerular damage score (0.01) were not statistically significant (**Figure 8, E-F**).

DISCUSSION

The goal of this study was to investigate whether renal disease in the DSS with or without a HS diet was mediated by excessive UMOD excretion, hypertension, or impaired MC. Excess sodium intake has been shown to induce several abnormalities such as hypertension, proteinuria, albuminuria, renal interstitial fibrosis, decreased glomerular filtration rate, and impaired vascular MC [32-34]. Some of these abnormalities follow the development of hypertension, yet others are independent of the elevated blood pressure [34-37]. We used HS diet to attempt to induce kidney disease in salt-sensitive DSS and salt-resistant SHR, measured renal pathology, and investigated the role of HS, hypertension, altered MC, and UMOD excretion in the observed renal pathology. Age of salt feeding initiation in the DSS was shown to be important for the speed of the CKD development, as weaning rats that were placed on HS developed hypertension, severe CKD, and ESRD much faster than 24-week-old rats [38]. To avoid effects of HS diet on nephron development, which occurs postnatally in the rat, we chose 12-week-old rats to initiate HS diet in our study.

We gave HS (8% NaCl) and NS (0.4% NaCl) diets to DSS, SHR, and their respective age-matched normotensive controls - BN13 and WKY. The BN13 is a DSS consomic strain that has its chromosome 13 substituted from Brown Norway (BN) rat

[39]; while the WKY are inbred from the same ancestral outbred, Wistar rat, as the SHR [40]. SHR develops hypertension at around 4-5 weeks [41, 42] but demonstrates little to no renal injury as a result [43]. This could be because SHR shows an augmented MC in its small renal arterioles due to increased thromboxane A2 secretion, protecting the kidneys from the chronically elevated systematic blood pressure [16]. DSS, on the other hand, develops hypertension and extensive renal injury upon salt feeding [43, 44]. Though, DSS rats and salt-sensitive humans develop hypertension over time even on a NS diet [45].

Our results showed that 16-week-old SHR were significantly more hypertensive (higher SBP) than DSS regardless of salt feeding (**Figure 1A**), which was similar to the findings of other groups at 20 weeks of age [46]. Despite this chronic and malignant hypertension, SHR kidneys suffered from minimal renal damage (**Figure 2, 5, 6, 7**). HS did not induce significant renal injury in WKY and BN13, except for increasing medullary interstitial fibrosis in the BN13 (**Figure 6C**). We also found that HS decreased pressure induced vasoconstriction (called MC) in the SHR-HS arcuate arteries compared to the SHR-NS (**Figure 4A**), but this was not associated with significant renal injury in the SHR. One reason could be that MC was not completely abolished but only reduced in the SHR (**Figure 4A**). However, MC of SHR-HS was not significantly different from DSS-HS (**Figure 4C**) suggesting that the enhanced MC in the SHR could not be the reason for the SHR renal protection. Contrary to the SHR, DSS suffered from extensive renal damage upon salt feeding measured by increased proteinuria, albuminuria, protein

casts (cortex and medulla), and medullary interstitial fibrosis (**Figure 2A, 2B, 5B, 5C, 6C**). DSS blood pressure (both SBP and DBP) also increased with HS feeding (**Figure 1A, 1B**). Several research groups have reported similar results [38, 44, 47]. For instance, Siege et al. found that feeding HS (HS: 4% NaCl vs NS: 0.2% NaCl) to 4-week-old SHR and DSS rats for 10 weeks induced hypertension and renal disease (i.e. higher albuminuria, glomerulosclerosis, tubulointerstitial fibrosis, and renal oxidative stress) in the DSS-HS compared to the DSS-NS and SHR-HS [48]. Additionally, our results showed that DSS-NS suffered from some renal injury (higher cortical and medullary interstitial fibrosis and serum creatinine) compared to the BN13-NS (**Figure 6B, 6C, 7A**). This is consistent with the literature reports that DSS rats develop hypertension and renal damage even on a NS diet [45, 49].

Further, the present study showed that HS abolished MC in the arcuate arteries of DSS compared to DSS-NS and BN13-HS as these vessels dilated with increasing intraluminal pressure similar to when the arteries were placed in Ca^{2+}-free buffer (**Figure 4B**). This could be one of the reasons that HS exacerbated renal injury in the DSS, however even though SHR-HS retained some of their MC, there was no statistical difference in the MC of the DSS-HS and SHR-HS. For this reason, MC alone could not explain sensitivity and insensitivity of the DSS and SHR, respectively, to HS feeding and renal injury. Also given that SHR is more hypertensive than DSS (**Figure 1A, 1B**) but has significantly less renal damage (**Figure 2, 5, 6, 7**), hypertension alone can not explain the observed renal disease in the DSS. In fact, there are mechanisms for improving renal

function independent of blood pressure. Samad et al. showed that elevated proteinuria and serum creatinine levels in HS-fed DSS rats were improved by inhibiting endothelin A receptor independent of blood pressure lowering (46), illustrating potential alternative mechanisms for DSS renal pathology other than merely the high blood pressure.

Genome-wide association studies conducted in 2009 examined the association of 900,000 single nucleotide polymorphisms (SNPs) across human genome with CKD and identified common non-coding variants for UMOD gene to have the strongest association with CKD [50], and even to have a causal link to CKD [26]. For this reason, we investigated urinary excretion of UMOD and its correlation with renal pathology in our animal models. To our knowledge, we are the first to measure and report excreted UMOD levels in the DSS and inbred-SHR rats (it has previously been measured in stroke-prone SHR rats [51, 52]). We are also the first to compare SHR and DSS rats on their excreted UMOD levels. Urinary UMOD western blot analysis in our study demonstrated two bands corresponding to approximately 60 to 75 kDa. Similarly, Mary et al. detected 2 bands at approximately 60 and 80 kDa in 24-hour urinary UMOD of pregnant WKY and stroke-prone SHR rats [52]. UMOD is a large 105 kDa glycoprotein that is cleaved into two isoforms prior to being excreted into the urine [52-54]. UMOD excretion into the urine follows a proteolytic cleavage by hepsin, a type II transmembrane serine protease, at the zona pellucida (ZP) domain [54, 55]. The ZP domain polymerizes into high molecular weight filaments that consist of a cysteine-rich domain and three epidermal growth factor-like (EGF-like) domains [55]. We discovered that UMOD

concentration (mg/ml urine) was higher in the DSS-HS versus SHR-HS (**Figure 3A**). HS diet did not change UMOD concentration in the DSS but decreased it in the SHR (**Figure 3A**). Conversely, HS diet increased total UMOD excretion (mg/24 hours) in the DSS (**Figure 3C**). Total UMOD (mg/24 hours) excretion was also higher in the DSS versus SHR regardless of diets (**Figure 3C**). A meta-analysis by Olden et al. showed that UMOD overexpression and overexcretion as a result of promoter and non-coding variants are associated with CKD in a human population of European descent [56]. These results suggest that increased UMOD excretion observed in our study may be strongly contributing to the renal disease in the DSS, particularly when fed HS diet. Cast forming proteins such as Bence Jones proteins and albumin bind to UMOD glycoproteins and form precipitated protein complexes that occlude nephron tubules, leading to nephron loss [57-59]. CKD progresses as more nephrons become dysfunctional, eventually leading to ESRD [57]. In this way, UMOD over-excretion in the DSS may result in excess protein cast filled tubules in the cortex and medulla (**Figure 5A, 5B**) as well as increased interstellar fibrosis (**Figure 6A, 6B**) resulting in exacerbated renal pathology, as was observed and demonstrated in this study.

Contrary to our findings that showed 4 weeks of HS (8% NaCl) consumption reduced UMOD concentration (mg/ml urine) but did not change total 24-hour UMOD (mg/24hour) excretion levels in the SHR (**Figure 3A, 3C**), Mary et al. (2021) reported that 3 weeks of HS consumption (1% NaCl) in drinking water decreased total UMOD excretion in 15 weeks-old stroke-prone-SHR rat. Regrettably, the authors did not assess

potential functional or histological changes associated with the observed alterations (50). The discrepancy between our findings could be explained by the use of different rat strains as stroke-prone-SHR are more sensitive to salt consumption than SHR rats (52). Moreover, Hoyer et al. conducted an immunomorphometric study of individual nephrons by injecting luminal immunoglobulin G (IgG) anti-UMOD antibodies to four rat models: 1) SHR, 2) aging Sprague-Dawley (SD), 3) SD injected with adriamycin (ADR), and 4) SD subjected to subtotal nephrectomy (NX) rats [60]. Interestingly the authors discovered more luminal UMOD deposits in long looped (LL) versus short looped (SL) nephrons, which were significantly correlated with 24-hour albuminuria levels in all their animal models except for the NX rats. The authors concluded that the NX rats display a differential pathogenesis compared to the other rat models [60].

We investigated the correlation between protein casts with urinary UMOD, proteinuria, albuminuria, fibrotic area, glomerular damage, and blood pressure in NS and HS fed SHR and DSS rats. Our results demonstrated that total 24-hour UMOD ($R^2 = 0.82$), proteinuria ($R^2 = 0.76$), albuminuria ($R^2 = 0.74$), and medullary interstitial fibrosis ($R^2 = 0.89$) were strongly and positively correlated with % protein casts area (**Figure 8A-D**). A limitation of these graphs is low sample numbers (N) particularly for the UMOD and the fibrosis graphs. Nevertheless, collectively, these results suggest that the increased protein casts area and the resulting nephron loss in the DSS may be mediated primarily through elements of proteinuria including excessive UMOD and albumin excretion but not high blood pressure per se even when accounting for renal protection from high blood

pressure by MC. These results are consistent with literature reports that hyaline casts, which are the most abundant type of protein casts [61], are primarily composed of UMOD and also commonly albumin [62, 63]. Thus, specifically targeting excessive UMOD excretion may be a viable treatment strategy to prevent nephron tubule obstruction. The question remains as to how to tackle UMOD overexcretion. Future studies should also examine potential structural alterations in the cleaved-external motif of UMOD, which may lead to further protein aggregations and nephron blockages. Also, since UMOD is matured, cleaved, and sorted in the endoplasmic reticulum, overexpression and overexcretion of UMOD may overwhelm this process and induce ER stress, which could contribute to renal pathology.

CONCLUSIONS

For the first time, the present study measured and compared urinary UMOD excretion levels in the DSS and SHR. MC was reduced to the same levels in the DSS and SHR arcuate arterioles upon salt loading, thus could not explain the increased renal pathology in the DSS rats. The observed CKD in the DSS was strongly correlated with UMOD excretion levels and was exacerbated with HS diet. These results suggest that increased UMOD excretion may contribute to the observed CKD in the DSS, but not the blood pressure elevation or loss of MC as a result of HS diet. This is the first evidence demonstrating that CKD progression in the DSS was independent of blood pressure and strongly associated with UMOD excretion levels.

AUTHOR CONTRIBUTIONS

SN and JD designed the study. SN, VY, and CL performed the experiments. SN and VY analyzed the data. SN and JD interpreted the results. SN prepared the figures and drafted the manuscript. SN and JD edited and revised the manuscript. All authors approved the final version of the manuscript.

CONFLICT OF INTEREST

The authors declare that the research was conducted in the absence of any commercial or financial relationships that could be construed as a potential conflict of interest.

REFERENCES

1.   Egan, B.M., Y. Zhao, and R.N. Axon, *US trends in prevalence, awareness, treatment, and control of hypertension, 1988-2008.* Jama, 2010. **303**(20): p. 2043-2050.

2.   System, U.R.D., *USRDS 2013 annual data report: atlas of chronic kidney disease and end-stage renal disease in the United States.* National Institutes of Health, National Institute of Diabetes and Digestive and Digestive and Kidney Diseases, Vol. 2014, 2013.

3.   Van Buren, P.N. and R. Toto, *Hypertension in diabetic nephropathy: epidemiology, mechanisms, and management.* Advances in chronic kidney disease, 2011. **18**(1): p. 28-41.

4.   Benjamin, O. and S.L. Lappin, *End-stage renal disease.* StatPearls [Internet], 2021.

5.   Rao, M.V., et al., *Hypertension and CKD: Kidney Early Evaluation Program (KEEP) and National Health and Nutrition Examination Survey (NHANES), 1999-2004.* American Journal of Kidney Diseases, 2008. **51**(4): p. S30-S37.

6.   Bikbov, B., et al., *Global, regional, and national burden of chronic kidney disease, 1990–2017: a systematic analysis for the Global Burden of Disease Study 2017.* The Lancet, 2020. **395**(10225): p. 709-733.

7.   Botdorf, J., K. Chaudhary, and A. Whaley-Connell, *Hypertension in cardiovascular and kidney disease.* Cardiorenal medicine, 2011. **1**(3): p. 183-192.

8.   Segura, J. and L.M. Ruilope, *Hypertension in moderate-to-severe nondiabetic CKD patients.* Advances in chronic kidney disease, 2011. **18**(1): p. 23-27.

9.   Hall, J.E., *Kidney dysfunction mediates salt-induced increases in blood pressure.* Circulation, 2016. **133**(9): p. 894.

10.   Buffet, L. and C. Ricchetti, *Chronic kidney disease and hypertension: A destructive combination.* 2012.

11.   Borrelli, S., et al., *Sodium intake and chronic kidney disease.* International Journal of Molecular Sciences, 2020. **21**(13): p. 4744.

12.   Weinberger, M.H., et al., *Definitions and characteristics of sodium sensitivity and blood pressure resistance.* Hypertension, 1986. **8**(6_pt_2): p. II127.

13.   Lerman, L.O., et al., *Animal models of hypertension: a scientific statement from the American Heart Association.* Hypertension, 2019. **73**(6): p. e87-e120.

14.   Mattson, D.L., et al., *Influence of diet and genetics on hypertension and renal disease in Dahl salt-sensitive rats.* Physiological genomics, 2004. **16**(2): p. 194-203.

15.   Yum, V., et al., *Endoplasmic reticulum stress inhibition limits the progression of chronic kidney disease in the Dahl salt-sensitive rat.* American Journal of Physiology-Renal Physiology, 2017. **312**(1): p. F230-F244.

16.   Nademi, S., C. Lu, and J.G. Dickhout, *Enhanced Myogenic Constriction in the SHR Preglomerular Vessels Is Mediated by Thromboxane A2 Synthesis.* Frontiers in Physiology, 2020. **11**: p. 853.

17.	Landry, D.W., S. Anubkumar, and J.A. Oliver, *Vascular Tone*, in *Clinical Critical Care Medicine*. 2006, Elsevier. p. 31-39.

18.	Endlich, N., et al., *Analysis of differential gene expression in stretched podocytes: osteopontin enhances adaptation of podocytes to mechanical stress.* The FASEB Journal, 2002. **16**(13): p. 1850-1852.

19.	Ingram, A.J., et al., *Activation of mesangial cell signaling cascades in response to mechanical strain.* Kidney international, 1999. **55**(2): p. 476-485.

20.	Noble, N.A. and W.A. Border. *Angiotensin II in renal fibrosis: should TGF-beta rather than blood pressure be the therapeutic target?* in *Seminars in nephrology*. 1997.

21.	Bidani, A.K. and K.A. Griffin, *Pathophysiology of hypertensive renal damage: implications for therapy.* Hypertension, 2004. **44**(5): p. 595-601.

22.	Bidani, A.K., et al., *Protective importance of the myogenic response in the renal circulation.* Hypertension, 2009. **54**(2): p. 393-8.

23.	Burke, M., et al., *Molecular mechanisms of renal blood flow autoregulation.* Curr Vasc Pharmacol, 2014. **12**(6): p. 845-58.

24.	Devuyst, O., E. Olinger, and L. Rampoldi, *Uromodulin: from physiology to rare and complex kidney disorders.* Nature Reviews Nephrology, 2017. **13**(9): p. 525-544.

25.	Kottgen, A., et al., *Uromodulin levels associate with a common UMOD variant and risk for incident CKD.* J Am Soc Nephrol, 2010. **21**(2): p. 337-44.

26.   Sjaarda, J., et al., *Blood HER2 and Uromodulin as Causal Mediators of CKD.* J Am Soc Nephrol, 2018. **29**(4): p. 1326-1335.

27.   Olden, M., et al., *Common variants in UMOD associate with urinary uromodulin levels: a meta-analysis*. 2014, Am Soc Nephrol.

28.   Yong-feng, C., et al., *Application of trichloroacetic acid-acetone precipitation method for protein extraction in bone tissue.* Zhongguo yi xue ke xue Yuan xue bao. Acta Academiae Medicinae Sinicae, 2011. **33**(2): p. 210-213.

29.   Youhanna, S., et al., *Determination of uromodulin in human urine: influence of storage and processing.* Nephrology Dialysis Transplantation, 2014. **29**(1): p. 136-145.

30.   Dickhout, J.G. and R.M. Lee, *Structural and functional analysis of small arteries from young spontaneously hypertensive rats.* Hypertension, 1997. **29**(3): p. 781-789.

31.   El Nahas, A.M., et al., *Chronic renal failure after nephrotoxic nephritis in rats: contributions to progression.* Kidney international, 1987. **32**(2): p. 173-180.

32.   Berger, R.C., et al., *Renal Effects and Underlying Molecular Mechanisms of Long-Term Salt Content Diets in Spontaneously Hypertensive Rats.* PLoS One, 2015. **10**(10): p. e0141288.

33.   Henry, C., et al., *Salt induces myocardial and renal fibrosis in normotensive and hypertensive rats.* Circulation, 1998. **98**(23): p. 2621-2628.

34.   Farquhar, W.B., et al., *Dietary sodium and health: more than just blood pressure.* J Am Coll Cardiol, 2015. **65**(10): p. 1042-50.

35.   Oberleithner, H., et al., *Salt overload damages the glycocalyx sodium barrier of vascular endothelium.* Pflugers Arch, 2011. **462**(4): p. 519-28.

36.   Gates, P.E., et al., *Dietary sodium restriction rapidly improves large elastic artery compliance in older adults with systolic hypertension.* Hypertension, 2004. **44**(1): p. 35-41.

37.   Todd, A.S., et al., *Dietary salt loading impairs arterial vascular reactivity.* Am J Clin Nutr, 2010. **91**(3): p. 557-64.

38.   DAHL, L.K., et al., *Effects of chronic excess salt ingestion: modification of experimental hypertension in the rat by variations in the diet.* Circulation Research, 1968. **22**(1): p. 11-18.

39.   Cowley Jr, A.W., et al., *Brown Norway chromosome 13 confers protection from high salt to consomic Dahl S rat.* Hypertension, 2001. **37**(2): p. 456-461.

40.   Zhang-James, Y., F.A. Middleton, and S.V. Faraone, *Genetic architecture of Wistar-Kyoto rat and spontaneously hypertensive rat substrains from different sources.* Physiological genomics, 2013. **45**(13): p. 528-538.

41.   Lais, L., et al., *Arterial pressure development in neonatal and young spontaneously hypertensive rats.* Journal of Vascular Research, 1977. **14**(5): p. 277-284.

42.   Dickhout, J. and R. Lee, *Increased medial smooth muscle cell length is responsible for vascular hypertrophy in young hypertensive rats.* American Journal of Physiology-Heart and Circulatory Physiology, 2000. **279**(5): p. H2085-H2094.

43.   Mohammed-Ali, Z., et al., *Animal models of kidney disease*, in *Animal Models for the Study of Human Disease*. 2017, Elsevier. p. 379-417.

44.   Karlsen, F.M., et al., *Dynamic autoregulation and renal injury in Dahl rats.* Hypertension, 1997. **30**(4): p. 975-983.

45.   Vasdev, S., et al., *Dietary lipoic acid supplementation attenuates hypertension in Dahl salt sensitive rats.* Molecular and cellular biochemistry, 2005. **275**(1): p. 135-141.

46.   Luo, Y., et al., *Blood pressure characterization of hypertensive and control rats for cardiovascular studies.* AHA, Atlanta: Charles River, 2008.

47.   Oguchi, H., et al., *Renal arteriolar injury by salt intake contributes to salt memory for the development of hypertension.* Hypertension, 2014. **64**(4): p. 784-791.

48.   Siegel, A.-K., et al., *Genetic linkage of albuminuria and renal injury in Dahl salt-sensitive rats on a high-salt diet: comparison with spontaneously hypertensive rats.* Physiological genomics, 2004. **18**(2): p. 218-225.

49.   Rafiq, K., et al., *Regression of glomerular and tubulointerstitial injuries by dietary salt reduction with combination therapy of angiotensin II receptor blocker and calcium channel blocker in Dahl salt-sensitive rats.* PloS one, 2014. **9**(9): p. e107853.

50.   Kottgen, A., et al., *Multiple loci associated with indices of renal function and chronic kidney disease.* Nat Genet, 2009. **41**(6): p. 712-7.

51.   Mary, S., et al., *Salt loading decreases urinary excretion and increases intracellular accumulation of uromodulin in stroke-prone spontaneously hypertensive rats.* Clinical Science, 2021. **135**(24): p. 2749-2761.

52.   Mary, S., et al., *Polymerization-incompetent uromodulin in the pregnant stroke-prone spontaneously hypertensive rat.* Hypertension, 2017. **69**(5): p. 910-918.

53.   Schaeffer, C., et al., *Analysis of uromodulin polymerization provides new insights into the mechanisms regulating ZP domain-mediated protein assembly.* Molecular biology of the cell, 2009. **20**(2): p. 589-599.

54.   Brunati, M., et al., *The serine protease hepsin mediates urinary secretion and polymerisation of Zona Pellucida domain protein uromodulin.* Elife, 2015. **4**: p. e08887.

55.   Zaucke, F., et al., *Uromodulin is expressed in renal primary cilia and UMOD mutations result in decreased ciliary uromodulin expression.* Human molecular genetics, 2010. **19**(10): p. 1985-1997.

56.   Olden, M., et al., *Common variants in UMOD associate with urinary uromodulin levels: a meta-analysis.* J Am Soc Nephrol, 2014. **25**(8): p. 1869-82.

57.   Sanders, P.W., *Dysproteinemias and amyloidosis.* Primer on Kidney Diseases E-Book, 2009: p. 232.

58.   Huang, Z.-Q., et al., *Bence Jones proteins bind to a common peptide segment of Tamm-Horsfall glycoprotein to promote heterotypic aggregation.* The Journal of clinical investigation, 1993. **92**(6): p. 2975-2983.

59.   Sanders, P.W., et al., *Mechanisms of intranephronal proteinaceous cast formation by low molecular weight proteins.* The Journal of clinical investigation, 1990. **85**(2): p. 570-576.

60.   Hoyer, J.R., et al., *Immunomorphometric studies of proteinuria in individual deep and superficial nephrons of rats.* Laboratory investigation, 2000. **80**(11): p. 1691-1700.

61.   Dvanajscak, Z., L.N. Cossey, and C.P. Larsen. *A practical approach to the pathology of renal intratubular casts.* in *Seminars in Diagnostic Pathology.* 2020. Elsevier.

62.   Fan, S.-L. and S. Bai, *Urinalysis*, in *Contemporary Practice in Clinical Chemistry.* 2020, Elsevier. p. 665-680.

63.   Wu, T.-H., et al., *Tamm–Horsfall protein is a potent immunomodulatory molecule and a disease biomarker in the urinary system.* Molecules, 2018. **23**(1): p. 200.
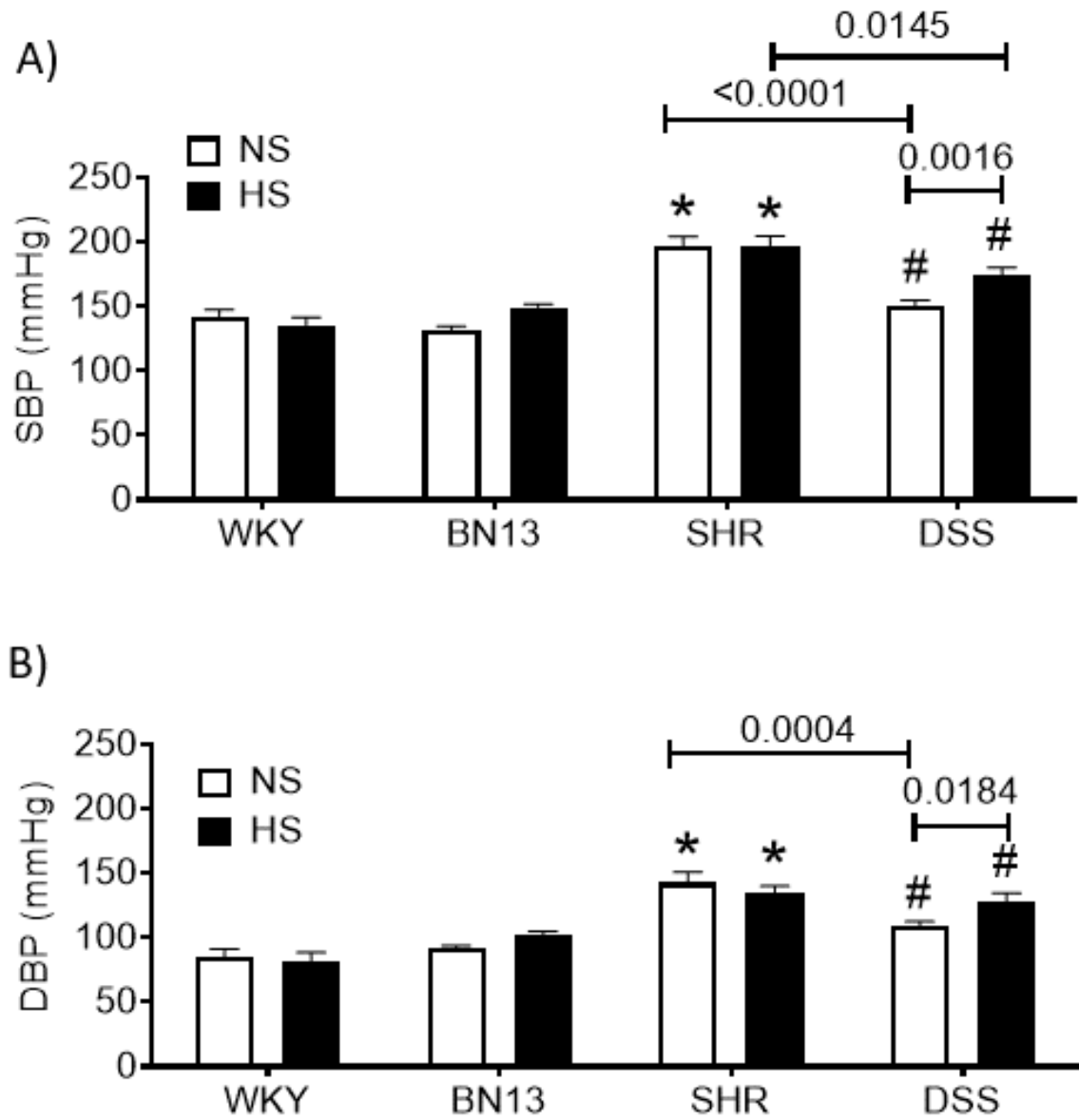
Figure 1.

Figure 1. Blood pressure comparison after 4 weeks of high salt (HS) feeding. A) Shows systolic blood pressure (SBP). **B)** Demonstrates diastolic blood pressure (DBP). Star (*) compares to the WKY of the same diet. Hash (#) compares to the BN13 of the same diet. P ≤ 0.05 was deemed statistically significant. Additional statistical significances were shown with P-values above markers. N (WKY-NS) = 5; N (WKY-HS) = 5; N (BN13-NS) = 6; N (BN13-HS) = 6; N (SHR-NS) = 5; N (SHR-HS) = 5; N (DSS-NS) = 10; N (DSS-HS) = 10.
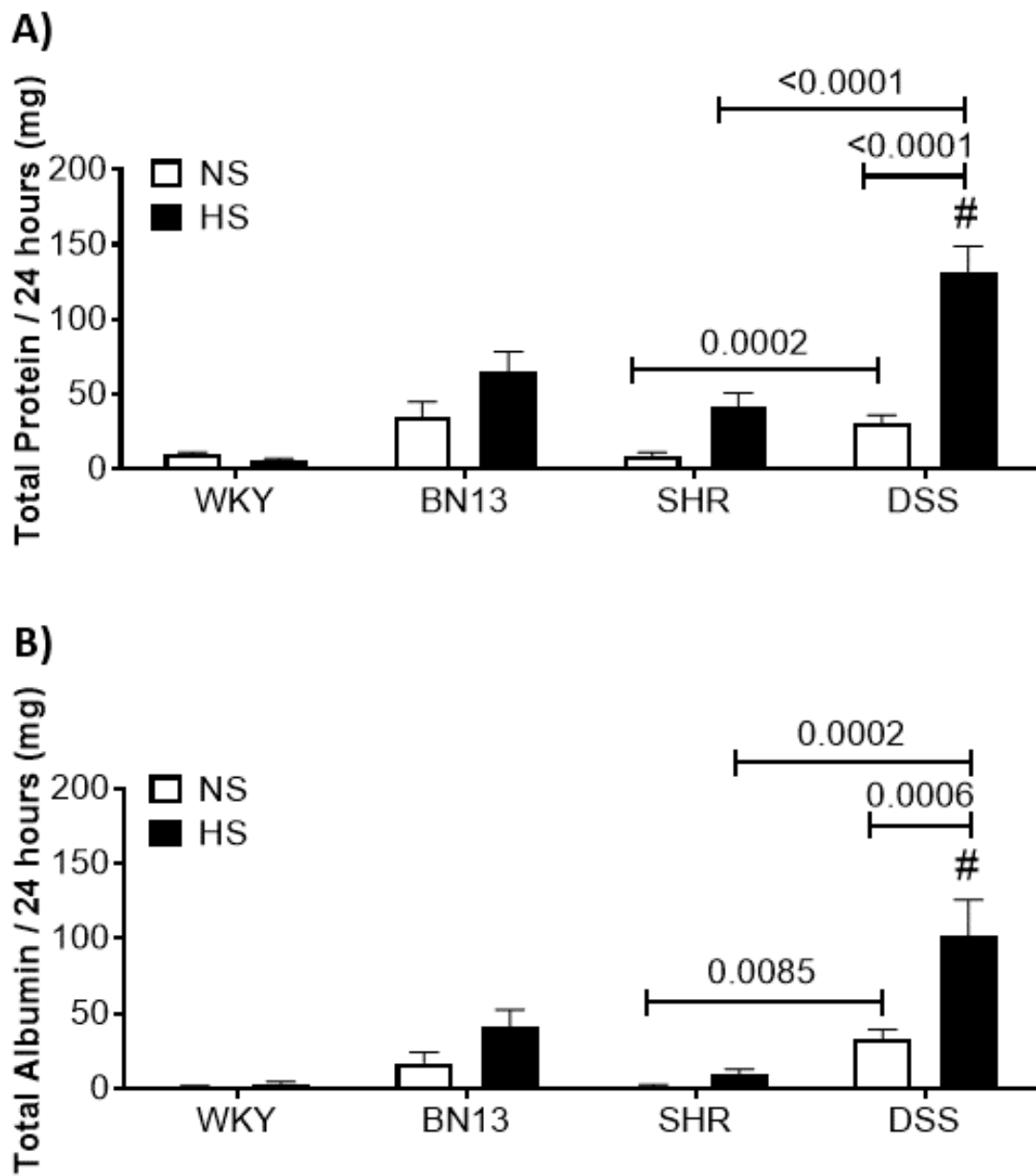
Figure 2.

Figure 2. Urinalysis of 24-hour urine samples after 4 weeks of diet consumption. A) Comparison of the total protein excreted over 24-hours (mg/24 hours). **B)** Comparison of the total albumin excreted over 24-hours (mg/24 hours). Hash (#) compares to the BN13 of the same diet. $P \leq 0.05$ was deemed statistically significant. Additional significant differences are shown with P-values above markers. N (WKY-NS) = 5; N (WKY-HS) = 5; N (BN13-NS) = 6; N (BN13-HS) = 6; N (SHR-NS) = 5; N (SHR-HS) = 5; N (DSS-NS) = 10; N (DSS-HS) = 10.
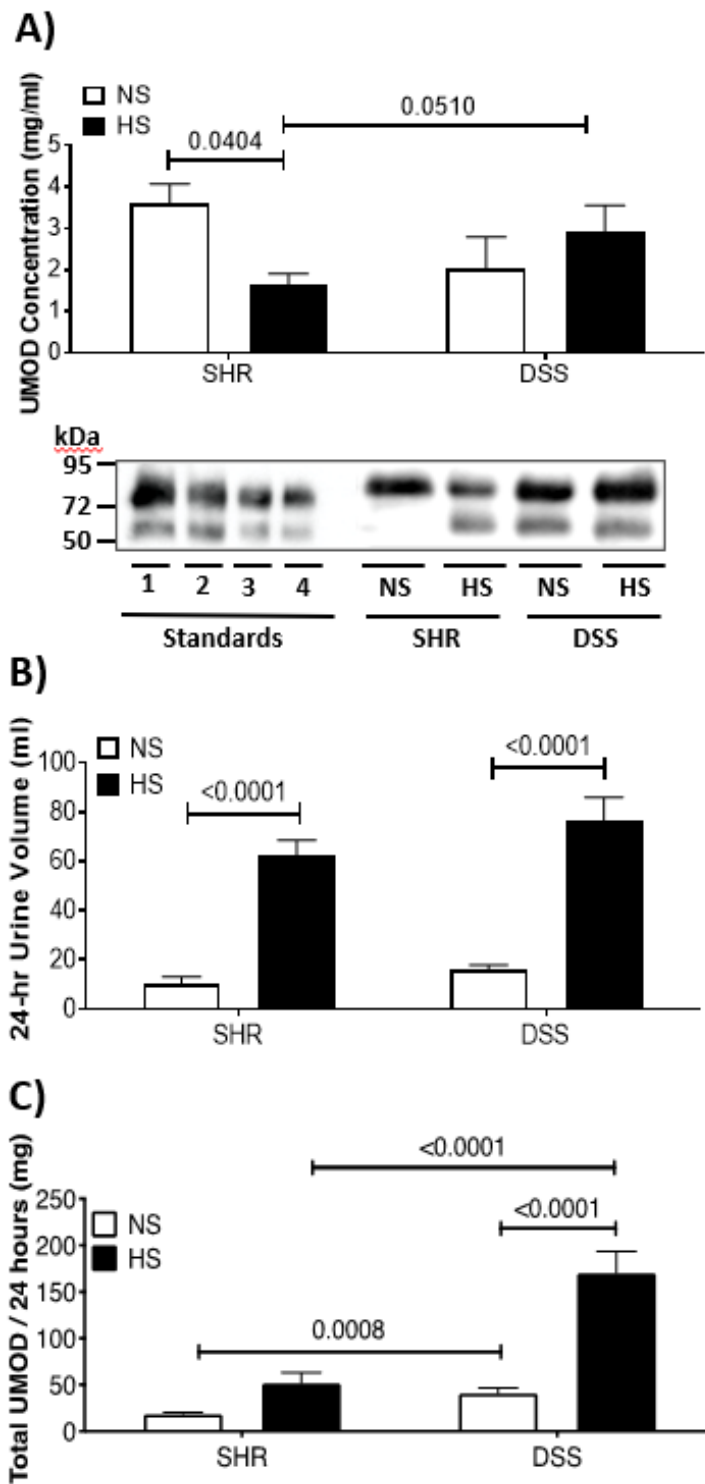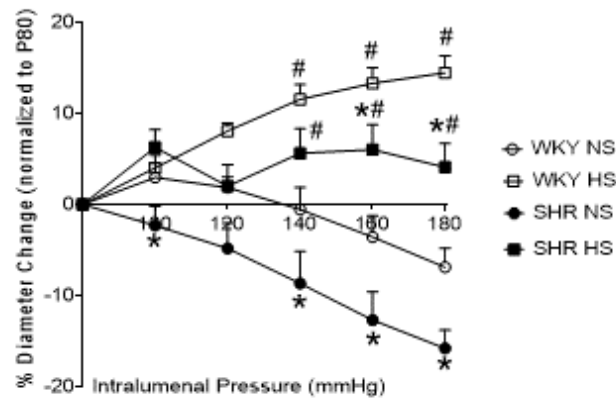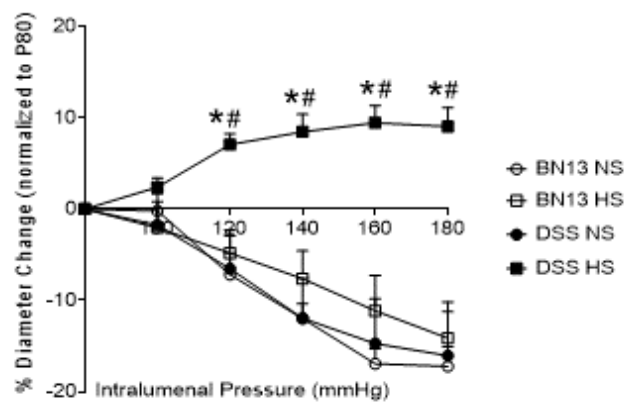
Figure 3.

Figure 3. Urinary uromodulin excretion after 4 weeks of diet consumption. Total urinary uromodulin (UMOD, mg/24 hour) was calculated using UMOD concentration (mg/ml urine), UMOD standards, and 24-hour urine volume (ml) as elaborated in the methods. **A)** Western blot analysis illustrating urinary UMOD concentration (mg/ml urine) after 4 weeks of salt feeding as well as the four purified UMOD standards (5, 2.5, 1, and 0.5 mg/ml). UMOD concentration was calculated by plotting band volumes in the standards' equation of the fitted standard curve. **B)** 24-hour urine volume (ml) comparison at endpoint. **C)** Total excreted UMOD (mg/24 hours) was calculated through multiplying UMOD concentration (mg/ml) by 24-hr urine volume (ml). Significant differences are shown between respective groups with P-values above markers. N (SHR-NS) = 10; N (SHR-HS) = 10; N (DSS-NS) = 6; N (DSS-HS) = 8.

Figure 4.

A) Myogenic Constriction (WKY vs SHR)

B) Myogenic Constriction (BN13 vs DSS)

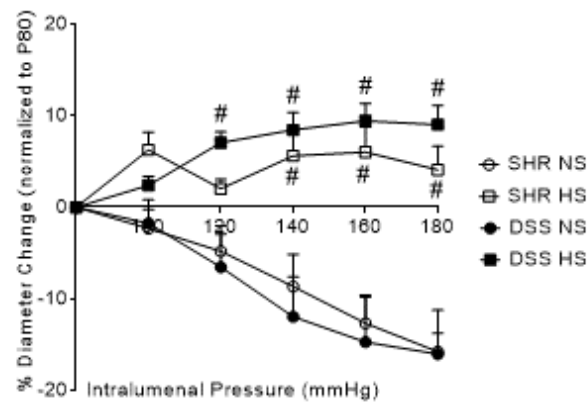C) Myogenic Constriction (SHR vs DSS)

Figure 4. Myogenic constriction (MC) comparison of renal arcuate arteries after 4 weeks of consuming diets. A) WKY and SHR MC comparison after 4 weeks of high salt (HS) or normal salt (NS) feeding. **B)** BN13 and DSS MC comparison after 4 weeks of diets. **C)** SHR and DSS MC comparison after 4 weeks of diets. The % Diameter Change was normalized to the vessel's diameter at pressure 80 mmHg (P80) as was elaborated in the methods. Star (*) depicts statistical significance between strains of the same diet; hash (#) shows significance between diets of the same strain; $P \leq 0.05$ was deemed statistically significant. N (WKY-NS) = 5; N (WKY-HS) = 5; N (BN13-NS) = 6; N (BN13-HS) = 6; N (SHR-NS) = 5; N (SHR-HS) = 5; N (DSS-NS) = 8; N (DSS-HS) = 8. "N" corresponds to the number of animals per group.
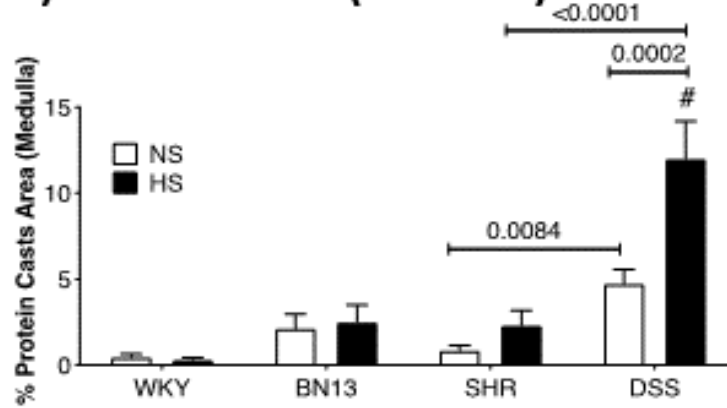
Figure 5.
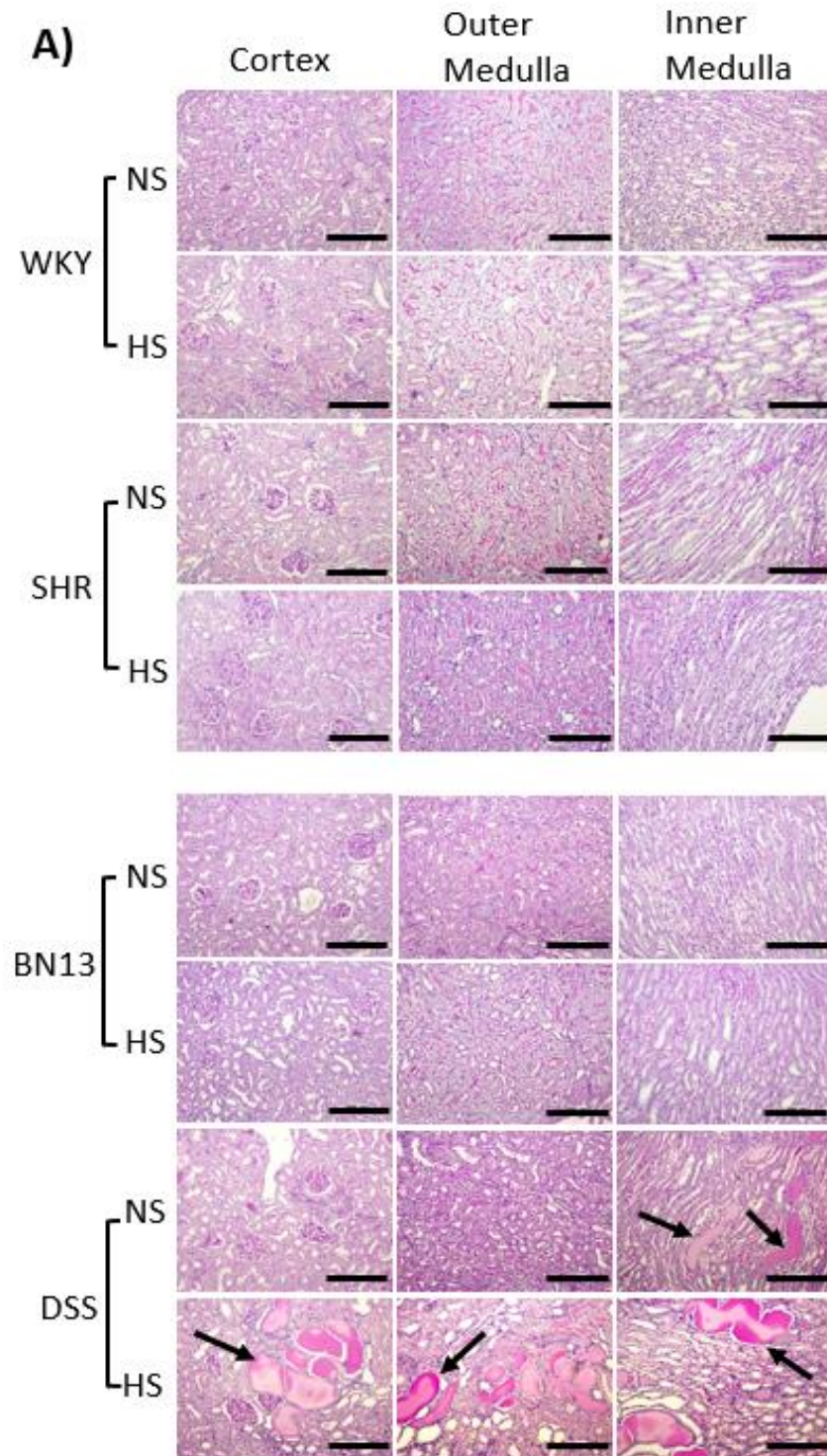
B) Protein Casts (Cortex)
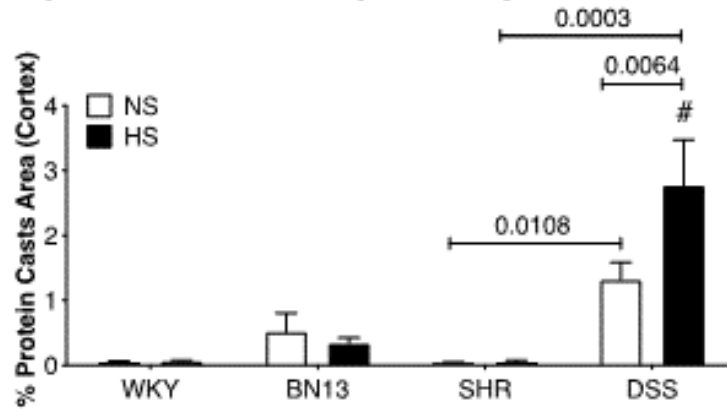
C) Protein Casts (Medulla)

D) Glomerular damage Score
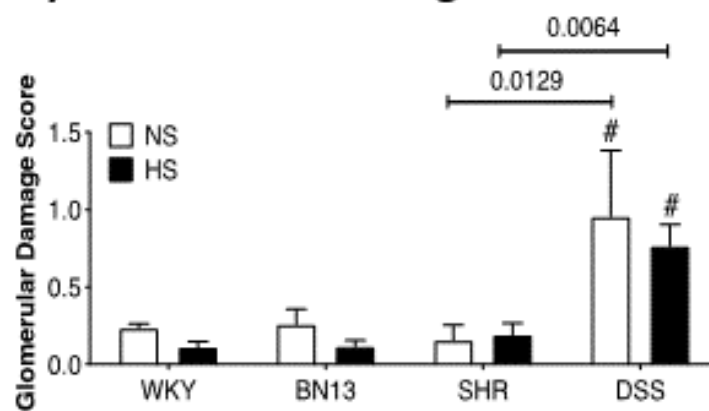
Figure 5. Histological assessments after 4 weeks of salt diets. A) Periodic acid-Schiff (PAS) staining demonstrating intratubular protein casts after 4 weeks of diet feeding. Images were taken with an Olympus BX41 microscope using 20X objective (scale bar 500 μm). **B)** Percent protein casts area in the cortex. **C)** Percent protein casts area in the medulla. **D)** Blinded glomerular damage score. The scoring scale was 0-4, with 0 showing no damage; 1 demonstrating 25% damage; 2 depicting 50% damage; 3 illustrating 75% damage; and 4 representing 100 % damage. Hash (#) is comparing to BN13 of the same diet. $P \leq 0.05$ was deemed significant. Additional significant differences are shown between respective groups with P-values above markers. For the PAS staining: N (WKY-NS) = 5; N (WKY-HS) = 5; N (BN13-NS) = 6; N (BN13-HS) = 6; N (SHR-NS) = 5; N (SHR-HS) = 5, N (DSS-NS) = 10, N (DSS-HS) = 10. For the glomerular damage: N was 5 rats per group.

Figure 6.
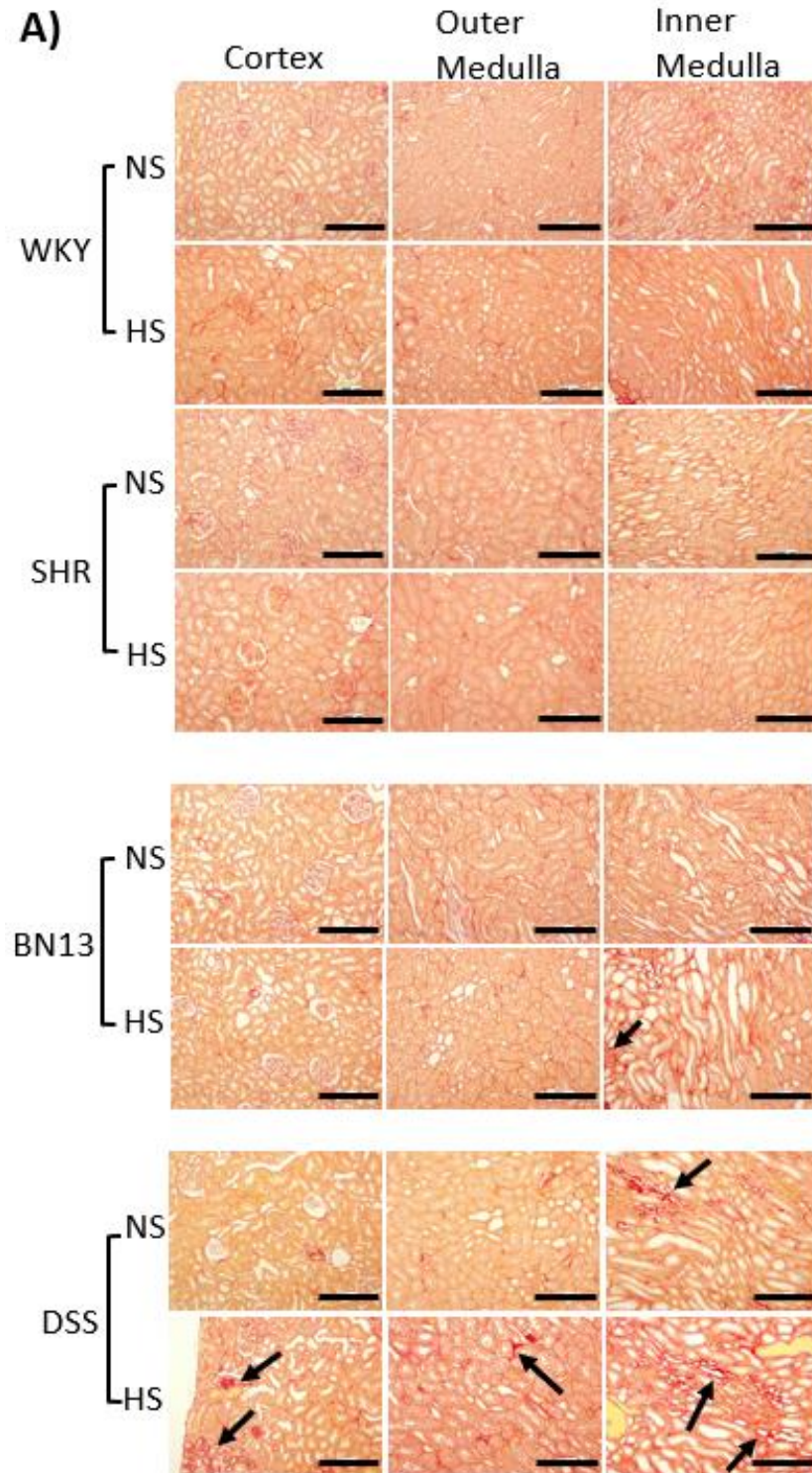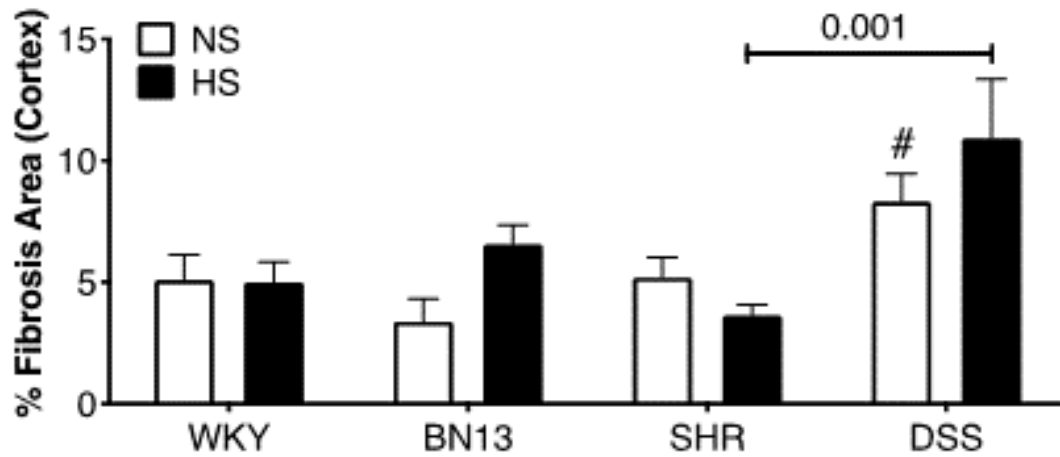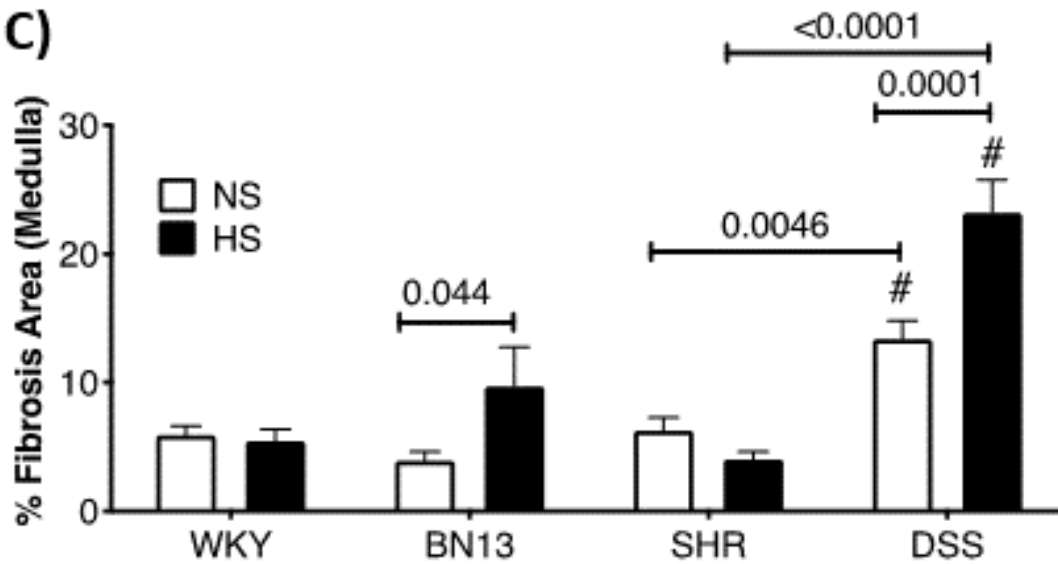
Figure 6. Periodic acid-Schiff (PSR) staining showing interstitial fibrosis after 4 weeks of salt feeding. A) PSR-stained micrographs demonstrating interstitial fibrosis as red. Images were taken with an Olympus BX41 microscope using 20X objective (scale bar 500 μm). **B)** Percent interstitial fibrosis in the cortex. **C)** Percent interstitial fibrosis in the medulla. Hash (#) compares to BN13 of the same diet. $P \leq 0.05$ was deemed statistically significant. Additional significant differences are shown between respective groups with P-values above markers. N (WKY-NS) = 5; N (WKY-HS) = 5; N (BN13-NS) = 5; N (BN13-HS) = 5; N (SHR-NS) = 5; N (SHR-HS) = 5, N (DSS-NS) = 6, N (DSS-HS) = 6.

Figure 7.
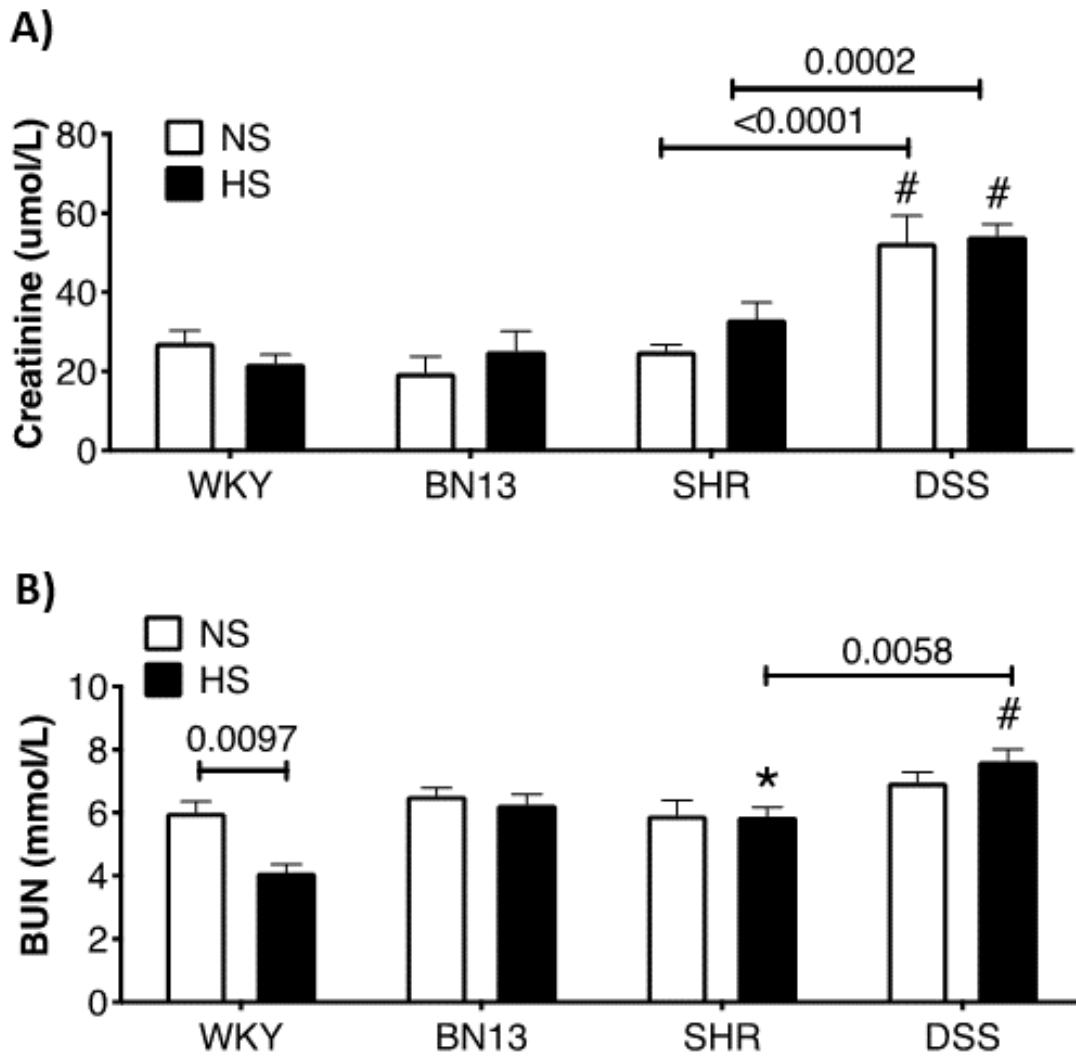
Figure 7. Plasma Analysis. A) Serum creatinine comparison. **B)** Blood urea nitrogen (BUN) levels comparison. Star (*) compares to WKY of the same diet. Hash (#) compares to BN13 of the same diet. $P \leq 0.05$ was deemed statistically significant. Additional significant differences are shown between respective groups with P-values above markers. N (WKY-NS) = 5; N (WKY-HS) = 5; N (BN13-NS) = 6; N (BN13-HS) = 6; N (SHR-NS) = 5; N (SHR-HS) = 5; N (DSS-NS) = 10; N (DSS-HS) = 10.

Figure 8.
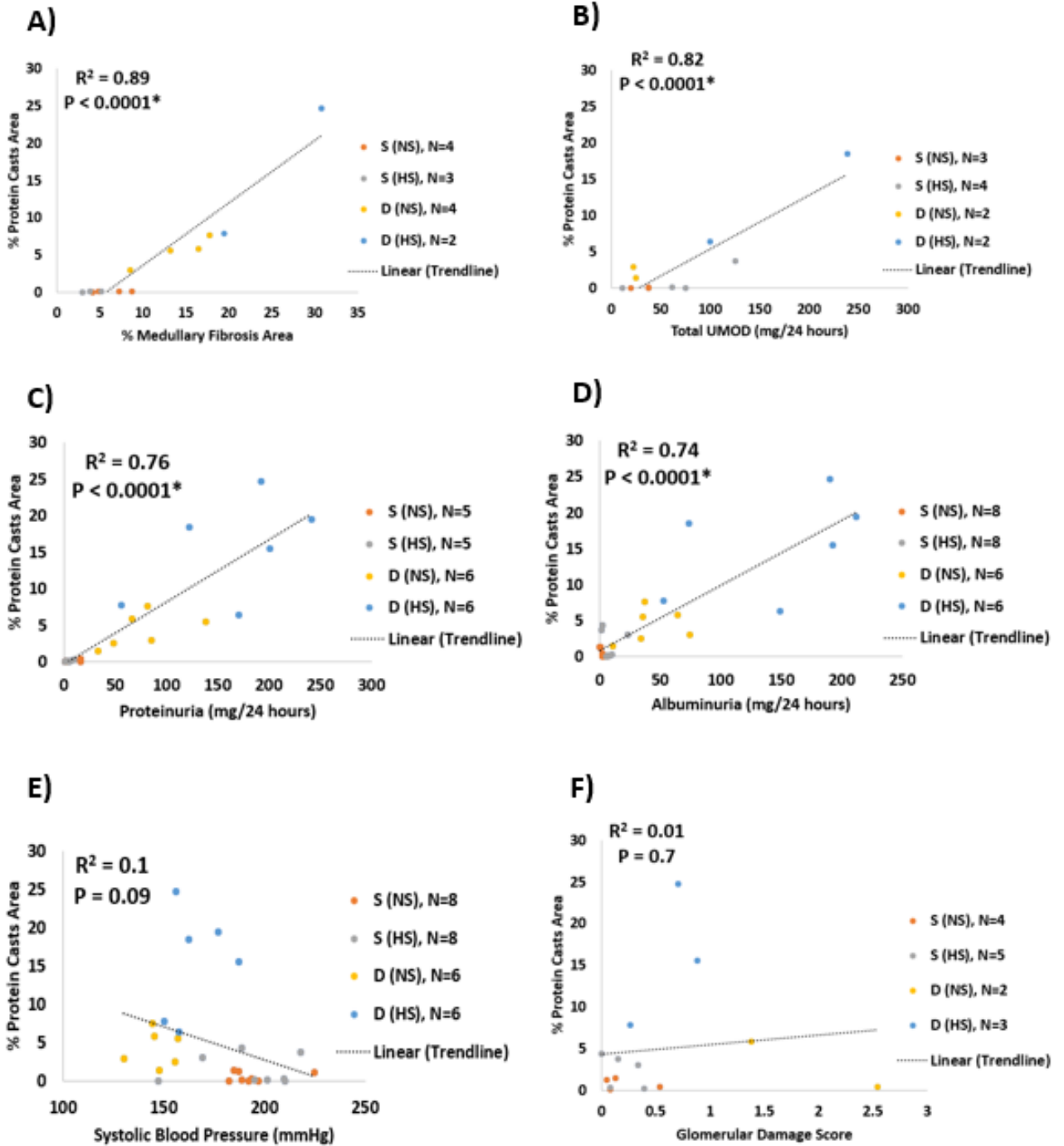
Figure 8. Correlation Studies. Correlation between % protein casts area and **A)** % medullary fibrosis area, **B)** 24-hour urinary uromodulin (UMOD) levels, **C)** 24-hour proteinuria, **D)** 24-hour albuminuria, **E)** systolic blood pressure (SBP), and **F)** glomerular damage score. Star (*) indicates statistical significance, $P \leq 0.05$.

Supplemental Figure 1.
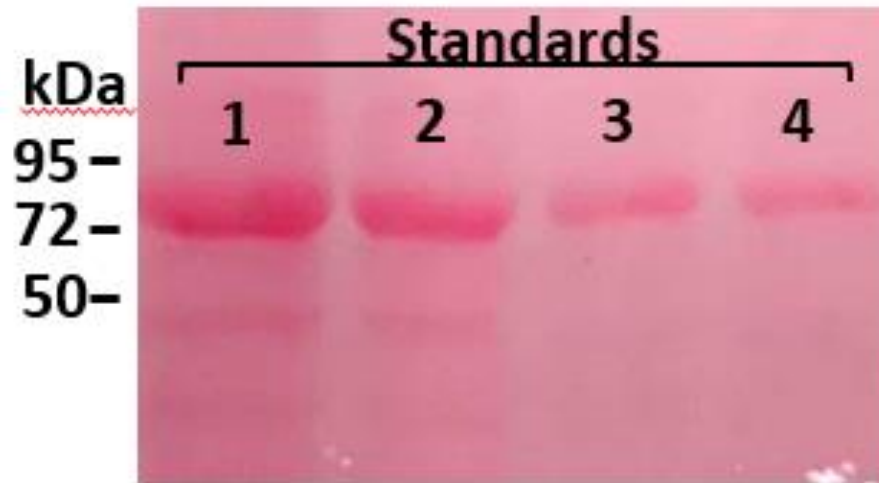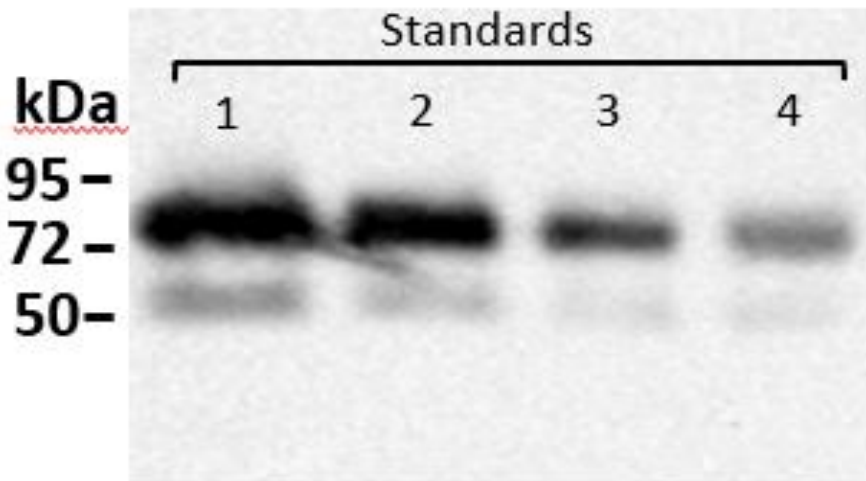
Supplemental Figure 1. Visual illustration of uromodulin (UMOD) extraction purity. UMOD was extracted using the Trichloroacetic (TCA) acid-acetone precipitation method. The extracted UMOD was serially diluted to 5, 2.5, 1, and 0.5 mg/ml standards. The standards were then diluted 1:2 with loading buffer and 5 ul of this mixture was loaded into the electrophoresis gel. **A)** Ponceau red staining showing all protein bands obtained from the extract. **B)** Antibody blot indicating that all the proteins shown in the ponceau staining were positively detected for UMOD.

CHAPTER 5

DISCUSSION, FUTURE DIRECTION, AND CONCLUSION

5.1 DISCUSSION

Hypertension can play a significant role in the onset and development of chronic kidney disease (CKD) particularly if the elevated blood pressure is transmitted to the glomerulus. Thus, preventing glomerular hypertension is important in preventing renal damage [1]. Myogenic constriction (MC), contraction of arterioles in response to increasing intraluminal pressure, regulates the blood pressure that the glomeruli receive, thus it helps control glomerular hypertension. The overall objective of this research project was to investigate if inhibiting MC worsens salt-induced hypertensive CKD and the involved mechanism(s). The overall hypothesis was that inhibiting MC worsens salt-induced hypertensive CKD. To examine this hypothesis, we first determined how MC functions. This thesis demonstrated that the enhanced MC in the preglomerular arteries of younger spontaneously hypertensive rat (SHR) (12-16 and 30-40 weeks old) was augmented due to increased thromboxane A2 synthesis from the tunica media (smooth muscle cells) and/or adventitia but not the endothelium (**Chapter 2**); MC in arcuate and mesenteric arteries was not dependent on the endothelium (removing endothelium did not change MC) (**Chapter 2**); MC was dependent on L-type calcium channels (blocking these channels impaired MC, although the arteries in most cases retained slight myogenic tone) (**Chapter 2**); inhibiting MC with nifedipine protected from salt-induced renal injury in older SHR rodents (51-54 weeks old) possibly through reducing the total excreted uromodulin (UMOD) and albumin (**Chapter 3**); comparing two hypertensive CKD animal models showed that MC was reduced to about the same levels in the Dahl salt sensitive (DSS) and SHR arcuate arterioles upon salt loading, therefore could not

explain the renal pathology in the DSS rats (**Chapter 4**); and CKD progression of DSS and SHR were independent of blood pressure and strongly associated with total UMOD excretion, albumin, and medullary fibrosis levels (**Chapter 4**). A summary of this thesis study's major findings is presented in **Table 2**.

Table 2. A summary of the thesis major findings

Main Findings	Chapter
Chapter 2	
Enhanced MC in the younger SHR was due to enhanced thromboxane A2 synthesis from either the smooth muscle cell layer or tunica adventitia.	Chapter 2, Figure 12
MC in the WKY and SHR arcuate and mesenteric arterioles was not dependent on the endothelium as removing it did not change MC.	Chapter 2, Figure 10, 11
MC in the WKY and SHR arcuate and mesenteric arterioles was dependent on the L-type calcium channels.	Chapter 2, Figure 6, 7, 8
Nifedipine-treated WKY and SHR arcuate and mesenteric arteries retained a slight myogenic tone.	Chapter 2, Figure 6, 7, 8
Nifedipine-treated SHR arcuate arteries (30-40 weeks old) showed significantly more myogenic tone compared to the WKY arcuate arteries.	Chapter 2, Figure 6C
Chapter 3	
Inhibiting MC while also reducing the blood pressure improved salt-induced CKD characteristics in older (51-54 weeks old) SHR rats.	Chapter 3
MC was not augmented in older (51-54 weeks old) SHR rats.	Chapter 3, Figure 5C
High salt increased 24-hour proteinuria, albuminuria, and total UMOD excretion in the SHR-HS rats versus SHR-NS.	Chapter 3, Figure 2, 3C

Co-treatment of high salt with nifedipine reduced the 24-hour proteinuria, albuminuria, and total UMOD excretion in SHR-HSN versus the SHR-HS.	Chapter 3, Figure 2
Proteinuria, total UMOD excretion, albuminuria, medullary fibrosis, and SBP were strongly and positively correlated with % protein casts area.	Chapter 3, Figure 9
Chapter 4	
DSS showed more renal injury (i.e., proteinuria, albuminuria, total excreted UMOD, casts, medullary fibrosis) than the SHR regardless of salt diet.	Chapter 4
DSS showed renal injury regardless of salt feeding but high salt diet worsened the pathology.	Chapter 4
MC was similar between SHR and DSS regardless of salt diets.	Chapter 4, Figure 4C
SHR was significantly more hypertensive than DSS regardless of salt feeding but showed minimal renal pathology.	Chapter 4, Figure 1
DSS excreted more 24-hour urinary UMOD, proteinuria, and albuminuria compared to the SHR regardless of salt feeding, but high salt exacerbated this.	Chapter 4, Figure 2, 3C
Medullary fibrosis, total 24-hr UMOD excretion, 24-hr proteinuria, and 24-hr albuminuria were strongly and positively correlated with % protein casts area.	Chapter 4, Figure 8

All Chapters	
Nifedipine did not entirely abolish myogenic constriction in the SHR, particularly the older (30-40 and 51-54 weeks old) SHR	Chapter 1 and 3
High dietary salt did not change MC in older SHR but decreased it in younger SHR.	Chapter 3 and 4
High dietary salt did not change blood pressure in the WKY and SHR regardless of age.	Chapter 3 and 4
UMOD and albumin may aggregate together and both contribute to the incident protein casts.	Chapter 3 and 4

Table abbreviations:

MC = Myogenic constriction

WKY = Wistar Kyoto rats

SHR = Spontaneously Hypertensive Rats

UMOD = Uromodulin

SBP = Systolic Blood Pressure

HS = High Salt

NS = Normal Salt

HSN = High Salt Plus Nifedipine

5.1.1 MC Was Not Enhanced in Older SHR

The precise correlation between laboratory rat and human age is still debatable. Rats have a brief and accelerated childhood compared to human, reaching their sexual maturity at about six weeks old. Nevertheless, their social maturity is not attained until about 5-6 months later [2]. During their adulthood, every month of the rat's life is equivalent to about 3 years of human life [2, 3]. While on average laboratory rats live for about 3 years (2-3.5 years), the life expectancy of human is approximately 80 years. Correlating rat and human life spans, 2 weeks of rats' life (13.8 rat days) is equivalent to about 1.5 year of human life [2, 4, 5].

Our results demonstrated that MC was augmented in preglomerular arcuate arterioles of 12–16 weeks old SHR rats (**Chapter 2, Figure 12A; Chapter 4, Figure 4A**) as well as 30-40 weeks old (**Chapter 2, Figure 2C**) compared to the WKY rats. However, MC in the older 51-54 weeks old rats was not augmented (**Chapter 3, Figure 5C**). These findings are consistent with other studies in the literature, reporting glomerular hemodynamic changes with aging. Respective to human life, late middle age SHR rats exhibited similar single nephron GFR and glomerular capillary plasma flow rate compared to younger rats [6]. However, older SHR rats showed reduced afferent arteriolar resistance. This reduction was associated with an increase in glomerular capillary hydraulic pressure even though the systematic blood pressure was not changed. Glomerular capillary ultrafiltration coefficient (Kf) was also decreased in older SHR rats, suggesting of a loss of afferent arteriolar responsiveness [6]. Similar patterns were also

observed in older healthy human kidney donors [7]. Kidney donors over 55 years old exhibited a reduced GFR, renal blood flow, and Kf compared to donors under 40 years old [7].

5.1.2 MC Was Dependent on L-Type Calcium Channels in All Animal Models Regardless of Age

We found that inhibiting L-type Ca^{2+} channels with nifedipine inhibited MC in 30-40-week-old WKY and SHR arcuate (**Chapter 2, Figure 6**) and mesenteric (**Chapter 2, Figure 7**) arteries. Nifedipine also blocked MC in older 51-54 weeks old (**Chapter 3, Figure 5**) as well as younger 12-16 weeks old arcuate arteries of WKY and SHR rats (**Chapter 2, Figure 8**). Changes in calcium concentration $[Ca^{2+}]$, required for muscle contraction, are produced by Ca^{2+} influx from voltage-dependent and -independent plasmalemmal Ca^{2+} channels, as well as Ca^{2+} release from the sarcoplasmic reticulum [8]. Intracellular Ca^{2+} release from the sarcoplasmic reticulum is facilitated through ryanodine and inositol-1,4,5,-trisphosphate receptors [9]. There are a few main plasmalemmal calcium permeable channels expressed in vascular smooth muscle cells (VSMCs) such as: L-type CaV1 channels, T-type Ca^{2+} channels, transient receptor potential (TRP) channel family, and Ca^{2+} release-activated channels [9]. Calcium entry through the L-type Ca^{2+} channels have been long deemed as the primary source of $[Ca^{2+}]$ in the cell [10]. L-type Ca^{2+} channels consist of one pore-forming (α) and a few auxiliary (β, $\alpha\delta$, and γ) subunits which modulate the channel functions. Dihydropyridine antagonists such as nifedipine, isradipine, and nicardipine prevent pressure-induced

calcium concentration changes by selectively inhibiting the pore-forming α subunit, thus diminishing MC [10]. In general, L-type Ca^{2+} channels predominantly contribute to the MC at lower intraluminal pressures and membrane potentials (~ -60 to -50 mV), while T-type Ca^{2+} channels are activated at greater intraluminal pressures when the membrane potential is more depolarized (~ -45 to -36 mV) [10]. Dihydropyridines such as nifedipine have been shown to have minimal effects on the T-type Ca^{2+} channels [11]. Another type of plasmalemmal calcium permeable channels is a superfamily of cationic channels called TRP channels which non-selectively permit Ca^{2+} entry to the VSMCs [12]. Dihydropyridines such as nifedipine generally do not affect the TRP channels [13].

5.1.3 Nifedipine Did Not Entirely Abolish Myogenic Constriction in the SHR

Inhibiting L-type calcium channels with nifedipine did not completely abolish MC in the SHR arteries, demonstrated by the negative % diameter change values in these vessels (**Chapter 1**). The % diameter change was calculated by subtracting the diameter of the vessel in calcium-free buffer ($D_{n\,(Calcium-free)}$) from the diameter of the vessel at that particular pressure point (D_n) in normal buffer, divided by the calcium-free diameter ($D_{n\,(Calcium-free)}$), multiplied by 100 (% Diameter Change $= \left(\frac{D_n - D_{n\,(Calcium-Free)}}{D_{n\,(Calcium-Free)}} \right) *$ 100). Negative % diameter values indicate that the vessel's diameter at that particular pressure point (D_n) in normal buffer was smaller than its diameter when it was in the calcium-free buffer ($D_{n\,(Calcium-free)}$). The arcuate arteries of 30-40 weeks-old SHR retained their myogenic tone at all pressure points (**Chapter 2, Figure 6B**) and there was a significant difference between nifedipine-treated WKY and SHR arterioles (**Chapter 2,**

Figure 6C). The mesenteric arteries of 30-40 weeks-old SHR also retained their myogenic tone at pressure points over 120 mmHg (**Chapter 2, Figure 7B).** As well, the arcuate arteries of 12-16 weeks-old SHR retained their myogenic tone at pressure points over 120 mmHg (**Chapter 2, Figure 8B).** Chapter 3 also showed that arcuate arteries of 51-55 weeks-old SHR and WKY rats retained their myogenic tone after nifedipine treatment at all pressure points (**Chapter 3, Figure 1A, 1B).**

As aforementioned, L-type calcium channels are the main source of cytosol calcium entry and the primary driving source for MC in smooth muscle cells [10]. Nevertheless, other calcium channels also contribute to the calcium influx and the myogenic tone [10]. One of these contributors is the sodium/calcium (Na^+/Ca^{2+}) exchanger (NCX) which uses sodium electrochemical gradient to efflux 1 calcium from the cell, at the expense of 3 sodium ions influx (3 Na^+ influx/1 Ca^{2+} efflux) [14]. Nevertheless, if sodium concentration is higher within the cell, sodium exits the cell down its concentration gradient but calcium enters the cell; in other words, NCX functions on a reverse-mode [15]. The reverse-mode NCX activity has been well documented in cardiac and vascular smooth muscle cells [15, 16]. In vascular smooth muscle cells, reverse-mode NCX contributes to substantial calcium influx and induces vascular tone [16]. This thesis study showed that SHR retained more vascular tone (in arcuate arteries) than the WKY after blocking L-type calcium channels. This is consistent with reports in the literature that demonstrated SHR to have more NCX in their vascular smooth muscle cells than the WKY [17]. The present research study also found that older

30-40 weeks-old SHR retained more myogenic tone in their arcuate arteries after blocking L-type calcium channels (**Chapter 2, Figure 6B, 6C**) compared to the younger 12-16 weeks-old SHR rats (**Chapter 2, Figure 8B, 8C**). This is consistent with the observation of Fowler et. al. that NCX activity in both WKY and SHR ventricular myocytes increased with aging as 32 weeks-old (8 months old) WKY and SHR rats showed more NCX activities compared to 20 weeks-old (5 months old) WKY and SHR rats [18]. Similarly, our thesis study found age-related differences in MC of high-salt fed rats.

5.1.4 HS Did Not Change MC in Older SHR But Decreased It in Younger SHR

In older rats, high dietary salt did not change MC in the SHR-HS versus SHR-NS (**Chapter 3, Figure 5B**) but decreased it in the WKY-HS versus WKY-NS (**Chapter 3, Figure 5A**). In younger rats however, HS attenuated MC in both SHR-HS and WKY-HS compared to SHR-NS and WKY-NS respectively (**Chapter 4, Figure 4A**). The observed results could be due to increased natriuretic ability in older SHR compared to the younger. It has been reported in the literature that older SHR rats excrete more sodium in their urine compared to the younger SHR [19, 20], possibly due to a reduction in the activity of Na^+/H^+ exchanger 3 (NHE3) [20]. NHE3 is an antiporter mainly expressed in the proximal tubules of the kidney. Another study conducted in large spinotrapezius muscle arterioles of 8-9 weeks old WKY and SHR found that HS (7% NaCl) reduced MC in WKY-HS but increased MC in SHR-HS compared to the low salt (0.45 % NaCl) fed

animals [21]. The discrepancy in our findings could be due to the use of different type and size of vascular beds.

5.1.5 High Dietary Salt Did Not Change Blood Pressure in the SHR Regardless of Age

We found that 4 weeks of HS (8% NaCl) diet did not change blood pressure in 16 weeks old WKY and SHR rats (**Chapter 4, Figure 1).** HS feeding for 8 weeks also did not change the blood pressure in older 51-54 weeks-old WKY and SHR rodents (**Chapter 3, Figure 1**). Contrary to our study, Yu et al. reported that HS diet (8% NaCl) for 8 weeks increased blood pressure, interstitial fibrosis, and hypertrophy (left ventricular and renal) in 8 weeks-old WKY and SHR rodents [22]. Similarly, Huang et al. showed that HS diet increased blood pressure in 5-6 weeks old SHR rats [23]. The discrepancy could be due to the age differences between the studies. Young SHR rats prior to the development of hypertension at around 5 weeks old have differential sodium metabolism compared to the older hypertensive animals [20]. This thesis study further demonstrated that HS changed blood pressure in 16 weeks old DSS rats which was consistent with other findings of the literature (**Chapter 3, Figure 1)** [24].

5.1.6 Blood Pressure and Kidney Damage Relationship Is Not Simple and Linear

In Chapter 3, we removed MC and reduced the blood pressure to ~ 170-180 mmHg with nifedipine treatment in the SHR-HSN (**Chapter 3, Figure 1 & 4**). This blood pressure was similar to the DSS rats (**Chapter 4, Figure 1**). Even though, 170-180

mmHg is still considered a high blood pressure, SHR-HSN had minimal renal damage, but the DSS rats suffered from extensive renal pathology. This suggests that BP and kidney damage do not have a simple and linear relationship with an increase in one, leading to an increase in the other. Even after the nifedipine treatment, SHR-HSN blood pressure was high (~170-180 mmHg) and for this reason, we expected the SHR-HSN kidneys to deteriorate after removing the MC (**Chapter 3**). However, the kidneys' pathology ameliorated despite the high blood pressure (**Chapter 3**), demonstrating a more complicated relationship between renal pathology and blood pressure [25].

5.1.7 UMOD and Albumin May Both Contribute to the Incident Protein Casts

Correlation studies showed that proteinuria ($R^2 = 0.92$), total UMOD ($R^2 = 0.89$), and albuminuria ($R^2 = 0.77$) excreted over 24 hours had the highest correlation with incident protein casts (**Chapter 3, Figure 9**). Nifedipine co-treated with HS significantly reduced 24-hour proteinuria, total excreted UMOD, and albuminuria; and these findings were associated with improved renal function (i.e., GFR, creatinine) and histopathology (i.e., protein casts, medullary fibrosis) in the SHR-HSN rats (**Chapter 3, Figure 2A, 3C**). These findings suggest that total excreted UMOD and albumin may play more significant roles in renal function and histopathology than MC and blood pressure. It is plausible that over-excreted UMOD and albumin in the SHR-HS aggregated in nephron tubules and formed protein casts. This is because UMOD and albumin are commonly found in protein casts, particularly in hyalin casts which are the most abundant type of protein casts [26-29]. Nevertheless, medullary fibrosis ($R^2 = 0.58$) and systolic blood pressure ($R^2 = 0.53$)

also positively contributed to the % protein casts area but their coefficient of determination (R^2) values were lower compared to the proteinuria ($R^2 = 0.92$), UMOD ($R^2 = 0.89$), and albuminuria ($R^2 = 0.77$) values. A limitation of these graphs, however, was low sample size, particularly in some of the groups for the total UMOD and fibrosis graphs (**Chapter 3, Figure 9**). Similar patterns were found when comparing SHR and DSS rats (**Chapter 4, Figure 8**). Incident protein casts was strongly and positively correlated with medullary fibrosis ($R^2 = 0.89$), total 24-hour UMOD ($R^2 = 0.82$), 24-hour proteinuria ($R^2 = 0.76$), and 24-hour albuminuria ($R^2 = 0.74$). A hallmark of fibrosis is increased pathological deposition of extracellular matrix proteins such as glycoproteins, proteoglycans, and collagens [30]; some of which can be found in protein casts [26, 31]. The correlation study results are consistent with the literature that reports UMOD as the major constituting protein in renal casts [26, 32]. In 1962, McQueen discovered that albumin was particularly effective at precipitating UMOD in nephrotic but not normal urines, even at low concentrations (i.e., 0.11 % grams). McQueen defined the "nephrotic urines" as samples belonging to proteinuric patients with urinary casts and albuminuria, while "normal urines" belonged to healthy individuals without proteinuria [33]. Thus, it is plausible that in our study, UMOD and albumin both contributed to the observed incident protein casts. Future research can investigate protein casts composition and UMOD precipitation capacity with different elements (i.e., albumin, collagens, proteoglycans, Bence-Jones proteins) with higher statistical power and confidence interval.

5.1.8 Relating Rats to Human Clinical Conditions

The rat models used in this thesis, SHR and DSS, were experimental models of human essential hypertension and salt-sensitive hypertension, respectively. Approximately 90-95% of hypertensive patients suffer from essential (also called primary) hypertension which means that the cause of the hypertension is unknown [34]. Similar to human, the hypertension in the SHR (which were inbred to be hypertensive) involves multiple genes [35]. The SHR also shows similar hypertension development and progression as humans do, based on the following 3 phases: a prehypertensive phase – spanning from birth to 6 weeks of age, a developing phase – starting from 6-7 to 17-19 weeks of age, and a sustained phase – after 17-19 weeks of age [36, 37]. This makes the SHR a great experimental model for hypertension as well as aging studies [36, 37]. In general as aforementioned, in adulthood, one month of rat's life is equivalent to approximately 3 years of human life [2, 3]. Just like in human, the MC in the SHR is augmented in certain vascular beds such as preglomerular [38], carotid [39], femoral [39], and cremaster muscle [40] arterioles, which help protect the SHR organs from the chronically elevated blood pressure [41]. This enhancement is also observed in humans who suffer from chronic essential hypertension [38, 41]. Hence, the SHR is an excellent experimental model to investigate the MC mechanism in the context of essential hypertension. DSS, on the other hand, is a well-established model of salt-sensitivity and hypertension similar to certain human populations such as African Americans [42]. DSS rats that are fed a high salt diet, rapidly develop progressive and proteinuric renal disease as well human hypertension features [43]. Utilization of these rat models of human

clinical conditions provides an element of genetic homogeneity (because these rats were inbred) as well as controlled environmental factors (such as diets), which are not possible to attain with the highly heterogeneous human populations [44]. Ultimately, the findings of these animal experimental models can be later tested in human clinical trials.

5.2 CONCLUSIONS

The central aim of this thesis was to communicate that: (i) the enhanced MC in the SHR is due to increased thromboxane A2 prostanoid independent of the endothelium, (ii) partially inhibiting MC while reducing the blood pressure protects from salt-induced renal injury in older SHR, and (iii) CKD progression of DSS and SHR are independent of blood pressure and strongly associated with proteinuria, albuminuria, and UMOD excretion levels. To present as a story, we first determined how MC works in terms of the role of endothelium, L-type calcium channels, and prostaglandins in the SHR and WKY rats. Blocking the MC through inhibiting L-type calcium channels lowered the blood pressure, but did not fully remove the MC, potentially resulting in its protective effects that included reduced urinary UMOD and albumin excretion levels leading to decreased incident protein casts and overall renal pathology. Comparing two animal models of hypertensive CKD, SHR and DSS, showed that even though their MC was similar and SHR was more hypertensive, the DSS suffered from more renal injury, which was associated with higher urinary UMOD and albumin as well as incident protein casts compared to the SHR. These results demonstrate a more complicated relationship between myogenic constriction, blood pressure, and renal pathology, and point to an

important role for the urinary UMOD and albumin. The significance of the findings of this thesis lies in the foundation that they have created for the future research and clinical works in hypertensive CKD.

5.3 FUTURE DIRECTIONS

In this thesis, the role of MC in the development of hypertensive CKD, and the use of nifedipine to inhibit the MC and subsequent pathology was investigated. However, some questions remain unanswered and are discussed below.

5.3.1 Determination of the Role UMOD Plays in the Development of CKD

While it has been established in this thesis that total 24-hour excreted UMOD is significantly correlated with incidents of protein casts, the mechanism has yet to be fully elucidated. Chapter 3 and 4 of thesis study demonstrated that overexcretion of total UMOD over 24 hours in the SHR-HS and DSS-HS rodents was associated with extensive renal damage, while reducing UMOD excretion with nifedipine treatment ameliorated the renal pathology (**Chapter 3 and 4**). After UMOD is synthesized, folded in the endoplasmic reticulum, and sorted by the Golgi, it is sent to the cell membrane where a membrane-bound serine protease called hepsin cleaves UMOD before being excreted into the renal tubules [45]. Nevertheless, an interesting point of inquiry is the specific role of UMOD expression and excretion in the development and progression of CKD. As such, future research can induce CKD (as previously established [46, 47]) in two knockout mouse models: 1) UMOD knockout to tackle UMOD expression; and 2)

hepsin knockout to tackle UMOD excretion. The combination of the 2 knockouts may provide interesting information on the role of UMOD expression and excretion in the development of CKD.

5.3.2 Determination of Salt Excretion Capabilities Between Younger and Older SHR Rats, and Its Relationship to Renal Injury

Chapter 3 and 4 demonstrated that MC was augmented in the younger but not the older SHR rats. The reason for this observation could be differential expression and activities in the sodium channels (i.e., sodium-hydrogen antiporter 3 and epithelial sodium channel) of younger and older SHRs, leading to differential sodium excretion. Yip et al. showed that 5 weeks-old prehypertensive SHR rats have higher expression of sodium-hydrogen antiporter 3 channels in their proximal tubules compared to older 12 weeks-old hypertensive SHR rats [20], leading to an increase in sodium excretion in 12 weeks-old SHRs. Paradoxically, epithelial sodium channel activity in renal epithelial cells was shown to be higher in 80 weeks-old SHR rats compared to 40- and 12-weeks old SHR rodents [48], suggesting that older SHR rats reabsorb more sodium from their proximal tubules than younger SHRs. Future research can investigate potential differential sodium metabolism in younger and older SHR rats, and explore its relationship to the pathogenesis of CKD.

5.3.3 Determination of the Mechanism Through Which Nifedipine Reduced UMOD Excretion.

Chapter 3 of this thesis illustrated that HS increased total UMOD excretion, however co-treatment of high salt with nifedipine significantly decreased total UMOD excretion. Future research could investigate whether the reduction in total UMOD excretion was as a result of alterations in UMOD mRNA or protein levels, or a change in hepsin expression or activity.

5.3.4 Validation of Our Findings in Human Clinical Trials

Chapter 1 of this thesis demonstrated thromboxane A2 to be the reason behind the enhanced MC in the SHR preglomerular arteries. However, whether this is also the case in human is unknown. Future clinical trials can extract preglomerular arterioles from kidney biopsies of patients with chronic essential hypertension to determine if increased thromboxane A2 drives the augmented MC in these vessels. The subsequent findings in these trials can lead to the development of pharmacological agents that stimulate the synthesis and release of thromboxane A2 in preglomerular arterioles of patients who suffer from other types of hypertensions, in an effort to induce enhanced MC to prevent hypertension-induced injury to the kidneys.

Additionally, even though nifedipine is a commonly used calcium blocker prescribed to patients [49] and non-coding variants in the UMOD gene were shown to have the strongest association with incident CKD [50], the effects of nifedipine on

UMOD excretion levels along with renal function and structure in CKD patients was never investigated before. Only one research study conducted in 1992 examined the effects of nifedipine on urinary UMOD excretion in hypertensive patients, but it is not clear whether the hypertensive patients in this study also suffered from CKD, and urinary albumin, renal function, and renal histopathology were not measured [51]. Previous research has shown that presence of even small amounts of albumin can precipitate UMOD in the urine of CKD patients [33]. This can also occur in renal tubules where both these elements exist, leading to the formation of protein casts. This thesis showed that nifedipine reduced high salt-induce urinary albumin and UMOD levels in hypertensive CKD rat models. Future human clinical trials should investigate if nifedipine decreases both urinary UMOD and albumin levels in hypertensive CKD; and if this potential reduction is accompanied with improved renal function and histopathology. This can potentially lead to the development of therapeutic agents that interfere with UMOD precipitation and protein casts formation to prevent the development of CKD. Collectively, these clinical trials following the animal model studies can fill in the current gaps of knowledge and pave the way for the treatment of hypertensive CKD.

CHAPTER 6

REFERENCES

1.   Pugh, D., P.J. Gallacher, and N. Dhaun, *Management of hypertension in chronic kidney disease.* Drugs, 2019. **79**(4): p. 365-379.

2.   Sengupta, P., *The laboratory rat: relating its age with human's.* International journal of preventive medicine, 2013. **4**(6): p. 624.

3.   Andreollo, N.A., et al., *Rat's age versus human's age: what is the relationship?* ABCD. Arquivos Brasileiros de Cirurgia Digestiva (São Paulo), 2012. **25**: p. 49-51.

4.   Quinn, R., *Comparing rat's to human's age: how old is my rat in people years?* Nutrition, 2005. **21**(6): p. 775.

5.   Sengupta, P., *A scientific review of age determination for a laboratory rat: how old is it in comparison with human age.* Biomed Int, 2011. **2**(2): p. 81-89.

6.   Tolbert, E.M., et al., *Onset of glomerular hypertension with aging precedes injury in the spontaneously hypertensive rat.* American Journal of Physiology-Renal Physiology, 2000. **278**(5): p. F839-F846.

7.   Hoang, K., et al., *Determinants of glomerular hypofiltration in aging humans.* Kidney international, 2003. **64**(4): p. 1417-1424.

8.   Amberg, G.C. and M.F. Navedo, *Calcium dynamics in vascular smooth muscle.* Microcirculation, 2013. **20**(4): p. 281-289.

9.   Ghosh, D., et al., *Calcium channels in vascular smooth muscle.* Advances in Pharmacology, 2017. **78**: p. 49-87.

10.   Knot, H.J. and M.T. Nelson, *Regulation of arterial diameter and wall [Ca2+] in cerebral arteries of rat by membrane potential and intravascular pressure.* The Journal of physiology, 1998. **508**(1): p. 199-209.

11.   Akaike, N., et al., *Low-voltage-activated calcium current in rat aorta smooth muscle cells in primary culture.* The Journal of Physiology, 1989. **416**(1): p. 141-160.

12.   Earley, S. and J.E. Brayden, *Transient receptor potential channels in the vasculature.* Physiological reviews, 2015. **95**(2): p. 645-690.

13.   Gao, H., et al., *Ca2+ influx through L-type Ca2+ channels and transient receptor potential channels activates pathological hypertrophy signaling.* Journal of molecular and cellular cardiology, 2012. **53**(5): p. 657-667.

14.   Yatabe, M.S., et al., *Effects of a high-sodium diet on renal tubule Ca2+ transporter and claudin expression in Wistar-Kyoto rats.* BMC nephrology, 2012. **13**(1): p. 1-9.

15.   Tykocki, N.R., W.F. Jackson, and S.W. Watts, *Reverse-mode Na+/Ca2+ exchange is an important mediator of venous contraction.* Pharmacological research, 2012. **66**(6): p. 544-554.

16.   Hirota, S.A. and L.J. Janssen, *Sodium and asthma: something borrowed, something new?* American Journal of Physiology-Lung Cellular and Molecular Physiology, 2007. **293**(6): p. L1369-L1373.

17.   Ashida, T., M. Kuramochi, and T. Omae, *Increased sodium-calcium exchange in arterial smooth muscle of spontaneously hypertensive rats.* Hypertension, 1989. **13**(6_pt_2): p. 890-895.

18.   Fowler, M.R., et al., *Age and hypertrophy alter the contribution of sarcoplasmic reticulum and Na+/Ca2+ exchange to Ca2+ removal in rat left ventricular myocytes.* Journal of molecular and cellular cardiology, 2007. **42**(3): p. 582-589.

19.   Zicha, J., *The age factor and salt-induced hypertension in the Brattleboro rat.* Hypertension, 1983. **5**(1): p. 156-157.

20.   Panico, C., et al., *Renal proximal tubular reabsorption is reduced in adult spontaneously hypertensive rats: roles of superoxide and Na+/H+ exchanger 3.* Hypertension, 2009. **54**(6): p. 1291-1297.

21.   Nurkiewicz, T.R. and M.A. Boegehold, *High dietary salt alters arteriolar myogenic responsiveness in normotensive and hypertensive rats.* American Journal of Physiology-Heart and Circulatory Physiology, 1998. **275**(6): p. H2095-H2104.

22.   Yu, H.C., et al., *Salt induces myocardial and renal fibrosis in normotensive and hypertensive rats.* Circulation, 1998. **98**(23): p. 2621-2628.

23.   Huang, B.S., B.N. Van Vliet, and F.H. Leenen, *Increases in CSF [Na+] precede the increases in blood pressure in Dahl S rats and SHR on a high-salt diet.* American Journal of Physiology-Heart and Circulatory Physiology, 2004. **287**(3): p. H1160-H1166.

24.   Sufiun, A., et al., *Association of a disrupted dipping pattern of blood pressure with progression of renal injury during the development of salt-dependent hypertension in rats.* International journal of molecular sciences, 2020. **21**(6): p. 2248.

25.   Farquhar, W.B., et al., *Dietary sodium and health: more than just blood pressure.* Journal of the American College of Cardiology, 2015. **65**(10): p. 1042-1050.

26.   Wu, T.-H., et al., *Tamm–Horsfall protein is a potent immunomodulatory molecule and a disease biomarker in the urinary system.* Molecules, 2018. **23**(1): p. 200.

27.   Lerma, E.V., M.A. Sparks, and J. Topf, *Nephrology Secrets E-Book.* 2018: Elsevier Health Sciences.

28.   Sanders, P.W., et al., *Mechanisms of intranephronal proteinaceous cast formation by low molecular weight proteins.* The Journal of clinical investigation, 1990. **85**(2): p. 570-576.

29.   Fan, S.-L. and S. Bai, *Urinalysis*, in *Contemporary Practice in Clinical Chemistry*. 2020, Elsevier. p. 665-680.

30.   Bülow, R.D. and P. Boor, *Extracellular matrix in kidney fibrosis: more than just a scaffold.* Journal of Histochemistry & Cytochemistry, 2019. **67**(9): p. 643-661.

31.   Fairley, J., J. Owen, and D. Birch, *Protein composition of urinary casts from healthy subjects and patients with glomerulonephritis.* Br Med J (Clin Res Ed), 1983. **287**(6408): p. 1838-1840.

32.   Fletcher, A., et al., *The chemical composition and electron microscopic appearance of a protein derived from urinary casts.* Biochimica et Biophysica Acta (BBA)-Protein Structure, 1970. **214**(2): p. 299-308.

33.   McQueen, E., *The nature of urinary casts.* Journal of Clinical Pathology, 1962. **15**(4): p. 367-373.

34.   Oparil, S. and M.A. Weber, *Hypertension: a companion to Brenner & Rector's The kidney*. 2000.

35.   Gardner, D.G., et al., *Vitamin D and the cardiovascular system*, in *Vitamin D*. 2011, Elsevier. p. 541-563.

36.   Mohammed-Ali, Z., et al., *Animal models of kidney disease*, in *Animal Models for the Study of Human Disease*. 2017, Elsevier. p. 379-417.

37.   Reckelhoff, J.F., L.L.Y. Cardozo, and M.L.A. Fortepiani, *Models of hypertension in aging*, in *Conn's Handbook of Models for Human Aging*. 2018, Elsevier. p. 703-720.

38.   Loutzenhiser, R., et al., *Renal autoregulation: new perspectives regarding the protective and regulatory roles of the underlying mechanisms.* American Journal of Physiology-Regulatory, Integrative and Comparative Physiology, 2006. **290**(5): p. R1153-R1167.

39.   Asano, M., et al., *Increased resting Ca2+ maintains the myogenic tone and activates K+ channels in arteries from young spontaneously hypertensive rats.* European Journal of Pharmacology: Molecular Pharmacology, 1993. **247**(3): p. 295-304.

40.   Huang, A. and A. Koller, *Endothelin and prostaglandin H2 enhance arteriolar myogenic tone in hypertension.* Hypertension, 1997. **30**(5): p. 1210-1215.

41.   Loutzenhiser, R., K.A. Griffin, and A.K. Bidani, *Systolic blood pressure as the trigger for the renal myogenic response: protective or autoregulatory?* Current opinion in nephrology and hypertension, 2006. **15**(1): p. 41-49.

42.   Williams, S.F., et al., *African Americans, hypertension and the renin angiotensin system.* World journal of cardiology, 2014. **6**(9): p. 878.

43.   Chackalamannil, S., D. Rotella, and S. Ward, *Comprehensive medicinal chemistry III*. 2017: Elsevier.

44.   Marín-García, J., *Post-genomic cardiology*. 2011: Academic Press.

45.   Brunati, M., et al., *The serine protease hepsin mediates urinary secretion and polymerisation of Zona Pellucida domain protein uromodulin.* Elife, 2015. **4**: p. e08887.

46.   Kirchhoff, F., et al., *Rapid development of severe end-organ damage in C57BL/6 mice by combining DOCA salt and angiotensin II.* Kidney international, 2008. **73**(5): p. 643-650.

47.   Mohammed-Ali, Z., et al., *Development of a model of chronic kidney disease in the C57BL/6 mouse with properties of progressive human CKD.* BioMed research international, 2015. **2015**.

48.   Kim, S.W., et al., *Increased expression of ENaC subunits and increased apical targeting of AQP2 in the kidneys of spontaneously hypertensive rats.* American Journal of Physiology-Renal Physiology, 2005. **289**(5): p. F957-F968.

49.   Snider, M.E., D.S. Nuzum, and A. Veverka, *Long-acting nifedipine in the management of the hypertensive patient.* Vascular health and risk management, 2008. **4**(6): p. 1249.

50.   Köttgen, A., et al., *Multiple loci associated with indices of renal function and chronic kidney disease.* Nature genetics, 2009. **41**(6): p. 712-717.

51.   Duława, J., M. Kokot, and F. Kokot, *Effects of furosemide, propranolol and nifedipine on urinary excretion of Tamm-Horsfall protein in patients with arterial hypertension.* Polskie Archiwum Medycyny Wewnetrznej, 1992. **88**(4): p. 212-218.